Industrial Electrical Engineering and Automation

# Harnessing Hydrogen and Batteries: Hybrid Energy Storage System for Versatile and Profitable Renewable Power Production
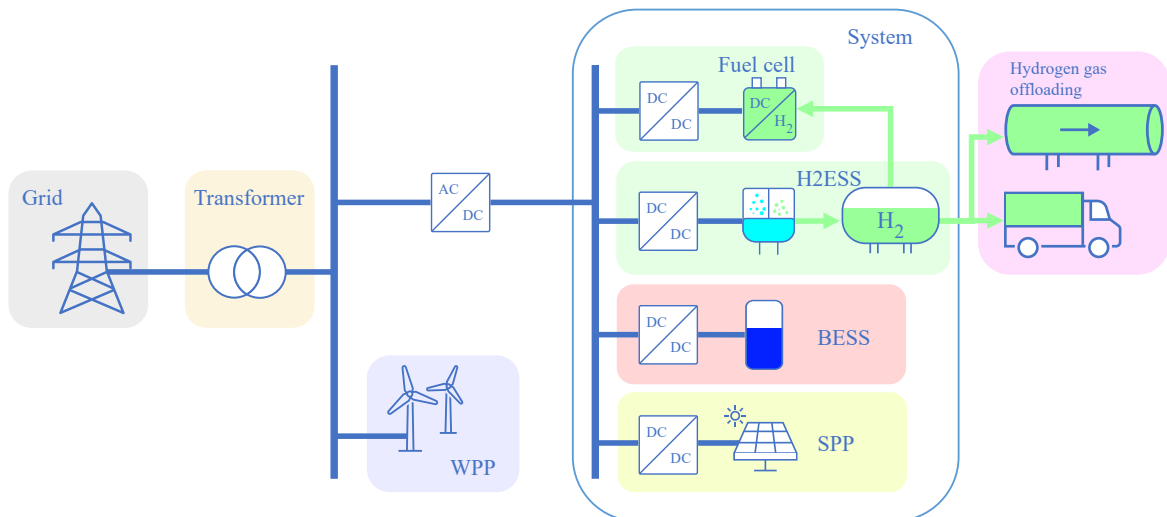
**Hugo Björling**
**Nora Jaredson Lilja**

Division of Industrial Electrical Engineering and Automation
Faculty of Engineering, Lund University

# Harnessing Hydrogen and Batteries

## Hybrid Energy Storage System for Versatile and Profitable Renewable Power Production

Hugo Björling

Nora Jaredson Lilja

Division of Industrial Electrical Engineering and Automation
Faculty of Engineering, Lund University
Lund

# Abstract

This thesis explores the integration of hydrogen and battery energy storage systems as a means to enhance the management of wind and solar power in the pursuit of a greener grid. The objective of the study is to identify the potential benefits and challenges associated with hybrid energy storage systems (HESS) and their role in renewable energy integration.

The thesis begins with a literature review, examining the energy system and markets, wind and solar power production, hydrogen energy storage system (H2ESS), and battery energy storage (BESS). This review serves as a foundation for the subsequent analysis and simulation.

A simulation method is employed to evaluate the performance and techno-economic aspects of the HESS. The OpenModelica software is used to model power generation, energy storage systems, grid infrastructure, and other relevant components. An operational strategy for the HESS is developed, including a Scheduler algorithm, which is making decisions based on market patterns, and a Controller algorithm, which assures technical functionality and makes the renewable variable power production plannable.

The economic decisions are made by the scheduler to maximise profit by either producing hydrogen, storing electricity, or delivering electricity to the grid. This is based on whichever market is momentarily most profitable. The scheduler dynamically adjusts the operation of the energy storage system to exploit price fluctuations and optimise revenue generation.

The techno-economic dimensioning method is utilised to assess the economic viability of the storage solution. Investment appraisal is conducted at various levels, including system, solar power plant, battery, electrolyser and hydrogen storage, and fuel cell levels. A simple optimisation process is employed to determine the optimal dimensions of the storage solution.

The results of the simulation and techno-economic analysis provide valuable insights. They demonstrate the potential of a HESS in improving the utilisation of renewable energy resources, enhancing grid stability, and reducing greenhouse gas emissions. The optimised HESS configuration offers a promising approach for future investments in renewable energy systems.

The discussion section highlights the implications of the findings, including the implications for investments in renewable energy and the potential for future market and technological developments. Furthermore, it identifies areas for further research to advance the understanding and implementation of HESS in the transition to a greener grid.

Overall, this thesis contributes to the ongoing efforts towards a sustainable and renewable energy future by investigating the role of HESSs in effectively managing wind and solar power, thereby facilitating the integration of clean energy into the grid.

# Acknowledgements

We would like to express our sincere gratitude to the following people and organisations for their invaluable contributions and support throughout the completion of this master thesis:

First and foremost, we want to extend our appreciation to our university supervisor, Jörgen Svensson, for his crucial contributions to our thesis work and his enthusiasm for the renewable energy transition as a whole. His knowledge has been instrumental in shaping the direction and execution of our research, and we are sure the thesis would not have been what it is today were it not for his help.

We would also like to express our gratitude to our supervisor at Eolus Vind AB, Andreas Möser, for his guidance and support throughout the thesis process. His experience and passion broadened our perspectives and helped shape our research. Thank you for your mentorship and dedication.

We also want to thank the rest of the team at Eolus Vind AB, the company with which we had the privilege to collaborate with. We are grateful for the time and enthusiasm the team has offered us, as well as all the words of motivation.

We would also like to acknowledge all other individuals who generously shared their time with us to facilitate interviews and discussions. These insights and perspectives have greatly helped our research.

To our friends and family, thank you for the continuous support and encouragement, not only during the writing of this thesis, but during our academic careers until this point. Thank you for believing in us and inspiring us to keep going.

Last but not least, we would like to express our appreciation to each other. With dedication, motivation, and unwavering optimism, we navigated the complexities of this thesis while supporting and challenging each other to produce our best work. The thesis is truly a testament to collaboration.

To everyone who played a part, whether big or small, in the realisation of this master thesis, we extend our deepest thanks. Your contributions have been invaluable, and we are grateful for the impact you have had on this journey.

Hugo Björling                                    Nora Jaredson Lilja
hugo.bjorl@gmail.com                 nora.jaredson@gmail.com

# Abbreviations

- AEL - Alkaline Electrolyser

- AEMEL - Anion Exchange Membrane Electrolyser

- AC - Alternating Current

- BESS - Battery Energy Storage System

- BOP - Balance of Plant

- BOS - Balance of System

- BRP - Balance Responsible Party

- CAPEX - Capital Expenditure

- CCS - Carbon Capture and Storage

- CSP - Concentrated Solar Power

- DC - Direct Current

- DOD - Depth of Discharge

- DSO - Distribution System Operator

- EU - European Union

- ESS - Energy Storage System

- FC - Fuel Cell

- FCEV - Fuel Cell Electric Vehicle

- GCP - Grid Connection Point

- GW, GWh - gigawatt, gigawatt-hour

- H2ESS - Hydrogen Energy Storage System

- HESS - Hybrid Energy Storage System

- IEA - International Energy Agency

- IRENA - International Renewable Energy Agency

- KPI - Key Performance Index

- kW, kWh - kilowatt, kilowatt-hour

- kV - kilovolt

- LCHS - Levelised Cost of Hydrogen Storage

- LCOE - Levelised Cost of Energy

- LOHC - Liquid Organic Hydrogen Carriers

- MW, MWh - megawatt, megawatt-hour

- NREL - National Renewable Energy Laboratory

- O&M - Operation & Maintenance

- OPEX - Operational Expenditure

- PEMEL - Polymer Electrolyte Membrane Electrolyser

- PPA - Power Purchasing Agreement

- PI Controller - Proportional Integral Controller

- PV - Photovoltaic

- RES - Renewable Energy Sources

- SPP - Solar Power Plant

- SOEL - Solid Oxide Electrolyser

- SoA - State-of-the-Art

- SOC - State of Charge

- SOH - State of Hydrogen

- TSO - Transmission System Operator

- VRES - Variable Renewable Energy Sources

- WPP - Wind Power Plant

# Contents

# List of Tables

# List of Figures

# 1 Introduction

This chapter will introduce the thesis by presenting its background and objectives. It also offers a brief method overview, followed by a lead-in to the Bäckhammar wind power plant, the location of which parts of this thesis is based on. After offering a report outline, the general system on which the thesis is based will be introduced.

## 1.1 Background

In light of the climate crisis, the EU announced a series of goals in its European Green Deal to ensure it becomes a "modern, resource-efficient and competitive economy" (European Commission [25]). Among these goals are the ambition to have zero net emissions of greenhouse gases by 2050 and to decouple economic growth from resource use. One subtarget is to reduce net greenhouse gas emissions by a minimum of 55% by 2030 compared to 1990.

Meanwhile, Sweden has a set goal to have net zero greenhouse emissions by 2045 (Regeringskansliet [59]). After this point, net negative emissions is the goal. One way to reach this goal is to increase the amount of renewable energy in the energy mix. However, increasing the amount of renewable, and often intermittent, energy comes with its own set of challenges. Until today, neither demand side response nor high electricity prices have done much to change the general electricity demand patterns. These are in large still decoupled from the solar and wind resource patterns.

Recent high energy prices in Sweden accentuate the need for cost-effective power production (Lejestrand [46]). One factor contributing to the high prices is that the electrical energy cannot be stored, causing dependency on current weather conditions. The higher ratio of unplannable electricity generation also increases the power system's sensitivity to smaller changes in supply and demand, causing a greater price variation.

One way to ensure competitive renewable energy is to shift it in time, through the use of energy storages. They can provide flexibility, stability, and reliability to the energy system (European Commission [27]). There are many different kinds of energy storages that each have different features, making them appropriate for various applications and allowing them to contribute to a range of decarbonisation goals. For example, batteries are considered more appropriate for reserve and response service as well as transmission and distribution grid support, while hydrogen storage is considered to be better adapted for bulk power management. Energy storage technologies are especially capable of supporting the increased integration of renewable energy, electrification of the economy, and decarbonisation of other economic sectors (such as transportation and industry).

Batteries help with integration of variable renewable energy sources (RES) at various scales (European Commission [24]). In grid and utility systems, they can store surplus energy and provide essential grid services including frequency and voltage control, peak shaving, con-

gestion management, and black start services. In commercial and industrial settings, batteries maximise self-consumption of renewable energy, help smoothly integrate electric vehicle (EV) recharge systems, and offer ancillary services. At the residential level, home batteries support RES and EV services on the demand side, while also providing grid-balancing services. In specialised applications like telecom or micro-grids, batteries are almost the only option for storage. With improved performance and cost-effectiveness, batteries are expected to compete with other storage technologies for long-term and long-duration stationary applications. Digitisation further amplifies their potential, allowing them to become an integrated and flexible addition to the grid.

While batteries have been developed for a long time, hydrogen gas as a means of energy storage is also becoming more important. The EU announced their hydrogen strategy for a climate-neutral Europe in 2020 as a solution to decarbonise hard-to-reach sectors and accelerate the green transition ([26]). It suggests that hydrogen is vital to support EU goals to achieve carbon neutrality by 2050 and the global attempt to implement the Paris Agreement. When produced from renewable sources, hydrogen has no $CO_2$ emissions, and also causes minimal air pollution when used. Although currently a small fraction of the energy mix, hydrogen is expected to grow rapidly due to falling renewable energy costs and increased investments. It has potential to bridge the gap in renewable energy storage, serve as a transport fuel, and replace fossil fuel in carbon-intensive industries. By 2050, it is expected to make up 13-14% of Europe's energy mix.

This thesis is done in collaboration with Eolus Vind AB.

### 1.1.1   Eolus Vind AB

Eolus Vind AB is a Swedish renewable energy company dating back thirty years (Eolus Vind AB [16]). Its main business areas are both on- and offshore wind power, solar power and energy storage. Its primary focus is on developing, establishing, and managing renewable energy projects. As one of the leading wind power developers in the Nordics, it offers attractive and competitive investment opportunities to both local and international investors alike. In 2021, Eolus had developed 1414 MW of wind power capacity in Sweden, Norway, the USA and Estonia, but also boasts business in Finland, Poland and Latvia. It has been listed on NASDAQ Stockholm since 2015.

## 1.2   Objectives

The main objective of this thesis is to examine the possibilities of a hybrid energy storage system (HESS) including a battery energy storage system (BESS) and a hydrogen energy storage system (H2ESS) which, together with a solar power plant (SPP), can be added to an onshore existing wind power plant (WPP). The goal is to make this system as technically and economically viable as possible. By doing so, it could contribute to the integration of variable renewable energy sources (VRES) in the power grid. In order to do this, the following questions will be answered.

- How can hydrogen gas and batteries be combined in an energy storage strategy?

- What dimensions of components make such a system the most profitable in a 2030 scenario?

- What drives profitability in a hybrid energy storage system with wind and solar power?

- How can such a system contribute to the green transition?

## 1.3   Method overview

The method of this thesis is divided into three parts. This method section provides a brief overview of the work. Another method chapter discusses the simulation methodology, found in Section 3. It covers aspects including data analysis, model design, energy storage strategy and operation, and implementation. This is followed by a techno-economic dimensioning method, found in Section 4, which includes economic methods, investment appraisal design, and a process used to dimension the components of the model.

The first part of this thesis consists of a literature study, making up the basis for what will be simulated in the latter part. For this reason, not all parts of the literature study provide the same depth, but relate closely to the scope of the simulation. The literature study will treat background knowledge relating to the Swedish electricity markets and system, the potential hydrogen market, wind and solar power production, as well as the characteristics and applications of hydrogen gas and batteries as energy storage.

The second part of the thesis details the operational strategy used to control the model simulation. This consists of two parts, a Scheduler which sets ideal values and a Controller which attempts to implement these ideal values while maintaining the system functions.

Then, simulations of the model are carried out using the OpenModelica software to determine the best dimensions for the model, based on both technical and economical feasibility. These results are then discussed before a conclusion is formed.

### 1.3.1 Scope and demarcations

The scope of this thesis is an investment in 2030 of a system added to complement an existing onshore wind production site. This means that the WPP itself is not economically included in the scope, although its production is included. Furthermore, the transportation of generated hydrogen at the site is not included in the scope, although it is briefly discussed to ensure technical feasibility. Finally, only one energy market is considered for the model, namely the future intraday market.

# 1.4 Case study

This project is based on the Bäckhammar WPP, located in the Kristinehamn and Degerfors municipalities in Sweden (Eolus Vind AB [15]). It has a total installed capacity of 130 MW, spread over 31 wind turbines. 22 of these are the Vestas V136 4.2 MW and the remaining 9 are the Vestas V150 4.2 MW. The WPP has been in operation since 2020. The specifications for the Bäckhammar WPP are shown in Table 1.1 (Vestas [87], Vestas [88]).

**Table 1.1:** Specifications of the Bäckhammar WPP turbines ([87], [88]).

|                          | V136  | V150  |
| ------------------------ | ----- | ----- |
| Rated power (MW)         | 4.2   | 4.2   |
| Cut-in wind speed (m/s)  | 3     | 3     |
| Cut-out wind speed (m/s) | 25    | 22.5  |
| Rotor diameter (m)       | 136   | 150   |
| Swept area (m$^2$)       | 14527 | 17671 |

The WPP has an external owner, KGAL, but Eolus continues to provide technical and administrative services. A Power Purchasing Agreement (PPA) has been established between KGAL and Amazon Web Services to provide the latter with green energy. PPAs will be further explained in Section 2.8.

The WPP is located in electricity price area 3 in Sweden, as can be seen in Figure 1.1. The concept of electricity price areas will be further explained in Section 2.1.1.
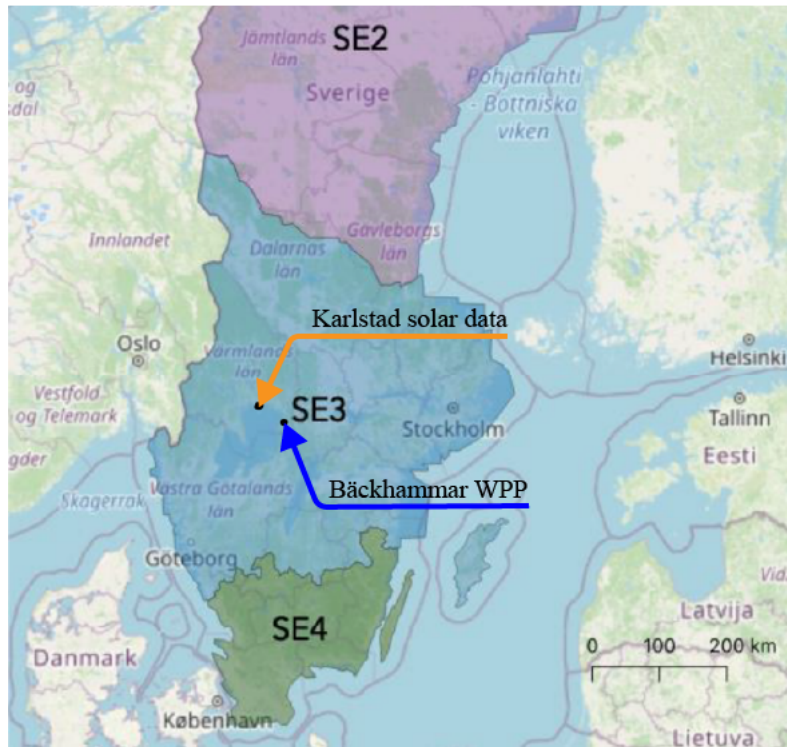
**Figure 1.1:** Map showing locations of Karlstad solar data measuring point [63] and Bäckhammar wind power plant [15], laid over a map of Sweden's electricity price areas [77].

The siting of the Bäckhammar WPP can be seen in Figure 1.2. There are three grid connection points (GCPs), but for the sake of this report, these will be assumed to act as one. The turbines are connected to a 30 kilovolt (kV) distribution grid. The transformer steps from 30 kV to 130 kV. The maximum active power of the transformer is limited to 130 MW. All additions in this project will be attached to this same GCP, before the transformer.
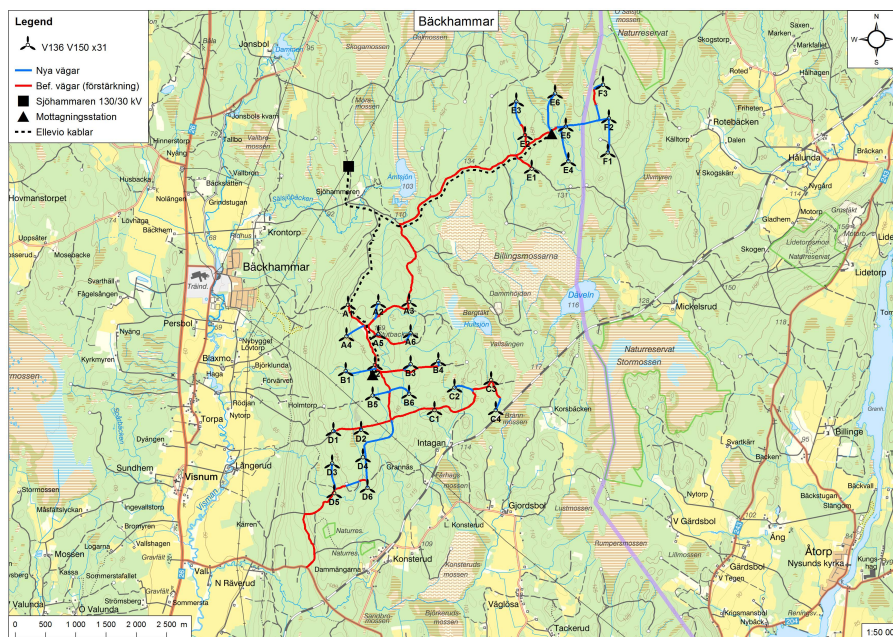


**Figure 1.2:** Siting of Bäckhammar wind power plant, provided by Eolus Vind AB.

One assumption made is that there is ample space at this site to install a SPP. Areas that could

be appropriate for this are some of the marshes seen to the East of the WPP, for example Billingsmossarna.

## 1.5   Report outline

Chapter 1 offers an introduction to the report, which includes background, introduction to Eolus Vind AB, objectives, method overview, scope and demarcations, a short case study on the chosen location, as well as a brief system introduction.

Chapter 2 consists of a literature review which covers the Swedish electricity system and other markets. It then goes on to give an overview of the two renewable power sources used in this thesis as well as some of their techno-economic characteristics. Then, it provides insights regarding H2ESS and BESS as well as their techno-economic characteristics. It also suggests some economic incentives for energy storage which motivate the existence of this thesis. Finally, it gives some background on management strategies for energy storage systems (ESSs).

Chapter 3 is the first method chapter which covers the simulation. It begins by reviewing simulation inputs and the coming initial data analysis. Then, it explains the system to be constructed as well as the software used. Finally, it explains the operational strategy used to control the ESS, and how it is implemented in the simulation tool.

Chapter 4 is the second method chapter, which focuses on the techno-economic dimensioning of the system. First, it gives some overview of the economics to be used in the dimensioning process. Then, it explains the investment appraisal inputs. Finally, the system evaluation method and optimisation process is presented.

In Chapter 5, results are presented for the simulation and techno-economic dimensioning, before Chapter 6 opens up for discussion. In Chapter 7, the thesis is concluded.

# 1.6 System introduction

In order to meet the objectives, a system containing several components will be constructed. As aforementioned, it will contain a WPP, SPP, BESS, H2ESS, and GCP. A very basic overview can be seen in Figure 1.3.
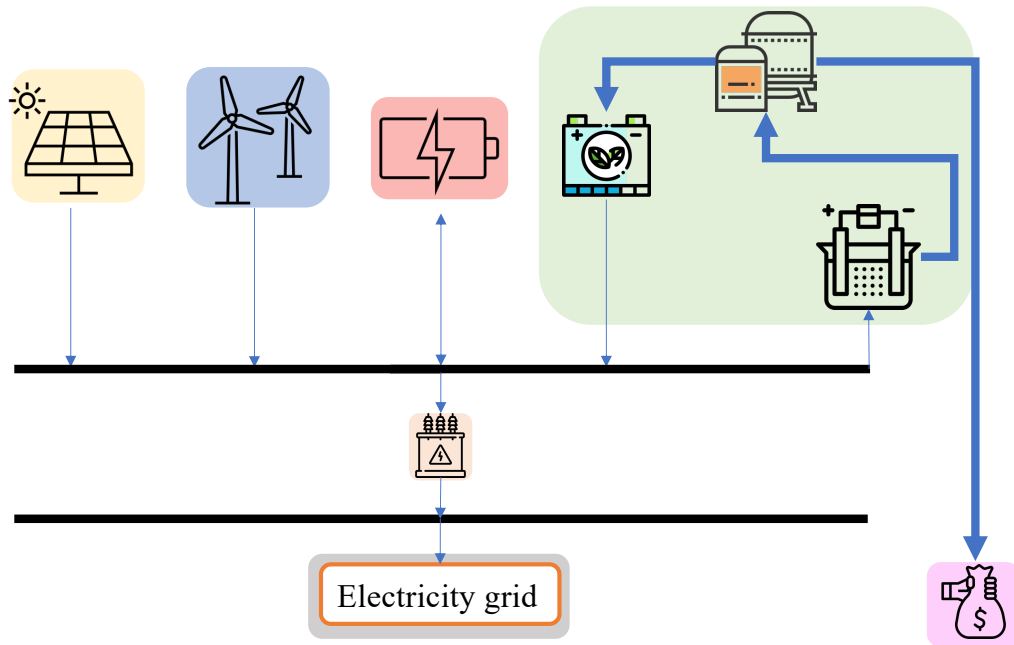


**Figure 1.3:** Introduction to system components.

10

# 2 Literature review

The following literature review will offer an overview of the energy markets, renewable power sources, and energy storages relevant to this thesis. Both technical and economic perspectives will be reviewed.

## 2.1 Energy system and markets

Traditionally, the electricity system of Sweden has consisted of large, centralised production from hydro and nuclear power (Swedish Energy Agency [74]). Production has been adjustable to variable needs. However, the contribution of wind and solar power have both increased significantly since the 2010s. As of 2020, Sweden's electricity production consisted of 45% hydro power, 29% nuclear power, 17% wind power and 1% solar power, see Figure 2.1. Although the total amount of solar power is low, the amount of grid connected solar installations saw a 46% increase between 2020 and 2021.

**Total supplied energy 1970–2020, TWh**
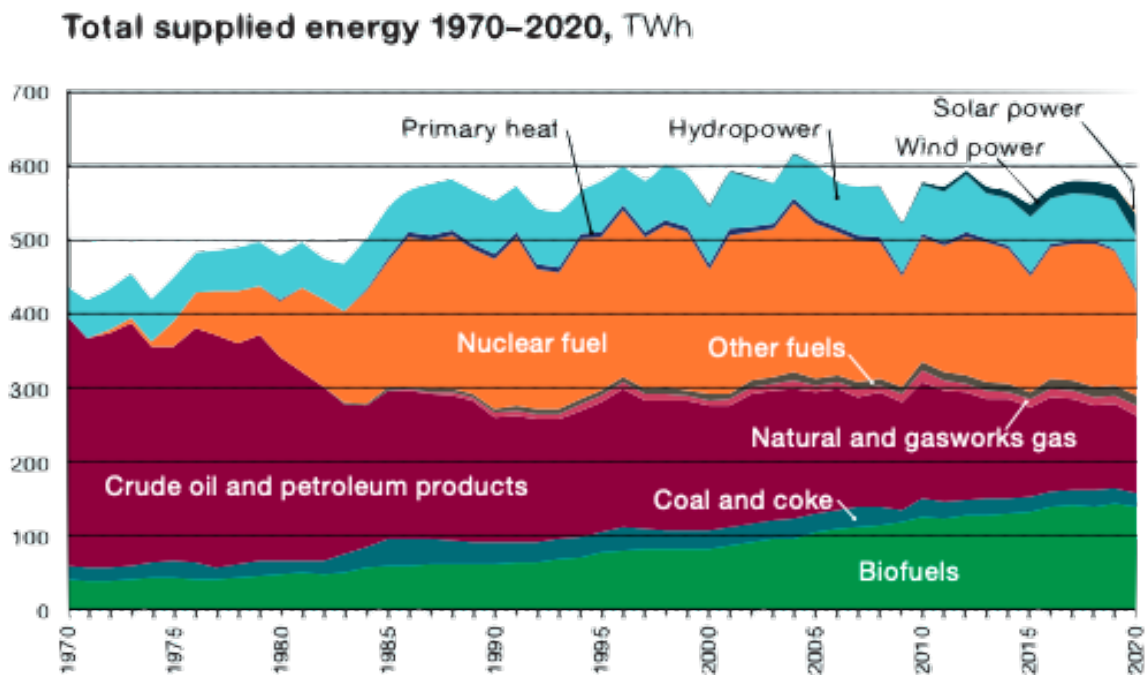
**Figure 2.1:** Swedish energy by source between 1970 and 2020 [74]. Note that wind power was included in hydropower until 1989.

The producer side of the Swedish electricity system is connected to the consumers through an electricity market (Svenska Kraftnät [69]). Sweden is part of a larger European electricity system, where electricity can flow freely between the Nordic and Baltic countries. The market is deregulated, meaning that there is free competition in order to encourage effective resource use. The Transmission System Operators (TSOs) are responsible for the

transnational trade and transmission of power to consumers. The Swedish TSO is Svenska kraftnät.

Electricity trade is done on different markets with different time horizons (Svenska Kraftnät [68]). The short term markets, consisting of a day-ahead market and an intraday market, are managed by Nord Pool. The long-term market is managed by Nasdaq OMX. The Nord Pool Spot market, also known as the day-ahead market, is an auction where electricity producers leave bids for the electricity they expect to produce the following day. This market closes at 12:00 the day before the forecasted generation. The intraday market is used to adjust for miscalculations in the spot market, for example if the weather forecast the day before generation did not match reality. Contrary to the spot market, this market is not run through an auction but by matching buyers to sellers continuously. Trade can be done whenever, but no later than one hour before the time of electricity consumption. Nasdaq OMX has a long-term market that offers large energy consumers contracts to secure electricity prices for several years ahead.

### 2.1.1 Electricity price areas

Sweden is divided into four electricity price areas, shown in Figure 2.2, in order to manage physical limitations in the transmission network (Svenska kraftnät [70]). The divisions are made to allow actors to trade under the same conditions regardless of what country they are in, as required by European legislation. Limitations or bottlenecks appear due to a mismatch of production and consumption in a given interface. For example, bottlenecks appear between the north and south of Sweden because of excess cheap electricity production in the north (hydro power) and excess consumption in the south (population centers). Where the network is physically unable to transmit enough electricity to meet the market demand, a division is made in order to send price signals to producers and consumers.
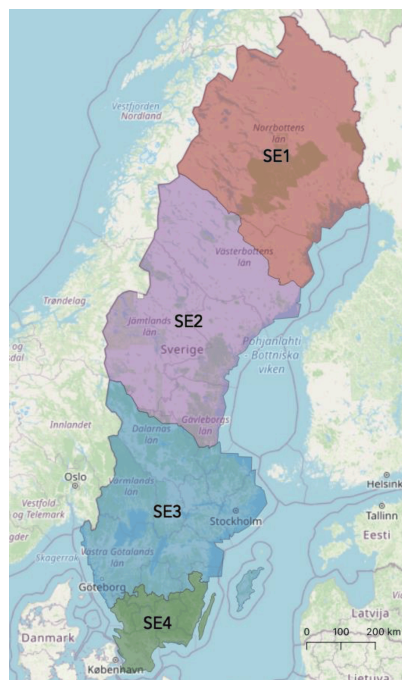


**Figure 2.2:** Swedish electricity price areas [77].

## 2.1.2 Nord Pool

Nord Pool is the organization in charge of the physical electricity trade in the Nordics (Sweden, Finland, Norway, Denmark, Estonia, Latvia, and Lithuania) (Energimarknadsinspektionen [13]). The market was founded in 1993 in Sweden and is owned by its member countries' TSOs. Nord Pool owns the day-ahead and intraday markets, which operate on different time horizons, see Figure 2.3. 85% of the electricity consumed in the Nordics is traded on a Nord Pool marketplace.

Nord Pool is overseen by its member countries' TSOs, and also has an overseeing requirement from the EU imposed on it. The EU directive REMIT controls the electricity trade in order to avoid market manipulation and insider trade. Also, market information is made available to all actors on the market through the Transparency Regulation (Swedish: transparensförordningen).
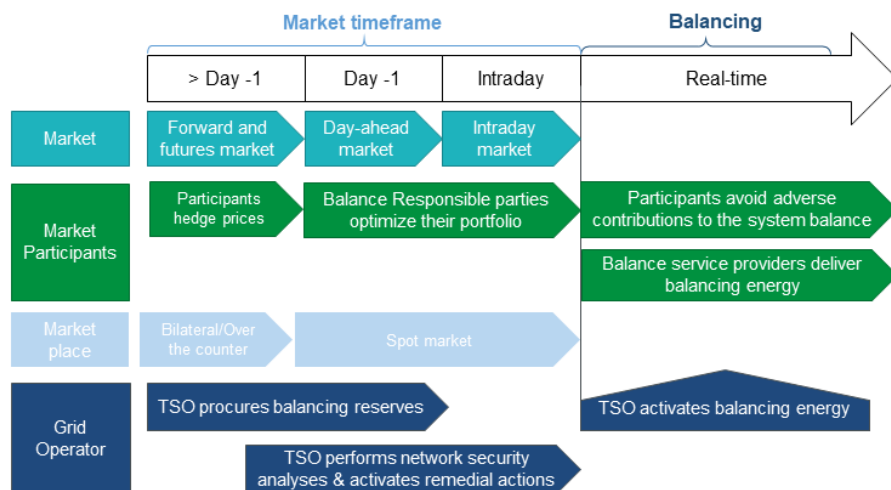


**Figure 2.3:** Time horizons for different markets, including the Nord Pool day-ahead and intraday markets [76].

**Day-ahead**

The day-ahead market acts as an auction forum to balance supply and demand. The buying bids from consumers are matched to the selling bids of producers through an auction. The bids specify the volumes to buy/sell (MWh/h) and the specific price (EUR/MWh) for each hour. As aforementioned, these bids are placed no later than 12:00 each morning for the following day, effectively coining the name day-ahead market. The final prices are published at 13:00 for the following day. The marketplace dictates the system and spot prices of the different electricity areas for each hour, one day ahead.

**Intraday**

The intraday market is an adjustment market acting as a complement for the day-ahead market. The market adjusts electricity trade contracts up until one hour before delivery the same day, hence the name intraday market. The adjustments are needed due to production or consumption not being in line with predictions, such as when the weather does not behave as expected.

A 15-minute intraday market is going to gradually launch in Sweden starting May 22nd 2023, meaning that bids will be able to be placed up to 15 minutes consumption as opposed to before one hour before (eSett Oy [21]).

### 2.1.3   Ancillary service markets

The Swedish TSO, Svenska kraftnät, uses so-called ancillary services to balance and manage disruptions in the power system (Svenska Kraftnät [72]). To do this, they buy different types of reserves from market participants in the electricity sector. Reserves are both managed in a bidding process on the balancing market, but also through longer-term contracts, depending on the service. The timeline for gate closure of different reserves can be seen in Figure 2.4. Providing ancillary services is not only very profitable for individual companies, but can also aid in the sustainable energy transition.
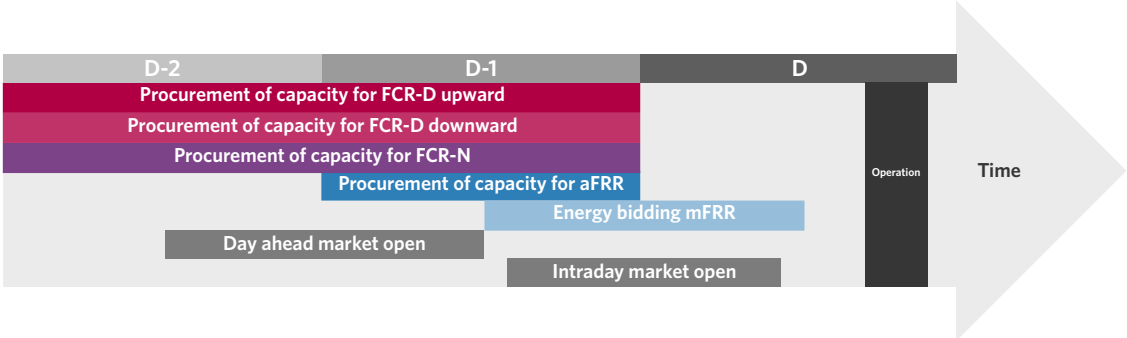


**Figure 2.4:** Gate closure time horizons for ancillary service markets, day-ahead market, and intraday market. [73].

## 2.1.4 Hydrogen market

Between late 2019 and early 2022, 15 countries and the EU commission had announced various hydrogen strategies, with a clear emphasis on both international collaboration and potential future trade (IRENA [41]). Many of these strategies have resulted in agreements, feasibility studies, memoranda of cooperation and more. Generally, these strategies fall into one of two categories - general technology collaboration to exchange knowledge and specific pilot projects or studies to investigate hydrogen trade between countries. The cumulative result of projects that have been announced between 2018 and 2022 can be seen in Figure 2.5.
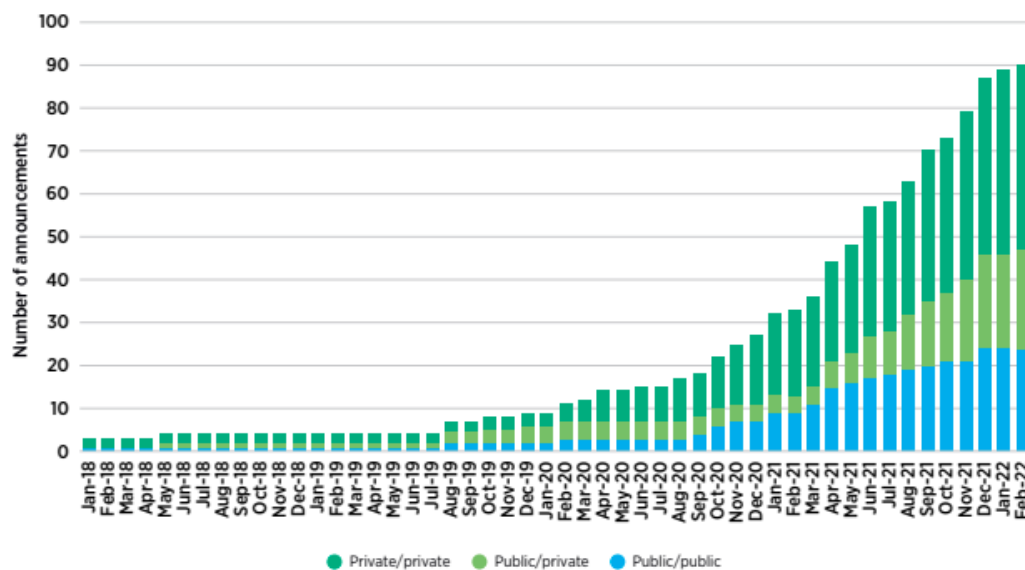


**Figure 2.5:** Cumulative hydrogen project announcements 2018-2022 [41]. Note that announcements are only included if they mention hydrogen trade explicitly.

Some countries that show good potential to be strong importers of hydrogen are Germany, Japan, and the Netherlands. For them, hydrogen can be a promising option considering lack of domestic renewable sources, limited hydrogen production potential, and restrictions on technology choices (for example, restrictions on use of nuclear energy in Germany). To ensure energy security and to hedge risks associated with future technology potential, their approaches are diversified by two aspects. Firstly, relationships are established with multiple countries to account for unforeseen events preventing their local hydrogen industry. Secondly, different hydrogen carriers are tested to see which would be most commercially feasible.

The EU has a clear commitment to achieve carbon neutrality by 2050, succeed in the implementation of the Paris Agreement, and emit zero pollution. Hydrogen is seen as a potential tool to decarbonise industrial processes and economic sectors that struggle to do this in other ways. In the EU Commission's "A hydrogen strategy for a climate-neutral Europe", three phases to ramp up and decarbonise hydrogen production are introduced (European Commission [26]).

In the first phase, spanning 2020 to 2024, the aim is to install at least 6 GW of renewable hydrogen electrolysers to produce a total of up to one million tonnes of hydrogen. To put this in perspective, the global installed electrolysis capacity for 2023 (based on projects under

construction or planned with a set start year of operation) is 5.52 MW, with the EU accounting for 30% of this capacity (IEA [40]). Besides this, the goal is to decarbonise existing hydrogen production, for example in the chemical sector, and to encourage consumption of hydrogen in new applications, such as in industrial processes and heavy-duty transport (European Commission [26]). The EU recognizes the need for increased electrolyser manufacturing during this phase and proposes that these electrolysers could be installed near the demand sources, such as steel plants.

To achieve these goals, the EU has identified the need to incentivise the production of low-carbon, electricity-based hydrogen, particularly with near-zero greenhouse gas emissions, in order to scale up production and obtain a greater market share. The retrofitting of existing hydrogen production plants with carbon capture and storage (CCS) technologies is also emphasised.

Policy making during the first phase will mainly focus on the regulatory framework for a hydrogen market, as well as incentivising supply and demand in key markets including making low-carbon hydrogen production less costly to match conventional hydrogen production through state aid rules. There will also be an emphasis on implementing framework conditions that support plans for large-scale renewable hydrogen production before 2030. The European Clean Hydrogen Alliance will be directing investments, and there will also be increased funding to support investment gaps in renewable production caused by the COVID-19 pandemic through various funding mechanisms.

The second phase of the plan, spanning from 2025 to 2030, has a strategic objective of installing at least 40 gigawatts (GW) of renewable hydrogen electrolysers and producing up to 10 million tonnes of renewable hydrogen. It is expected that by this point, renewable hydrogen will be cost-competitive with other forms of hydrogen production. However, further policies will be necessary to support the industrial demand for new applications, such as steel production. In addition, hydrogen will have an increased role in the electricity system as it will be used for seasonal storage and frequency balance. Retrofitting of existing fossil hydrogen production with CCS will continue.

To achieve these objectives, there is a need for an EU-wide logistical infrastructure, which will include attempts to transport hydrogen from areas with good renewable potential to other member states. Planning for a pan-European grid and establishing hydrogen refuelling stations will be essential. The existing gas grid will be partially repurposed, and large-scale hydrogen storage will be developed. International trade with the EU's neighbours could also be developed. The policies established in this phase aim to stimulate investments in building a complete hydrogen system. By 2030, the EU aims to create an open, competitive hydrogen market with unobstructed cross-border trade and efficient allocation across sectors.

In the third phase of the plan, spanning from 2030 to 2050, renewable hydrogen production is expected to have matured and scaled up significantly to meet the decarbonisation needs of all sectors. As a result, renewable electricity production will also need to increase, with a quarter of it being used for hydrogen production by 2050. Hydrogen-derived synthetic fuels are anticipated to penetrate a wide range of sectors.

In addition, the United States has made a significant commitment to hydrogen (U.S Department of Energy [83]). The Infrastructure Investment and Jobs Act of 2021 has allocated

9.5 billion USD towards clean hydrogen, and the Inflation Reduction Act of 2022 provides further incentives for hydrogen through a production tax credit.

Aurora Energy has made predictions for the levelised cost of green hydrogen (hydrogen produced entirely through renewable energy sources) for 2030 (Aurora Energy Research [6]). For Germany, this number was put in a range between 3.9 to 5 €/kgH$_2$, in the case where the electrolysers are not connected to the electricity grid.

## 2.2 Wind power production

### 2.2.1 Theory

Electricity production through wind turbines involves converting the kinetic energy of air into rotational energy in the blades, which is then transferred via a shaft to the generator, resulting in the production of electrical energy (IRENA [44]). In recent years, wind energy has experienced significant growth, see Figure 2.6.
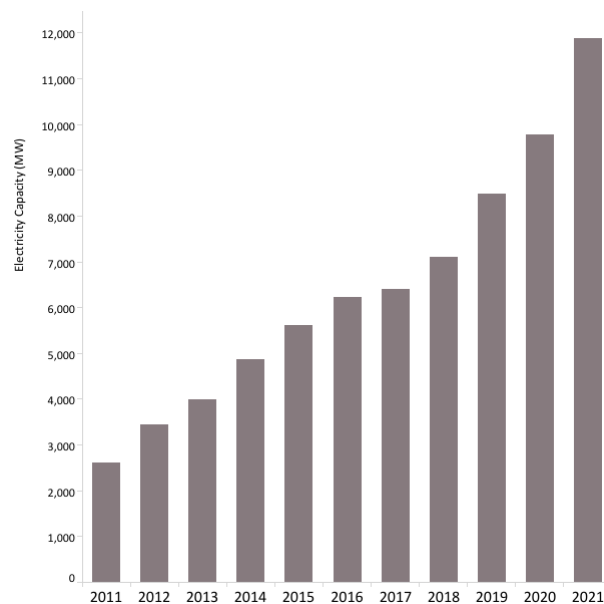


**Figure 2.6:** Installed onshore electricity capacity in Sweden [44].

Since the 2000s, the wind energy sector has witnessed a remarkable expansion, made possible both by favorable governmental policies and technological advancements. The continuous increase of capacity factors for wind turbines over time points is one factor pointing towards technological advancement. A capacity factor is the relationship between the energy produced by a source and its peak capacity. The capacity factors of wind turbines have increased over time, as turbines become larger and more powerful. In 2020, the capacity factor for new installed onshore wind in Sweden was estimated to be about 37% (Svensk Vindkraft [67]). The same number for 2025 is projected to be about 40%. Onshore wind turbines have a typical output power between 3 to 4 MW, while the highest performing onshore wind turbine has a rated power of 7.58 MW (Enercon [12]). The increase in turbine size is due to the relationship between power and wind (IRENA [44]). The output of wind turbines is proportional to the swept area of the blades and the cube of wind speed, and

as wind speeds are typically higher at a larger height, this makes the development of taller wind turbines beneficial.

The wind turbines used at the case study location, Bäckhammar, are 22 of the V136 4.2 MW turbines and nine of the Vestas V150 4.2 MW turbines (Eolus Vind AB [15]). Their specifications are shown in Table 1.1.

To be able to produce power and avoid high stress on the rotor blades, wind turbines have cut-in and cut-out speeds (Manwell et al. [48]). The output power of the turbine increases between the cut-in speed and the speed at which it reaches its rated power. The rotors are stopped at the cut-out speed to prevent excess stress on the blades. This behaviour can be seen in Figure 2.7.
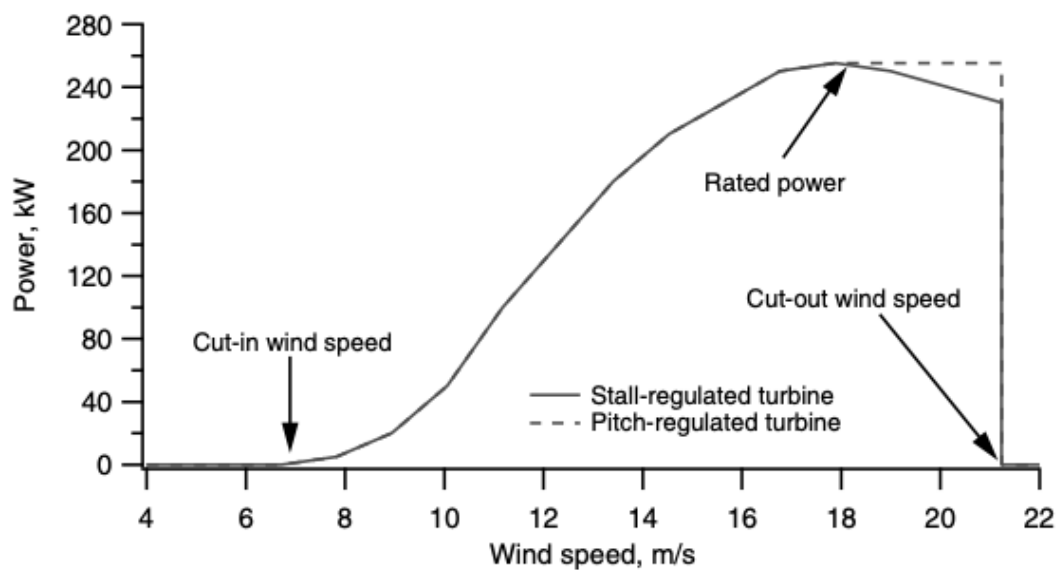


**Figure 2.7:** Sample power curve for a wind turbine [48]. Note that the Bäckhammar wind turbines are pitch-regulated and therefore correspond to the dotted line.

As wind is intermittent by nature, wind power is a VRES. This involves challenges both with regards to grid connection, and with regards to making applications profitable.

## 2.2.2   Techno-economic characteristics of wind power

As this thesis is centred around the contribution of adding a SPP and energy storage to an existing onshore WPP, the techno-economic characteristics of wind power are not within the scope. However, having some knowledge of how onshore wind power operates is beneficial to get a deeper understanding of this thesis.

In order to see how WPP production varies throughout one year, the capacity factor can be studied. Based on simulations by Renewable Ninja, using data from the MERRA-2 database, the daily mean capacity factors for onshore wind power production in Sweden in 2019 could be generated (Pfenninger and Staffell [56], Pfenninger and Staffell [54], Pfenninger and Staffell [55]). This can be seen in Figure 2.8.
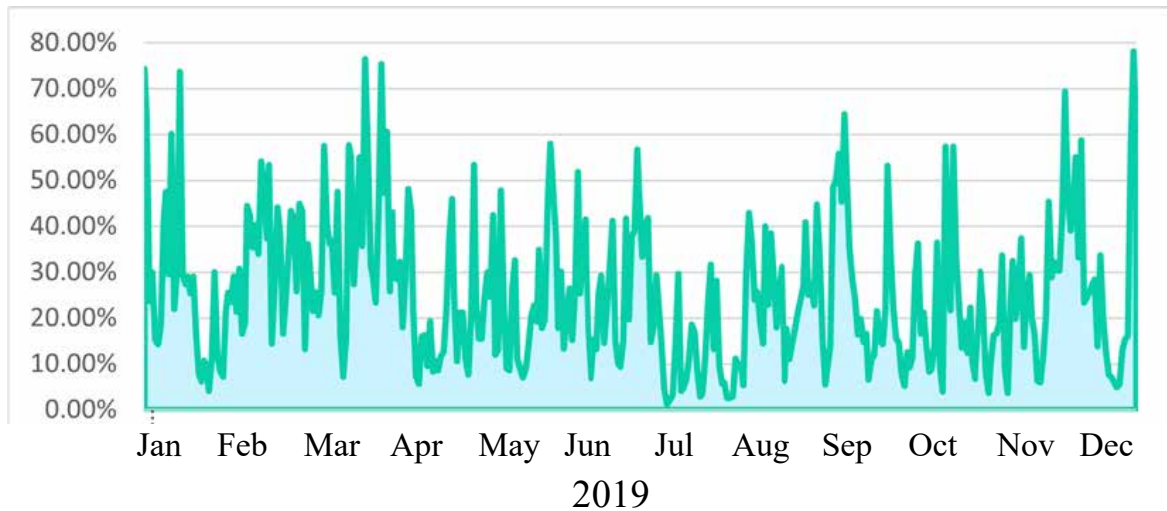
**Figure 2.8:** Mean daily capacity factors of onshore wind power for 2019 in Sweden ([56], [54], [55]).

The pattern of power production reflects typical behaviour for a WPP. WPP production varies seasonally and generally produces much more power during winter and fall compared to summer (Heide et al. [36]). There are also daily variations.

The monthly average capacity factors for onshore wind power in Sweden in 2019 is shown in Figure 2.9.
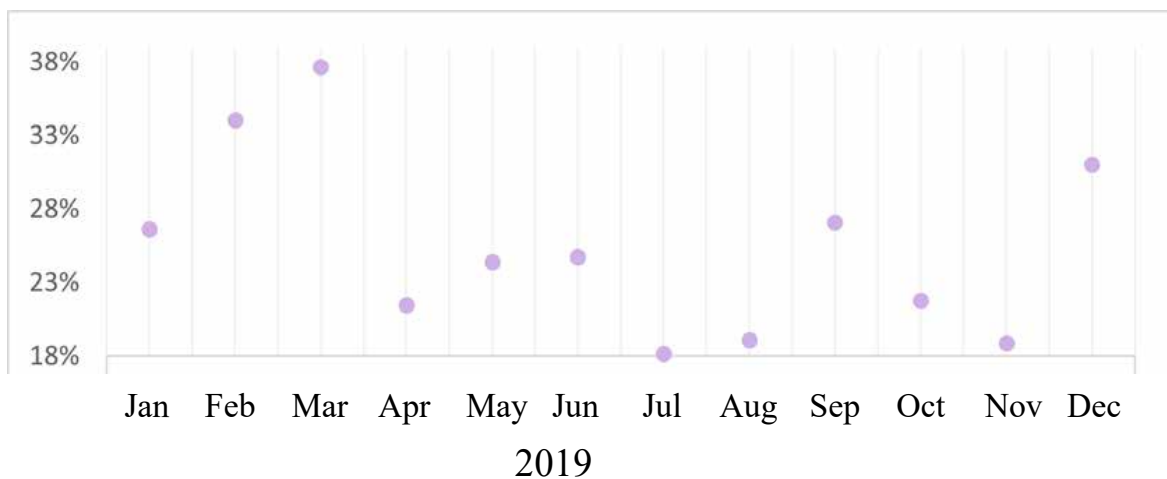


**Figure 2.9:** Mean average capacity factors of onshore wind power for 2019 in Sweden ([56], [54], [55]).

In 2021, The LCOE for new onshore wind power in Sweden was the lowest out of all energy sources, ranging from 240 to 360 SEK/MWh depending on the plant size (Elmqvist et al. [11]). The LCOE for onshore wind power in the EU in 2018 ranged between 41 and 89 EUR/MWh, with 75% of countries reporting an LCOE below 66 EUR/MWh (Trinomics for the European Commission [78]). Considering the average annual exchange rate of 2021, this amounts to about 670 SEK/MWh (European Central Bank [22]).

## 2.3 Solar power production

### 2.3.1 Theory

Solar power is a popular renewable energy source for electricity generation and desalination of water (IRENA [43]). This is done mainly through two technologies, solar photovoltaic (PV) and concentrated solar power (CSP).

PV technology involves the use of electronic devices, namely solar cells, which directly convert sunlight into electricity. This technology is one of the fastest-growing renewable energy technologies. It has a modular design that allows for a range of applications, from small solar home kits and rooftop installations of 3 - 20 kilowatts (kW) to large-scale installations with hundreds of megawatts (MW) in capacity. The manufacturing cost of solar PV cells has decreased significantly since the 2010's, often making it one of the cheapest forms of electricity globally. In the period 2010 to 2020, a 93% price decrease was seen in solar modules along with an 85% decrease in LCOE for utility-scale solar PV.

CSP uses mirrors to concentrate the sun's rays, which heat a fluid that generates steam to drive a turbine and in turn generate electricity. This technology is typically used in large scale power plants, in places with a high amount of direct solar irradiation.

In Sweden however, there is not generally enough direct solar irradiation for this technology to be feasible. Figure 2.10, showing a map of global solar irradiation, makes it clear that solar irradiation is comparatively quite low in Sweden (Alshahrani et al. [3]). That is one reason why, after discussions with Eolus Vind AB, the solar panels assumed for this project are solar PV cells. PV cells are deemed to be the most mature technology for this scope and are the market standard in Sweden.
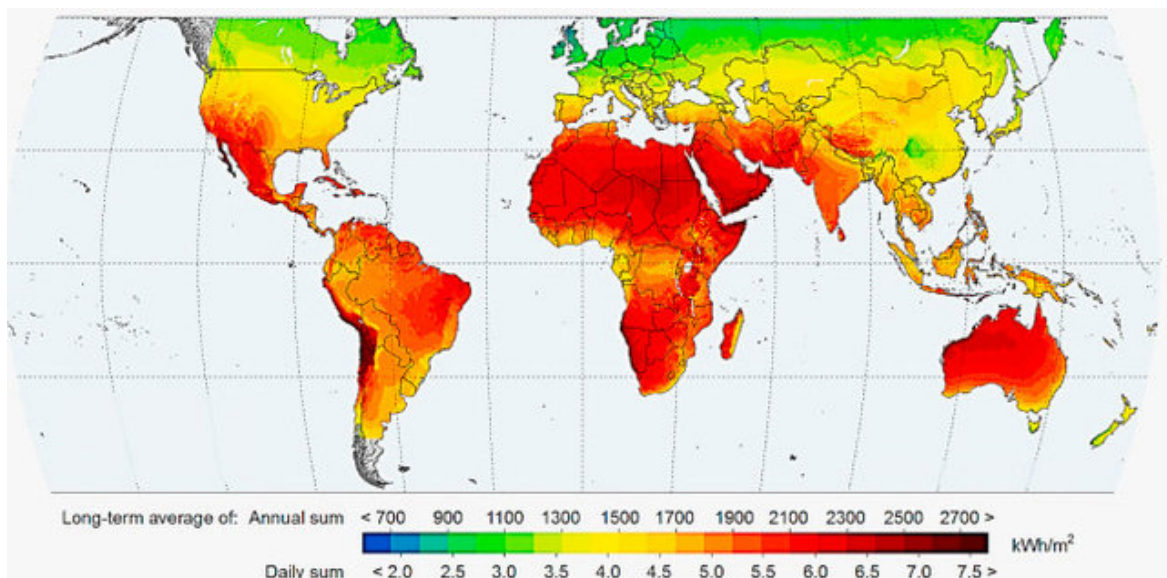


**Figure 2.10:** Map showing global solar energy [3].

## 2.3.2 Techno-economic characteristics of solar power

To show the solar power production variation during one year, a simulation was run for a generic SPP placed in Bäckhammar. The daily mean capacity factors for this SPP is generated for 2015 and can be seen in Figure 2.11 (Pfenninger and Staffell [56], Pfenninger and Staffell [54], Pfenninger and Staffell [55]).
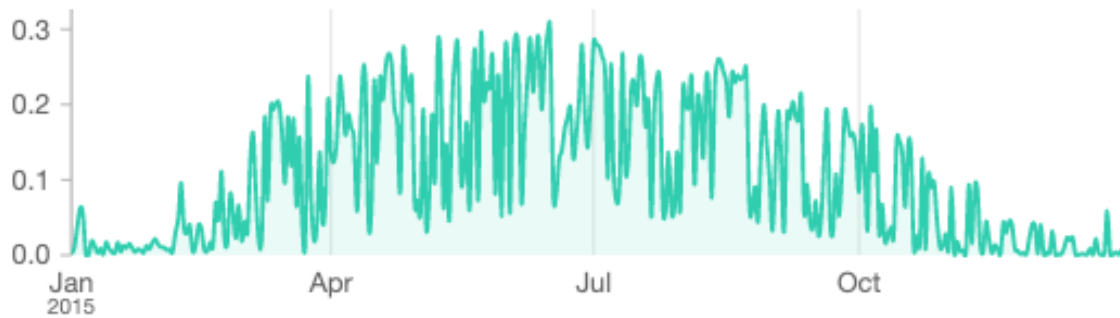


**Figure 2.11:** Mean daily capacity factors in 2015 for a SPP in Bäckhammar ([56], [54], [55]).

This simulation confirms the well-established pattern that solar production is much higher in the summer months compared to the winter months (Heide et al. [36]). The sun also follows another distinct pattern - the production increases during the day and is zero during the night.

The monthly average capacity factors for this simulation are shown in Figure 2.12. It can be observed that the capacity factors are much higher during the summer months. The total mean capacity factor is 10.7% for this year and location.
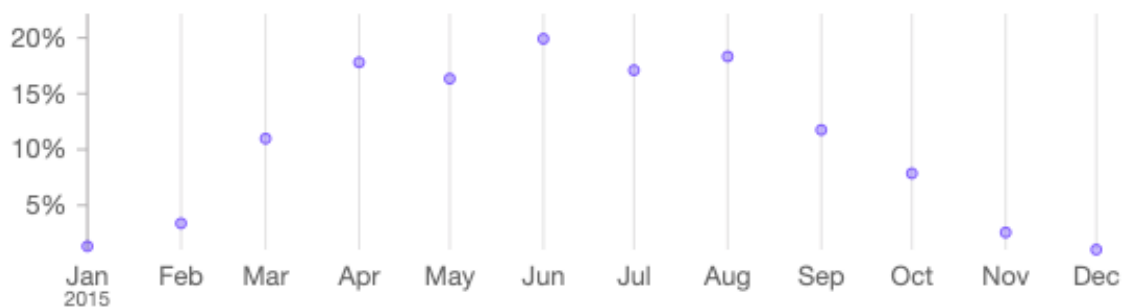


**Figure 2.12:** Monthly average capacity factors in 2015 for a SPP in Bäckhammar ([56], [54], [55]).

To get the maximum amount of full load hours, it is common practice to overdimension the peak power of an aggregated PV module compared to its inverters (Möser [51], Hazim et al. [35]). Oversizing the solar output by 30% compared to the inverter is one method. For example, if the wanted maximum power output of a SPP is 100 MW, its total direct current (DC) capacity will be 100 * 1.3 = 130 MW. The production will then be capped by setting the maximum inverter capacity to 100 MW.

There are advantages and disadvantages to different solar photovoltaic technologies. Some of these can be seen in Table 2.1 (Ud-Din Khan et al. [79]). In this case, mono-crystalline silicon PV cells are chosen for their high efficiency and long lifetime of 25 years.

**Table 2.1:** Comparison of photovoltaic cell types [79].

| PV type | Efficiency (%) | Advantages | Disadvantages |
|---|---|---|---|
| Mono-crystalline silicon | 15-20 | • Energetically efficient <br> • Space efficient | • Expensive <br> • Fragile panels <br> • Material waste during manufacturing |
| Poly-crystalline silicon | 13-16 | • Simple, cost-effective manufacturing <br> • Less manufacturing waste | • Space inefficient <br> • Lower heat tolerance <br> • Energy-intensive manufacturing |
| Flexible amorphous thin film | 9-12 | • Simple mass production <br> • Cost-efficient <br> • Enables flexible configurations <br> • High shading tolerance | • Space inefficient <br> • High degradation rate |
| Copper indium gallium selenide thin film | 10-12 | • Simple mass production <br> • Good heat resistance <br> • Requires fewer toxic materials (cadmium) | • High fabrication cost |

It is worth noting that mono-crystalline silicone PV cells are estimated by some to have a higher efficiency than the one presented in Table 2.1, namely up to 24% (Ameur et al. [4]).

In 2021, LCOE for new utility-scale SPP's in Sweden ranged from 290 to 520 SEK/MWh (Elmqvist et al. [11]). In 2018, this same number for the EU was estimated between 43 and 168 EUR/MWh, with 75% of these results being below 112 EUR/MWh (Trinomics for the European Commission [78]). This amounts to about 1140 SEK/MWh according to the 2021 annual average exchange rate (European Central Bank [22]).

## 2.4 Combined wind and solar power production

There are many potential benefits to combining wind and solar resources, including sharing of project costs, improved power generation, and more efficient land use (Agrawal et al. [2]).

The blend of wind and solar power generation can share project costs through the use of common resources. Instead of developing separate infrastructure for wind and solar projects, much of this can be shared - for example the grid infrastructure, including the substation equipment and transmission lines, as well as support infrastructure.

Also, the intermittent nature of wind and solar power can be mitigated to some extent through their combination. Wind speeds are generally higher at night and in the early morning, while solar production peaks during the day. By combining these two resources, the power generation can be more consistent throughout the day, ultimately improving the efficiency of the system. It is also evident from Figure 2.8 and 2.11 that the wind and solar power can complement each other's seasonal variations to some extent, since wind power production is higher in fall and winter, while solar power production is higher during summer.

Finally, because the placement of wind turbines is optimised to avoid wake losses, there is a lot of excess land between each turbine. This land could be used for solar panel installation, thus reducing the additional cost of land.

## 2.5 Hydrogen energy storage

As the energy demand in the world increases and the transition to more climate neutral energy is accelerating, the hydrogen market is growing (IRENA [41]). As a fuel that can be produced to be void of harmful emissions, with only water as its byproduct, it has great potential to be useful in the path to a sustainable future.

It is a very energy dense fuel by mass, as seen in Figure 2.13, having almost three times the energy content of gasoline (120 MJ/kg vs 44 MJ/kg) (U.S Department of Energy [82]). However, on a volume basis, gasoline has a density of 32 MJ/L while liquid hydrogen has a density of 8 MJ/L. Independent of outdoor temperature, a fuel cell electric vehicle (FCEV) can drive about 600 km on a full tank (Vätgas Sverige [89]). The range is determined by both the efficiency of the fuel cell as well as the amount of hydrogen that can be contained in the vehicle. Today, the cost to fuel a passenger FCEV is about 9 SEK/10 km in Sweden, which is slightly less than the cost for fueling a passenger car with diesel or gasoline.
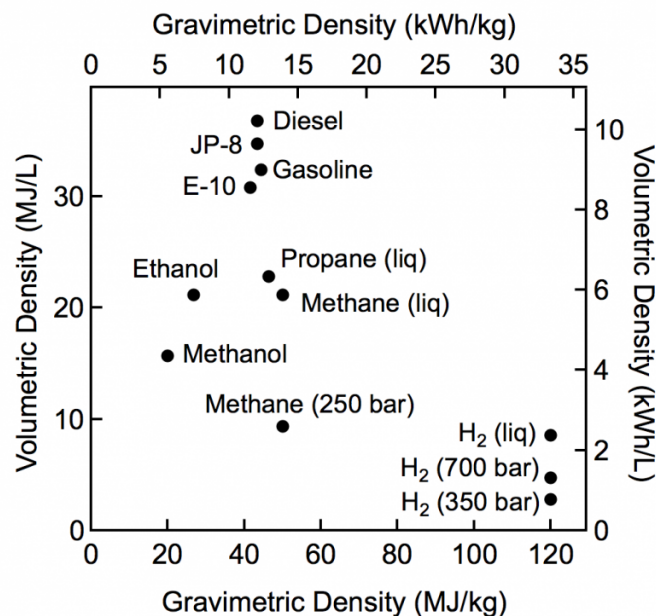


**Figure 2.13:** Comparison of volumetric density (MJ/L or kWh/L) and gravimetric density (kWh/kg or MJ/kg) for different fuels based on lower heating values [82].

While there are a number of ways to produce hydrogen, and several that are fossil fuel free, about 95% of all hydrogen produced today is produced through fossil fuels (U.S Department of Energy [80]). In order to understand hydrogen as a means of energy storage better, its generation, storage methods, and conversion to useful energy will be summarised in the following sections.

## 2.5.1 Hydrogen production through electrolysis

One way to produce clean renewable hydrogen is through water electrolysis using renewable electricity. Water electrolysis works by splitting water to produce hydrogen gas and oxygen using electricity. Electrolysers consist of an anode and cathode separated by an electrolyte.

However, different electrolyser technologies work in slightly different ways (U.S Department of Energy [81]).

The configuration of alkaline electrolysers (AEL) are shown in Figure 2.14a. They work by transporting hydroxide ions from their cathode to their anode through the electrolyte, while generating hydrogen on the cathode side. The electrolytes that have been commercially available up to this point are a liquid alkaline solution of sodium or potassium hydroxide, but there are also new approaches being researched.

Polymer electrolyte membrane electrolysers (PEMEL), their configuration shown in Figure 2.14b, have an electrolyte consisting of a solid specialty plastic material. In this process, water reacts at the anode to form oxygen and positively charged ions (protons). This causes electrons to flow through an external circuit while the hydrogen ions move across the membrane to the cathode. Once at the cathode, they combine with electrons from the external circuit to form hydrogen gas.

Finally, the solide oxide electrolyser (SOEL), uses a solid ceramic material as its electrolyte. The configuration of the SOEL is shown in Figure 2.14c. This electrolyte conducts negatively charged oxygen ions at higher temperatures to generate hydrogen. This process differs slightly from AEL and PEMEL technologies - steam at the cathode combines with electrons from the external circuit to generate hydrogen gas and negatively charged oxygen ions. Then, these negatively charged ions pass through the electrolyte and react to form oxygen gas and generate electrons to power the external circuit. In order for the electrolyte to function, this must be done at high temperatures (700 - 800°C) compared to AELs and PEMELs (which both function below 100°C).
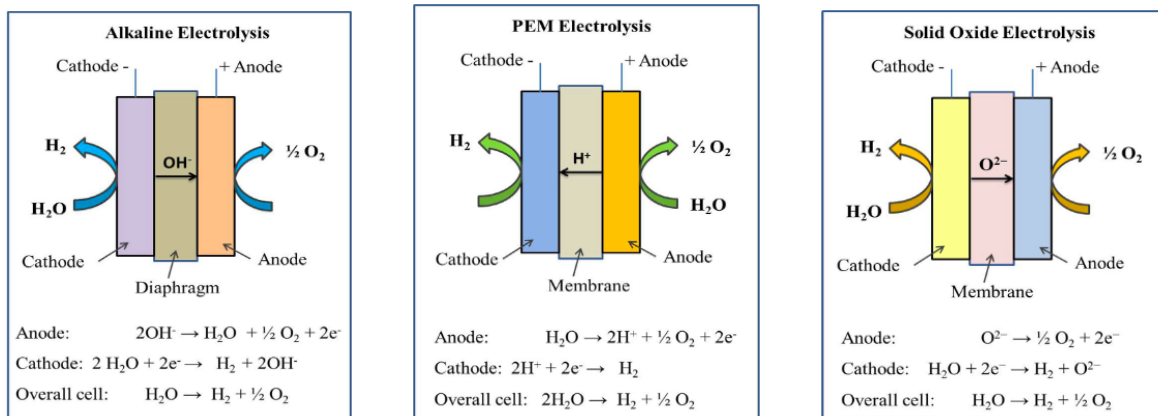


**(a)** AEL configuration.  **(b)** PEMEL configuration.  **(c)** SOEL configuration.

**Figure 2.14:** Schematic configuration of alkaline, polymer electrolyte, and solide oxide electrolyser technologies [61].

The electrolytic process is not only fossil free with the right electricity source, but it also generates a purer hydrogen compared to steam reformation of natural gas (Shiva Kumar and Himabindu [61]). There are currently four types of electrolysers used to produce hydrogen, the three mentioned previously and anion exchange membrane electrolysers (AEMEL). As can be seen in Figure 2.15, AEMEL is the least mature out of the technologies, and will not be further reviewed in this thesis. AEL and PEMEL are both commercially available at scale today while AEMEL and SOEL are still on the prototype or large scale demonstration level (IEA [40]).

There are a number of hydrogen production projects using water and steam electrolysis already (Clean Hydrogen Europe [7]). These projects use AEL, PEMEL and SOEL technologies and are already scaled up to a few MWs. Other projects between 20 and 100 MW are under development with hydrogen costs of 5-8 €/kg.
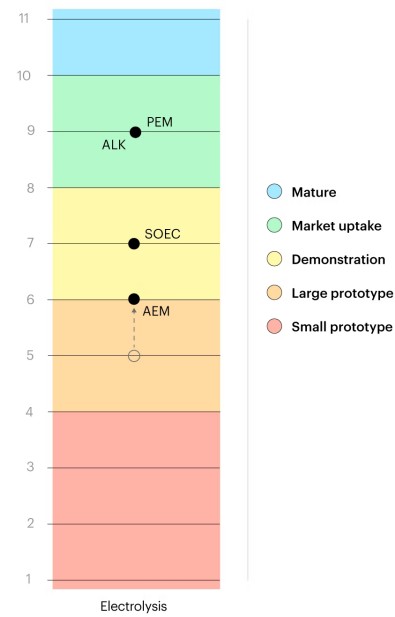


**Figure 2.15:** Technology readiness levels of electrolyser technologies [40].

## 2.5.2 Transportation of hydrogen

The method of storing hydrogen is significantly influenced by the form in which the hydrogen will later be transported or converted back to power. The transportation cost of hydrogen is mainly a function of two parameters: volume transported and distance (IRENA [42]). The three ways of transporting hydrogen are via truck, pipeline and ship. When transporting short distances and small volumes, the truck can be the most cost effective alternative. As the volume and distance increase, the density of the hydrogen needs to be increased making liquid hydrogen trucks the more appropriate option. With even greater volumes or distances, transmission pipelines are a better alternative. For very long distances or for hydrogen transportation across water, ships are the most viable option. In Figure 2.16, the different transportation alternatives and their respective appropriate distances and volumes are presented as well as the cost per kg of hydrogen transported.
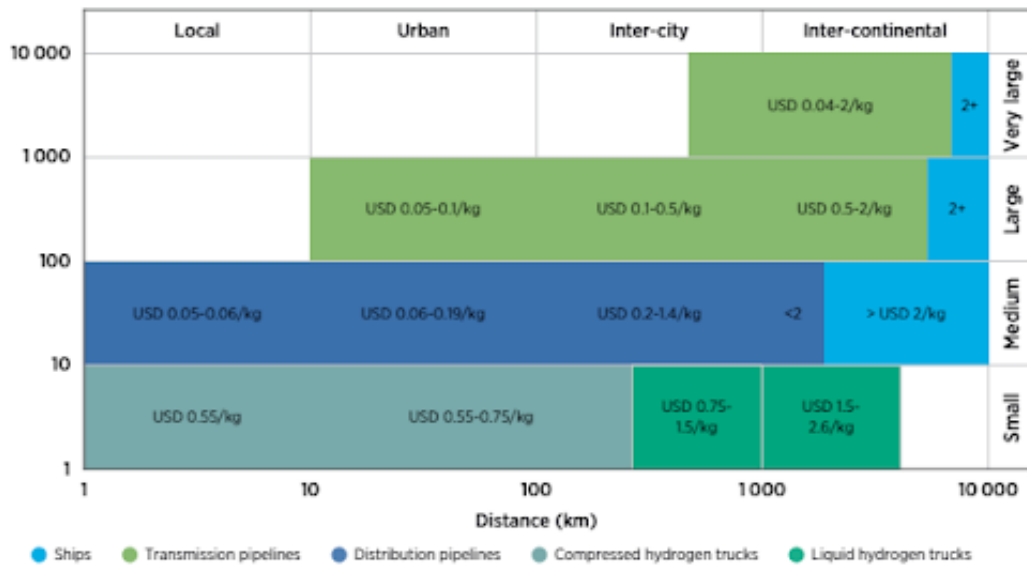
**Figure 2.16:** Hydrogen transport costs and options based on distance and volume [42].

For a small and local hydrogen producer on land, the best alternatives are most likely compressed hydrogen trucks or compressed hydrogen through a distribution pipeline. Pipelines are the most cost-effective at distances up to 1000 km with at least 0.3 - 0.4 million tonnes of hydrogen transported per year. With less volume and distance compressed hydrogen trucks become more attractive. Even more so when the delivery of hydrogen might become intermediate as it's acting as energy storage for a power producing facility.

### 2.5.3 Energy storage using hydrogen

In order for hydrogen to be of help during the global energy transition, large-scale hydrogen distribution is needed (Abdin et al. [1]). Stationary storage is a necessary part of this to act as a buffer between production facilities and demand fluctuations, and for renewable-based hydrogen generation systems. Large-scale hydrogen storage does present with some challenges in terms of safety, economics and efficiency.

Studies have shown that compressed hydrogen gas storage dominates in stationary hydrogen storage systems. A study by Gahleitner analysed 48 hybrid stationary hydrogen production plants built between 1990 and 2012. 88% of these stored hydrogen via compressed gaseous storage, while only 12% used metal hydride storage. Similarly, Abdin analysed 19 renewable hybrid stationary hydrogen production plants built between 1989 and 2017, and 74% of these used compressed gaseous storage, while 26% used metal hydride storage. Compressed gaseous storage being so dominant is likely due to its maturity as a technology and its commercial availability compared to some other storage methods.

Salt caverns have been used for underground compressed hydrogen storage, and are promising candidates for large-scale hydrogen storage. However, they are naturally geographically limited and come with more challenges. Therefore, this technology has not been tried in many countries. At this point, liquid hydrogen storage has not been a preferred technology for stationary storage at a large scale, even though cryogenic storage of liquid hydrogen is already well-established in the space industry. This is because of the energetically drain-

ing (ca. 10 kWh/kg) and financially draining (ca. 40-50% of system capital expenditure) liquefaction process it involves.

Another promising alternative to compressed gaseous storage is liquid organic hydrogen carriers (LOHCs) for stationary hydrogen storage. Several studies have been conducted on LOHCs, including techno-economic analyses. They concluded that LOHC-based pathways have potential especially for smaller-scale hydrogen demand.

Other alternatives for stationary hydrogen storage include ammonia and methanol. Ammonia has many different use cases, but most of it is used in fertilisers and other chemical and process industries. However, it could be used both as a hydrogen carrier and as a hydrogen-rich fuel or fuel additive in internal combustion engines. Similarly, methanol could be used as a hydrogen carrier. It also has many use cases, such as fuel and feedstock in various chemical processes.

All hydrogen storage technologies have some essential elements in common. A generic H2ESS is shown in Figure 2.17.
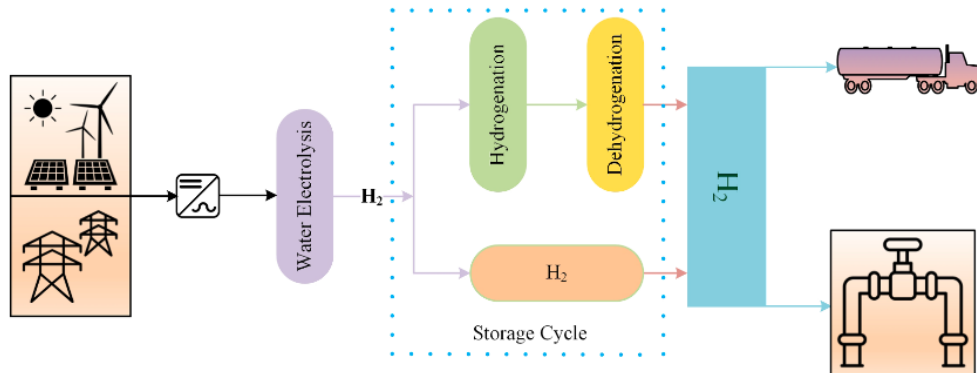


**Figure 2.17:** A generic hydrogen energy storage system [1].

## 2.5.4   Electricity generation with fuel cells

Fuel cells can be used to transform stored energy in the form of hydrogen to electricity. In comparison to other energy conversion technologies, such as internal combustion engines and turbines, a fuel cell operating alone generally boasts a higher efficiency of approximately 65% (Godula-Jopek and Friedrich Westenberger [32]). However, the process of creating hydrogen, storing it, and subsequently converting it back into electricity incurs losses from every component involved in the process. As a result, the overall round trip efficiency is exceptionally low (Kungl. Ingenjörsvetenskapsakademien (IVA) [45]). Figure 2.18 presents the efficiencies of different components involved, as well as the cumulative efficiency of the entire system, highlighting the substantial losses involved.
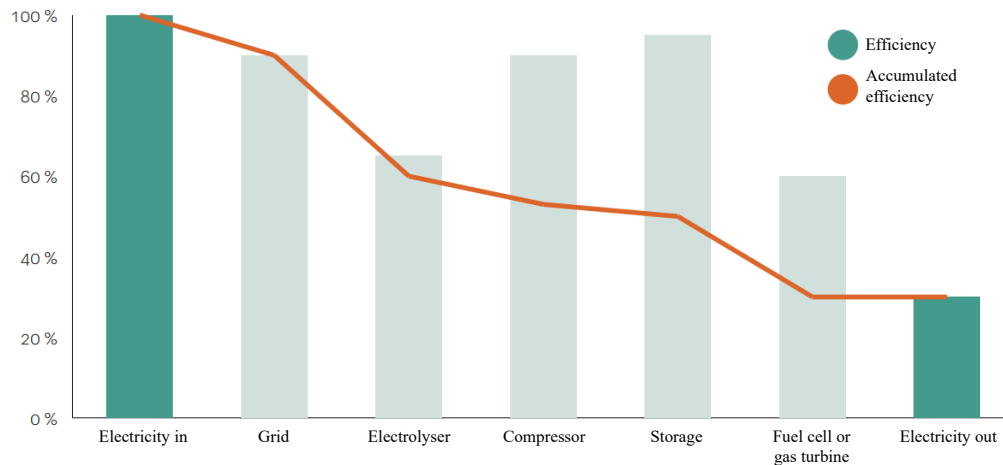
**Figure 2.18:** Efficiencies of system components and cumulative efficiency in a power-to-hydrogen-to-power system [45]. Translated from Swedish to English.

The different fuel cell technologies that exist today vary significantly in output power, required temperature, and efficiency, resulting in a varied range of applications and suitabilities for different industries and use cases. A comparison of the different fuel cell technologies can be seen in Figure 2.19

| Fuel Cell Type | Operating Temperature | Typical Stack Size | Electrical Efficiency (LHV) | Applications | Advantages | Challenges |
|---|---|---|---|---|---|---|
| Polymer Electrolyte Membrane (PEM) | <120°C | <1 kW - 100 kW | 60% direct H$_2$ 40% reformed fuel | • Backup power<br>• Portable power<br>• Distributed generation<br>• Transportation<br>• Specialty vehicles | • Solid electrolyte reduces corrosion & electrolyte management problems<br>• Low temperature<br>• Quick start-up and load following | • Expensive catalysts<br>• Sensitive to fuel impurities |
| Alkaline (AFC) | <100°C | 1 - 100 kW | 60% | • Military<br>• Space<br>• Backup power<br>• Transportation | • Wider range of stable materials allows lower cost components<br>• Low temperature<br>• Quick start-up | • Sensitive to CO$_2$ in fuel and air<br>• Electrolyte management (aqueous)<br>• Electrolyte conductivity (polymer) |
| Solid Oxide (SOF C) | 500 - 1000°C | 1 kW - 2 MW | 60% | • Auxiliary power<br>• Electric utility<br>• Distributed generation | • High efficiency<br>• Fuel flexibility<br>• Solid electrolyte<br>• Suitable for CHP<br>• Hybrid/gas turbine cycle | • High temperature corrosion and breakdown of cell components<br>• Long start-up time<br>• Limited number of shutdowns |

**Figure 2.19:** Comparison of fuel cell technologies [84].

### 2.5.5 Techno-economic characteristics of H2ESS

**Electrolysers**

All electrolysers consist of their stack (up to 100 cells) and their Balance of Plant (BOP), and can be configured in parallel using the same BOP infrastructure (IEA [39]). This makes them highly modular and flexible. However, this means that the effects of economies of scale are limited for electrolysers, meaning that electrolysers increase linearly in price with size.

As previously presented, there are four main types of electrolysers in use today. Some of their key performance indices (KPIs) as of 2020 will be presented in Figures 2.20, 2.21, and 2.22.

PEMELs and AELs are the most mature electrolysis methods (IEA [40]). PEMELs have the fastest ramp times (both hot idle and cold start) coupled with a fairly low degradation rate (Clean Hydrogen Europe [7]). PEMELs and SOELs have the best cost reduction potential in the future (IEA [39]). PEMELs are especially interesting since they have the highest current density and operational range, which can reduce capital costs and improve operational flexibility. Currently, cell lifetime is a limiting factor for both PEMEL and SOEL technologies.

| No | Parameter | Unit | SoA | Targets | |
| | | | 2020 | 2024 | 2030 |
| --- | --- | --- | --- | --- | --- |
| 1 | Electricity consumption @ nominal capacity | kWh/kg | 55 | 52 | 48 |
| 2 | Capital cost | €/(kg/d) | 2,100 | 1,550 | 1,000 |
| | | €/kW | 900 | 700 | 500 |
| 3 | O&M cost | €/(kg/d)/y | 41 | 30 | 21 |
| 4 | Hot idle ramp time | sec | 2 | 1 | 1 |
| 5 | Cold start ramp time | sec | 30 | 10 | 10 |
| 6 | Degradation | %/1,000h | 0.19 | 0.15 | 0.12 |
| 7 | Current density | A/cm$^2$ | 2.2 | 2.4 | 3 |
| 8 | Use of critical raw materials as catalysts | mg/W | 2.5 | 1.25 | 0.25 |

**Figure 2.20:** KPIs for polymer electrolyte membrane electrolysers [7].

| No | Parameter | Unit | SoA | Targets | |
| | | | 2020 | 2024 | 2030 |
| --- | --- | --- | --- | --- | --- |
| 1 | Electricity consumption @ nominal capacity | kWh/kg | 50 | 49 | 48 |
| 2 | Capital cost | €/(kg/d) | 1,250 | 1,000 | 800 |
| | | €/kW | 600 | 480 | 400 |
| 3 | O&M cost | €/(kg/d)/y | 50 | 43 | 35 |
| 4 | Hot idle ramp time | sec | 60 | 30 | 10 |
| 5 | Cold start ramp time | sec | 3,600 | 900 | 300 |
| 6 | Degradation | %/1,000h | 0.12 | 0.11 | 0.1 |
| 7 | Current density | A/cm$^2$ | 0.6 | 0.7 | 1.0 |
| 8 | Use of critical raw materials as catalysts | mg/W | 0.6 | 0.3 | 0.0 |

**Figure 2.21:** KPIs for alkaline electrolysers [7].

| No | Parameter | Unit | SoA | Targets | |
|---|---|---|---|---|---|
| | | | 2020 | 2024 | 2030 |
| 1 | Electricity consumption @ nominal capacity | kWh/kg | 40 | 39 | 37 |
| | Heat demand @ nominal capacity | | 9.9 | 9 | 8 |
| 2 | Capital cost | €/(kg/d) | 3,550 | 2,000 | 800 |
| | | €/kW | 2,130 | 1,250 | 520 |
| 3 | O&M cost | €/(kg/d)/y | 410 | 130 | 45 |
| 4 | Hot idle ramp time | sec | 600 | 300 | 180 |
| 5 | Cold start ramp time | h | 12 | 8 | 4 |
| 6 | Degradation @ $U_{TN}$ | %/1,000h | 1.9 | 1 | 0.5 |
| 7 | Current density | A/cm$^2$ | 0.6 | 0.85 | 1.5 |
| 8 | Roundtrip electrical efficiency | % | 46 | 50 | 57 |
| 9 | Reversible capacity | % | 25 | 30 | 40 |

**Figure 2.22:** KPIs for solide oxide electrolysers [7].

**Fuel cells**

80% of fuel cells in 2015 were used for stationary applications (incl. co-generation, back-up and remote power systems) (IEA [39]). Although they show potential for hydrogen conversion, they are still limited by high investment costs and limited lifetimes. Investment costs depend on manufacturing costs and, unlike electrolysers, could be benefitted by effect of economies of scale. Polymer electrolyte membrane fuel cells (PEMFCs) for FCEVs have the greatest cost reduction potential, while investment costs for stationary applications are expected to reduce their costs more slowly, as the focus for stationary applications is to increase efficiencies and lifetimes.

Figures 2.23 and 2.24 compare PEMFCs and solid oxide fuel cells (SOFCs) (Clean Hydrogen Europe [7]). PEMFCs have a lower capital expenditure (CAPEX), higher electrical efficiency, and lower availability than SOFCs. Also, PEMFCs have a lower degradation rate than SOFCs while maintaining a significantly lower stack production cost.

| No | Parameter | | Unit | SoA | Targets | |
|---|---|---|---|---|---|---|
| | | | | 2020 | 2024 | 2030 |
| System | | | | | | |
| 1 | CAPEX | <5 kWe<br>5-50 kWe<br>51-500 kWe | €/kW | 6,000<br>2,500<br>1,900 | 5,000<br>1,800<br>1,200 | 4,000<br>1,200<br>900 |
| 2 | O&M cost | <5 kWe<br>5-50 kWe<br>51-500 kWe | €ct/kWh | 10<br>10<br>5 | 8<br>7<br>3 | 4<br>3<br>2 |
| 3 | Electrical Efficiency $\eta_{el}$ | <5 kWe<br>5-50 kWe<br>51-500 kWe | % LHV | 50<br>45<br>50 | 50<br>50<br>52 | 56<br>56<br>58 |
| 4 | Availability | <5 kWe<br>5-50 kWe<br>51-500 kWe | % | 97<br>97<br>98 | 97<br>97<br>98 | 98<br>98<br>98 |
| 5 | Warm start time | | sec | 60 | 15 | 10 |
| Stack | | | | | | |
| 6 | Degradation @ CI | | %/1,000h | 0.4 | 0.2 | 0.2 |
| 7 | Stack Production cost | | €/kWe | 400 | 240 | 150 |
| 8 | Non-recoverable CRM as catalyst | | mg/$W_{el}$ | 0.1 | 0.07 | 0.01 |

**Figure 2.23:** KPIs for polymer electrolyte fuel cells [7].

| No | Parameter | | Unit | SoA | Targets | |
|---|---|---|---|---|---|---|
| | | | | 2020 | 2024 | 2030 |
| System | | | | | | |
| 1 | CAPEX | <5 kWe<br>5-50 kWe<br>51-500 kWe | €/kW | 10,000<br>10,000<br>10,000 | 6,000<br>5,000<br>5,000 | 3,500<br>2,500<br>2,000 |
| 2 | O&M cost | <5 kWe<br>5-50 kWe<br>51-500 kWe | €ct/kWh | 10<br>12<br>10 | 8<br>7<br>5 | 2,5<br>2.0<br>1,5 |
| 3.1 | Electrical Efficiency $\eta_{el}$ | <5 kWe<br>5-50 kWe<br>51-500 kWe | % LHV $CH_4$ | 35-55 (90)<br>55 (85)<br>55 (85) | 55 (90)<br>58 (85)<br>60 (85) | 55 (90)<br>62 (85)<br>65 (85) |
| 3.2 | Electrical Efficiency $\eta_{el}$ | <5 kWe<br>5-50 kWe<br>51-500 kWe | % LHV $H_2$ | 47 (85) | 52 (90) | 57 (95) |
| 4 | Availability | 5-50 kWe | % | 99<br>98<br>98 | 99<br>99<br>99 | 99<br>99<br>99 |
| 5 | Warm start time | | min | 15 | 10 | 2 |
| Stack | | | | | | |
| 6 | Degradation @ CI & FU=75% | | %/1,000h | 0.6 | 0.4 | 0.2 |
| 7 | Stack production cost | | €/kWe | 4,000 | 2,000 | ≤800 |
| Technology Related | | | | | | |
| 8 | System roundtrip electrical efficiency in reversible operation | | % | 32 | 38 | 50 |

**Figure 2.24:** KPIs for solide oxide fuel cells [7].

In the IEA's Technology Roadmap for Hydrogen and fuel cells, parameters of a few key electrolyser and fuel cell technologies are given for 2015 and predicted for 2030 (IEA [39]). These can be seen in Figure 2.25. Among others, predictions for lifetimes were given. The lifetime for PEMEL's and PEMFC's are comparable at 75 000 and 80 000 hours, respect-

ively. However, the lifetime for AEL's are quite a bit higher, at 95 000 hours, while alkaline fuel cells have lifetimes of just 20 000 hours.

| | | | Hydrogen generation and conversion | | | | | | | |
|---|---|---|---|---|---|---|---|---|---|---|
| | | Unit | Alkaline electrolyser | PEM electrolyser | NG SMR | NG SMR with CCS | Coal CCS | Biomass gasification | Alkaline FC | PEM FC |
| Today | Efficiency | - | 74% | 73% | 77% | 70% | 56% | 50% | 50% | 43% |
| | Life time | hours or years | 75 000 | 40 000 | 30 | 30 | 30 | 30 | 7 000 | 60 000 |
| | Investment cost conversion | USD/kW | 1 150 | 2 600 | 550 | 1 370 | 1 670 | 4 930 | 700 | 3 200 |
| | Investment cost storage | USD/kWh | - | - | - | - | - | - | - | - |
| | Fixed O&M | - | 5% | 5% | 3% | 5% | 5% | 5% | 5% | 5% |
| 2030 | Efficiency | - | 75% | 82% | 82% | 73% | 57% | 50% | 50% | 54% |
| | Life time | hours or years | 95 000 | 75 000 | 30 | 30 | 30 | 30 | 20 000 | 80 000 |
| | Investment cost conversion | USD/kWh | 870 | 800 | 440 | 700 | 1 280 | 1 320 | 450 | 830 |
| | Investment cost storage | USD/kWh | - | - | - | - | - | - | - | - |
| | Fixed O&M | - | 5% | 5% | 3% | 5% | 5% | 5% | 5% | 5% |

**Figure 2.25:** Parameters of key electrolyser and fuel cell technologies in 2015 and 2030 [39].

**Hydrogen storage**

The choice of hydrogen storage technology depends on several parameters including efficiency, CAPEX, operational expenditure (OPEX), and levelised cost of hydrogen storage (LCHS).

The charts presented in Figure 2.26 present the efficiency and CAPEX for a 5000 tonne hydrogen storage system, the OPEX to store 4000 tonnes of hydrogen at different cycle times, LCHS to store 4000 tonnes of hydrogen for a daily and 4-monthly storage cycle

length, as well as change of LHCS over time (Abdin et al. [1]). 5000 tonnes of installed capacity corresponds to about 167 GWh at lower heating value. Note that the storage cycle is considered to be 4000 tonnes for safety and maintenance reasons, but that it still corresponds to the storage system with a 5000 tonne installed capacity.
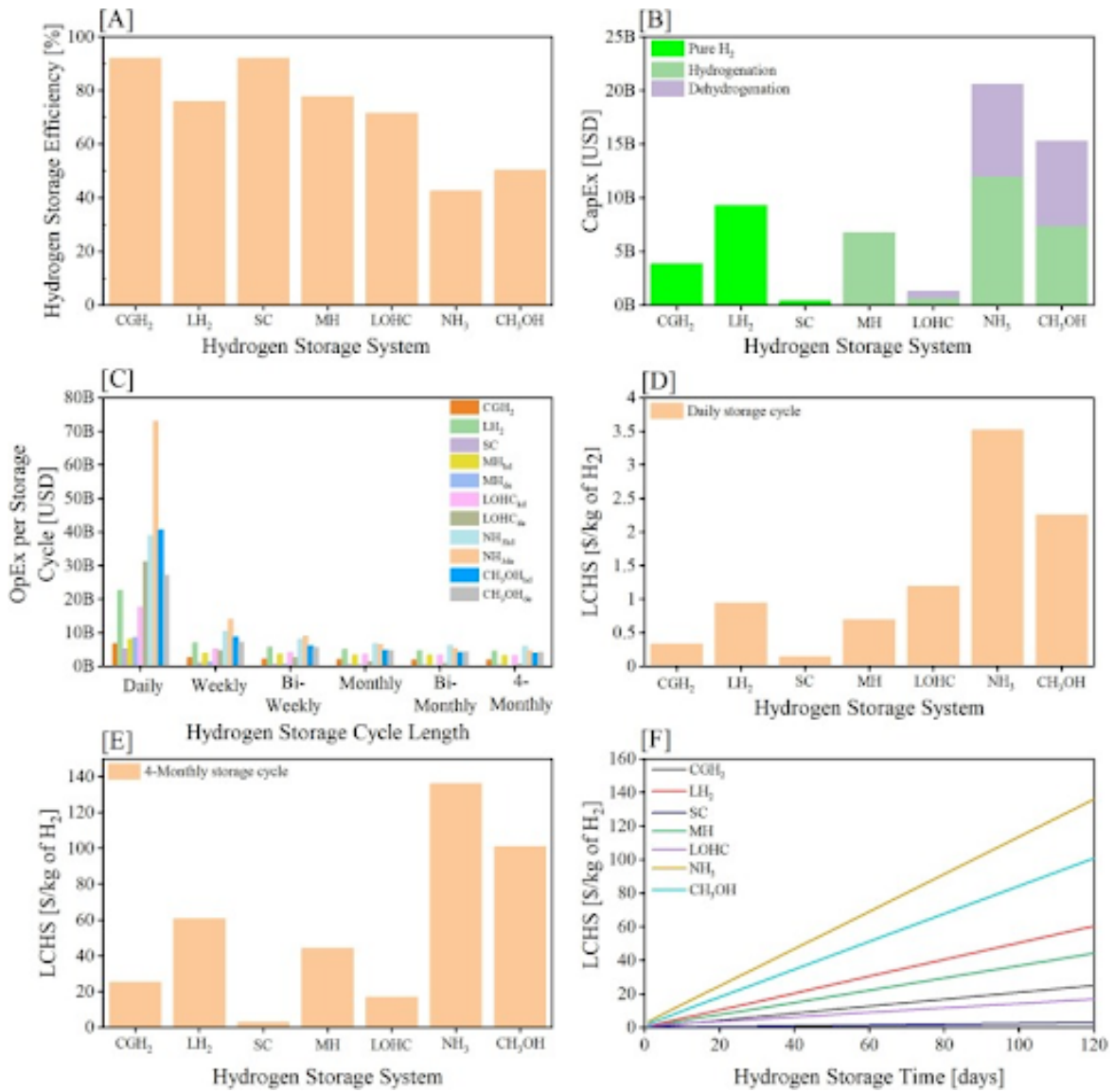


**Figure 2.26:** Techno-economic characteristics of different hydrogen storage technologies [1].

Note that:

- $CGH2$ refers to compressed gaseous hydrogen

- $LH2$ refers to liquid hydrogen

- $SC$ refers to salt cavern compressed gaseous hydrogen

- $MH$ refers to metal hydride

- $LOHC$ refers to liquid organic hydrogen carrier

- $NH3$ refers to ammonia

- $CH3OH$ refers to methanol

The conclusion of the paper by Abdin et al. is that above-ground compressed gaseous storage is one of the more economical options, with a low LCHS of around 0.33 USD/kg of $H_2$ for daily storage, but this number jumps to 25.20 USD/kg of $H_2$ for 4-month storage. Storage in salt caverns has the lowest LCHS at 0.14 USD/kg of $H_2$ for daily storage, while ammonia has the highest LCHS at about 3.51 USD/kg of $H_2$, followed by methanol at 2.25 USD/kg of $H_2$. Storage efficiency is highest for compressed gaseous storage, at 92%, followed by methanol at 50% and ammonia at 42%.

## 2.6 Battery energy storage

Battery technology has been deployed in all five power circles in Europe, being local, community, Distribution System Operator (DSO), TSO, and pan-European (European Commission [24]). The deployment of batteries is not necessarily linear, since it is heavily dependent on geopolitical circumstances - for example beneficial legal provisions, a weak electrical grid and climatic conditions that cause periods of excessive solar or wind power supply. However, BESS costs are still an obstacle for wide deployment.

Batteries can significantly contribute to VRES integration on both grid and utility-scale by allowing excess energy to be stored and by providing grid services. These include frequency and voltage control, peak shaving, congestion management, and black start services. They can also help with smooth integration of electric vehicles and provide ancillary services to the grid.

The generic layout of a BESS, including its additional functions, can be seen in Figure 2.27 (Hajeforosh et al. [33]). The electrical energy flows between the batteries and the grid through two power-electronic converters as well as a transformer. Each of these elements have built-in protective devices, and the power flow through them is controlled locally. This local control is based on local measurements and information given by the grid controller, which comes from other remote controllers and/or remote measurements.
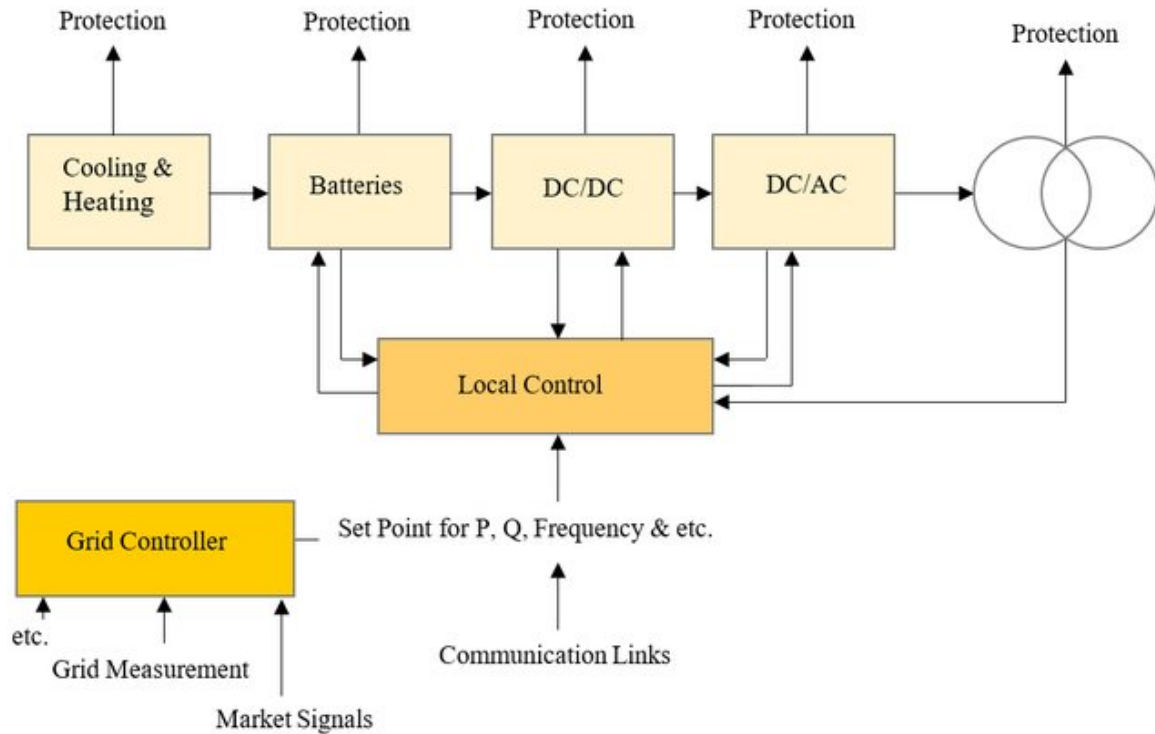
**Figure 2.27:** A generic battery energy storage system [33].

While there are many different types of batteries, the type chosen for this thesis is the lithium ion battery, for its long lifetime and low life cycle costs (Diouf and Pode [9]).

### 2.6.1 Lithium ion batteries

Use of lithium ion batteries for BESSs is the most common strategy, in part due to them being the only type of batteries used for electric vehicles. Lithium demand continues to rise due to both the expansion of electromobility and stationary applications. Lithium prices have been on the rise since 2020, reflecting the rapidly growing demand for electromobility (Gielen and Lyons [31]).

Lithium cells are electrochemical cells (Åkesson [92]). Inside them, there is a positive electrode and a negative electrode separated by an electrolyte. The electrons are transferred via an external circuit, from one electrode to the next, while ions are transferred through the electrolyte to keep the cell balanced. A secondary cell is a cell able to repeat the cycle in reverse, and is therefore chargeable. A battery pack consisting of secondary cells is a rechargeable battery pack.

Lithium ion batteries exist in different configurations, but typically have graphite as its negative electrode material. This is chosen because graphite has a low potential, making it highly reactive, and a good ability to add and remove large amounts of lithium ions. For the positive electrode, different materials are chosen for different properties, but some common ones are lithium cobalt oxide, lithium iron phosphate, and lithium manganese oxide. Depending on the chosen material, the cell voltage is 3 to 4 V. When multiple cells are series coupled, the voltage capacity can be increased, while parallel coupling increases the total

capacity of the battery. The desired battery pack can be created by connecting multiple cells and multiple battery packs.

## 2.6.2 Techno-economic characteristics of BESS

The base year costs for utility-scale BESS accounts for major components including the lithium ion battery pack, the inverter, and the BOS necessary to install the BESS (National Renewable Energy Laboratory (NREL) [52]). When the National Renewable Energy Laboratory (NREL) constructed detailed cost models, the base year costs for a 60 MW BESS were coupled with durations ranging from 2 to 10 hours in 2 hour intervals. These are shown in Figure 2.28. Figure 2.28a shows dependency on energy capacity ($/kWh) while Figure 2.28b shows dependency on power capacity ($/kW). The figures demonstrate that the CAPEX of the installation in terms of energy capacity decreases with increased energy capacity, while the costs in terms of power rating increases. This is an inverse behavior which can be seen for all energy storage technologies, and highlights the importance of differentiating between energy and power capacity.
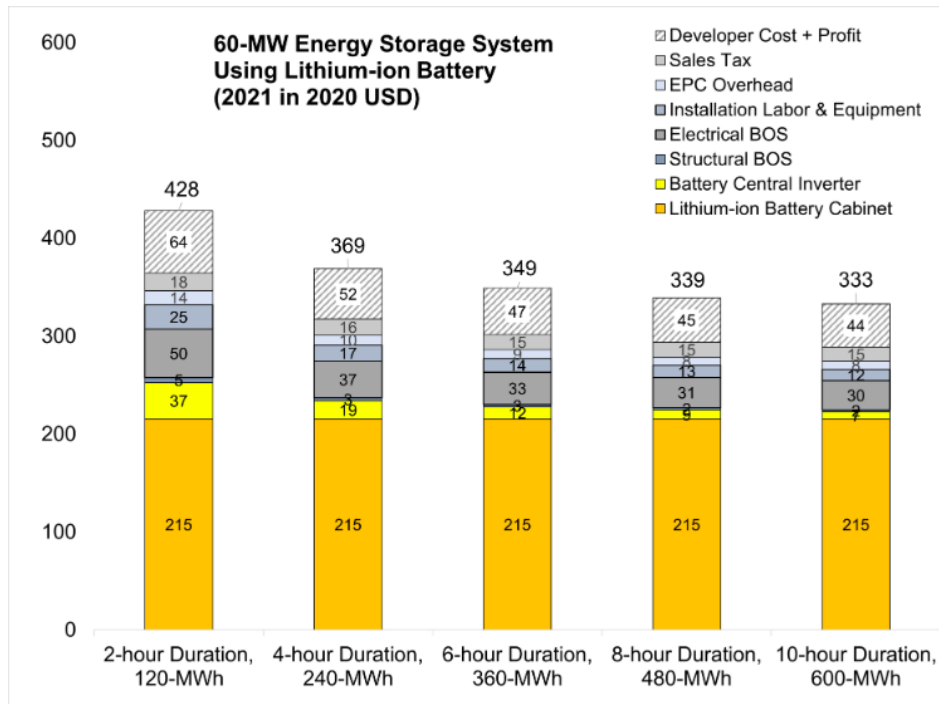
**(a)** Cost per energy capacity (USD/kWh).
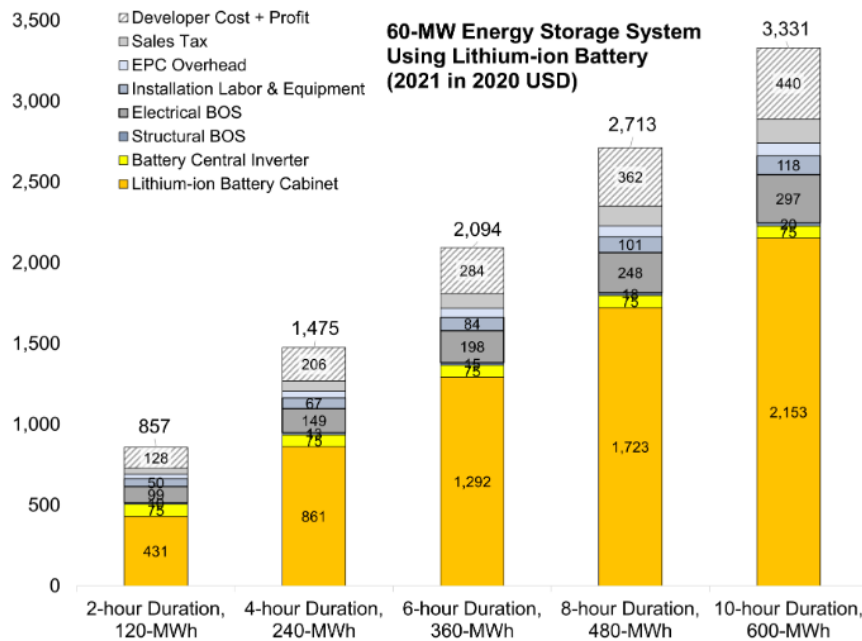


**(b)** Cost per power rating (USD/kW).

**Figure 2.28:** BESS CAPEX distribution for energy and power capacity [52].

To project BESS costs and performances for 2020 to 2050, NREL performed a literature review of 13 sources published between 2018 and 2019. Three projections are made, the conservative scenario, the moderate scenario, and the advanced scenario. These can be seen in Figure 2.29. The scenarios refer to the projected degree of technological innovation in the time period 2020 to 2050. The scenarios have several characteristics in common, though. For all scenarios, the costs for BESS are expected to decline, mainly due to cost decrease in the battery pack component. Some causes for this are the growth of the battery industry, changes in the lithium ion chemistry (such as finding alternatives to expensive metals), and

the amount of research being carried out on batteries. Also, there is an expected growth in the market (due to learning-by-doing) and diversification of chemistries that is expected to result in a change of dynamics in the supply chains of the batteries, ultimately resulting in cheaper inputs for the battery pack.
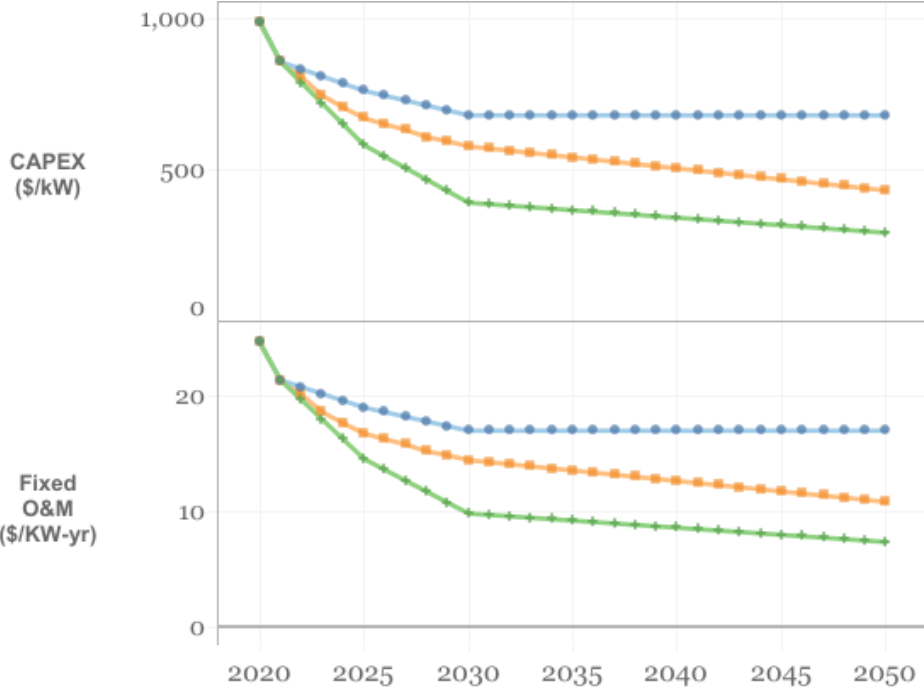


**Figure 2.29:** CAPEX ($/kW) and fixed operation and maintenance (O&M) ($/kW-yr) projections in a conservative, moderate, and advanced technological innovation scenario [52].

Please note that:

- The blue line is the conservative scenario

- The orange line is the moderate scenario

- The green line is the advanced scenario

- The cost recovery period is 30 years

- The battery referred to is a utility-scale battery for four hour storage

Some important terms for batteries are C-rate, lifetime, depth of discharge (DOD), and state of charge (SOC) (Åkesson [92]). C-rate signifies the current needed to discharge the battery's capacity in one hour. So, for example, a battery with a capacity of 4000 mAh is discharged by a current of 4000 mA, making this its C-rate. The lifetime of a battery is the number of cycles it can be charged and discharged. The DOD is how deep the battery has been discharged, where 0% means there has been no discharge (the battery is full) and 100% means that the battery is fully discharged (the battery is empty). It is related to lifetime, as a higher DOD decreases the lifetime of the battery. The SOC is inversely related to the DOD, as it signifies the current energy available in the battery (100% corresponding to a full battery and 0% to an empty battery). As aforementioned, a 0% SOC should be avoided as this decreases the lifetime. Lithium ion batteries have efficiencies of 85-95%, making them

one of the most efficient energy storage technologies (Environmental and Energy Study Institute [14]).

## 2.7   Combined energy storage

Each ESS comes with its unique set of advantages and disadvantages (Atawi et al. [5]). In the case of batteries and hydrogen storage, batteries have a major advantage in their fast response time while hydrogen has the advantage of being able to retain large amounts of energy.

One advantage to using a HESS is that it increases the power quality. The system's power quality is its ability to yield clean and stable power with a constant power output, while maintaining high availability and providing pure, noise-free sinusoidal voltages and currents within the acceptable limits. Using a quick-response ESS can improve this, but to mitigate drawbacks of different ESSs, using several is best.

Also, HESSs can improve intermittence. Compared to a single ESS, a HESS gives better smoothing since it can combine both high and low speed responses.

Furthermore, frequency regulation can be made more efficient by implementing a HESS. A high penetration of VRES can significantly lower the system inertia, which increases risk of system crashes and blackouts. By regulating frequency, these risks can be mitigated, which can lead to smoother VRES integration into the power grid.

Also, thermal and power disturbances caused by multiple pulse loads can be reduced by using a HESS. Pulse loads require very high instantaneous power but a low average power, which an ESS with high power density can help with. They can reduce frequency variance, voltage deviation, and more. However, in the case of several pulsed loads at once, use of more than one ESS is more efficient.

HESSs are also useful for peak load shaving, the act of shifting energy production from times of high demand to times of lower demands. In practice, this means that too much variable renewable energy generation can be stored and supplied later when demands are high. To do this, the ESS must be scalable and able to deliver energy for minutes to hours. Using just one ESS for this can cause problems with efficiency, reliability, stability, and cost. Optimal peak shaving can be realised with a HESS. The most common hybridisation tactic for peak shaving is combining fuel cells and batteries.

Finally, unbalanced loads can be avoided with the fast and accurate voltage regulation a well-constructed HESS can provide.

## 2.8 Economic incentives for energy storage

The ability to shift production in time can yield income, for example by taking part in energy arbitrage. Energy arbitrage is the concept of using price variations on the electricity market to earn money (Zhang et al. [91]). The idea is to buy energy from the grid at a low price and sell it back at a higher price.

The ability to shift production in time can also yield income by mitigating the cannibalisation effect (Prol et al. [58]). The cannibalisation effect is the concept that increased penetration of VRES can cause a decrease in electricity price, which undermines the value of the technology. A study from the journal Energy Economics analysed the California electricity market's day-ahead data between January 2013 and June 2017 and found that the cannibalisation effect was prominent for both wind and solar power. The effect was more evident at low consumption and high wind and solar penetration levels. By increasing the flexibility of the energy distribution, for example by using a ESS, this effect can be reduced. This is because the transfer of electricity loads between periods of low or high value can flatten the price distribution. As the cannibalisation effect increases, the value of energy storage thus increases.

Another economic incentive is that energy storage can decrease costs caused by curtailment (Denholm [8]). Curtailment both decreases environmental benefits of VRES, as well as increases costs. When energy is curtailed, the capacity factor is reduced, which results in less energy being sold to the grid. Since VRES often have no fuel costs, their levelised cost of energy (LCOE) is inversely proportional to the capacity factor, making it extra critical. Energy storage can reduce curtailment in two ways: by moving energy from periods of excessive production to periods of lower production, and by delivering grid flexibility. The grid flexibility can reduce the minimum generation constraints of baseload generators, which lessens the likelihood that curtailment occurs due to saturated transmission lines.

Furthermore, ESSs make it possible to operate on markets besides the electricity market, such as the ancillary service market and hydrogen market (Lindgren [47]). Lithium ion batteries are known for their rapid response time (milliseconds) and high efficiencies, making them excellent candidates for ancillary services, such as frequency reserves. By adapting the chemical makeup of the battery, its characteristics can be made optimal for the service being offered - characteristics that can be adapted include charge and discharge rate, number of cycles in one lifetime, operating voltage, and energy density.

As detailed in Section 2.1.4, the hydrogen market shows potential to increase moving forward, which is another incentive to use hydrogen gas as a means of energy storage. Hydrogen gas can both be used as an intermittent source when converting the energy back to electricity with a fuel cell, and it can be sold as a source of energy for industry (for example steel) and transportation. As technology continues to develop in the future, higher round-trip efficiencies for fuel cells as well as an increased market for hydrogen gas can be expected, increasing the economy of hydrogen production.

Other economic incentives for energy storage include contractual value increasing due to new market models and shifting customer values. One example of this is that the use of energy storage could enable more Baseload PPAs.

PPAs are long-term agreements between electricity generators and customers (corporate or utility) during which the customer purchases energy at a set pre-negotiated price from the producer (Stene Bakke and Maznic [66]). The use of PPAs for VRES makes revenues more predictable, reducing the risk for investors and lenders in renewable energy projects. There are fundamentally two types of PPAs: pay-as-produced PPAs and Baseload PPAs.

Pay-as-produced PPAs, which are the most common today, means that the project owner receives a fixed price per unit of energy produced, as the PPA covers only part of the generation volume (typically expressed in percentage or MW). The generation volume for each hour is split according to the agreement between the purchaser and residual revenues not covered by the PPA. This residual volume is sold on the spot market.

Baseload PPAs are growing in popularity as they reduce the risk of being impacted by the variability of VRES for the customer. This is done by expressing the purchasing volume as a fixed amount of power (MW) to be delivered every hour of the year. The surplus generation at high production hours is sold to the spot market, while volumes needed to complement generation at low production hours are purchased from the spot market by the electricity generator. What this can look like for a set time period can be seen in Figure 2.30.
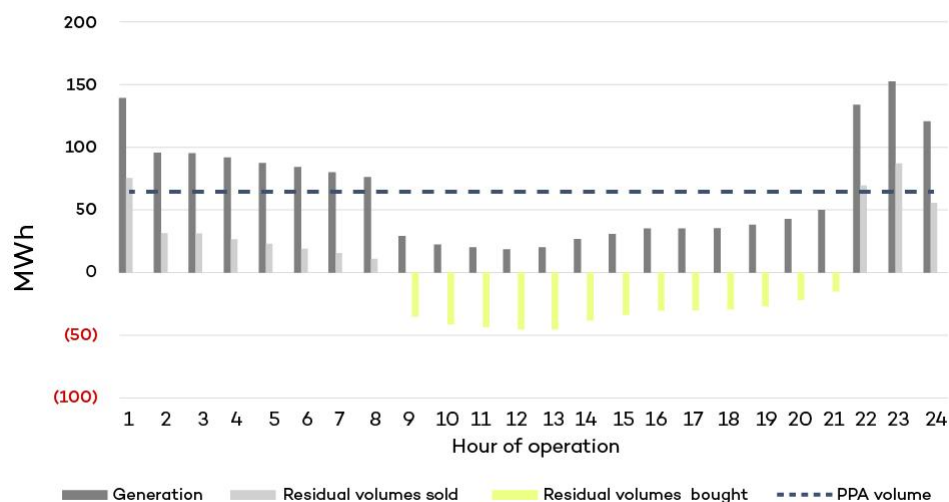


**Figure 2.30:** Illustration of the operation of baseload PPAs [66].

Economic incentives due to contractual value being added to reflect customer priorities are also present for energy storage technologies. Being able to guarantee renewables 100% of the time is a very good selling point, as demonstrated by the 24% increase of clean energy purchased by companies through PPAs from 2020 to 2021 (Henze [37]). This increased the clean energy acquired through PPAs from 25.1 GW to 31.1 GW. This strong growth can in part be attributed to interest from technology companies, who were responsible for about half of these deals. Alas, the PPA struck between Amazon and KGAL for the Bäckhammar wind power plant is not the first of its kind (Eolus Vind AB [15]). In 2021, contracts were announced by over 137 companies in 32 different countries, corresponding to 10% of all renewable capacity increase that year (Henze [37]). These numbers reflect an increased demand for both clean energies and PPAs from corporations.

By incorporating energy storage technologies in combination with VRESs, baseload PPAs should be able to be offered more broadly to customers. Since baseload PPAs offer a higher

degree of security compared to the more common pay-as-produced PPAs, while they also incorporate the selling point of 100% renewable energy at all times, it is reasonable to assume that these types of agreements should be very economically advantageous.

There are also economic incentives for energy storage based on political actions. The EU has adopted strategies for increasing the flexibility in the grid in order to enable more VRES in the system (European Commission [28]). Several principles were decided in order to enable this in the Clean Energy for all Europeans package adopted in 2019. For financing of energy storage, the EU suggests increasing the predictability and long-term visibility of revenue to make financing easier, for example by compensating storage operators for certain services that they may already be providing. It is also suggested that EU countries should consider economic instruments within individual state aid rules that could stimulate increased investments, such as competitive bidding procedures.

In March 2023, the Staff Working Document was released, which cohesively covers the role and application of energy storage in the EU transition (European Commission [27]). Among other things, the document covers both public financing and support by the EU. The financing tools offered come both from the EU's long-term budget and from the NextGenerationEU package. Amongst others, both hydrogen and batteries are covered by the research and innovation programme Horizon Europe, which offers substantial funding support. Energy storage can also be funded under the InvestEU programme, supporting market-based and demand-driven projects.

Furthermore, using energy storages could reduce the costs attributed to balancing by the TSO, in this case Svenska kraftnät (Svenska Kraftnät [71]). The balance responsible party (BRP) is charged with an imbalance fee by the Svenska kraftnät, the level for 2023 being 1.15 EUR/MWh, which is subsequently reflected in a fee given by the BRP to the power producer. The purpose of the imbalance fee is to cover the costs which imbalance causes.

## 2.9   Energy storage operational strategy

With the shift towards more sustainable energy, the demand for ESSs has increased substantially (Mitali et al. [49]). Requirements for ESSs are expected to triple by 2030 compared to values today. Because of this, researchers are continuously developing strategies that are more efficient and reliable in order to deliver renewable power in a controller manner.

A set of requirements necessary to facilitate the system for this thesis have been set up, and are as follows:

1. To at all times protect components from operating outside their operating ranges. That is, to never completely empty or exceed the capacity of the battery or hydrogen storage and never to exceed power ratings of components (including the GCP).

2. To facilitate decision-making based on market data.

3. To minimise curtailment of the additional solar power production.

A study by Phan Van et al. outlines a state machine based strategy for renewable energy production which combines a H2ESS and a BESS (Phan Van et al. [57]). The strategy combines a state machine with a hysteresis band to integrate the VRES in a microgrid. The method considers the power difference between the VRES, current load demand, battery SOC, and hydrogen state of charge (SOH). Based on this, the strategy can control the power output of fuel cells, electrolysers, and batteries in the microgrid as well as the power import and export to the main power grid. The strategy was successful in balancing the microgrid supply and demand, extending the lifetime of the electrolyser and fuel cell components, and ensuring the appropriate SOC and SOH.

# 3 Simulation method

In this chapter, methods relating to the simulation will be presented. The first section provides the simulation inputs and initial dimensioning of components. The second section briefly describes the method for initial data analysis. Then, the third section introduces the system that is constructed as a basis for simulation, as well as the software used, the different system components, and their technical assumptions. After this, the fourth section presents the operational strategy which controls the system. The fifth and final section demonstrates the system implementation in the simulation software.

## 3.1 Simulation inputs

Sources used for different simulation data, their resolution, units, and years, can be seen in Table 3.1. Global irradiation data at one minute intervals for the Karlstad measuring location are generously provided by SMHI. The one minute irradiation data is transformed to 10 minute averages to match the 10 minute wind power data for the Bäckhammar WPP provided by Eolus Vind AB. Nord Pool provides access to market data to students. This provided the SE3 day-ahead price data used in this simulation.

**Table 3.1:** Simulation input data.

| Data | Resolution | Unit | Years | Source |
|---|---|---|---|---|
| Global irradiation in Karlstad | 1 minute average | W/m2 | 2021 | SMHI |
| Wind power | 10 minute average | MW | 2021 | Eolus |
| SE3 Day-ahead price | Hourly | SEK/MWh | 2021 | NordPool |

The power production profile at Bäckhammar WPP can be seen in Figure 3.1. The WPP production profile is in line with the literature presented in Section 2.2.2. More power is produced during the fall and winter months compared to the summer months.
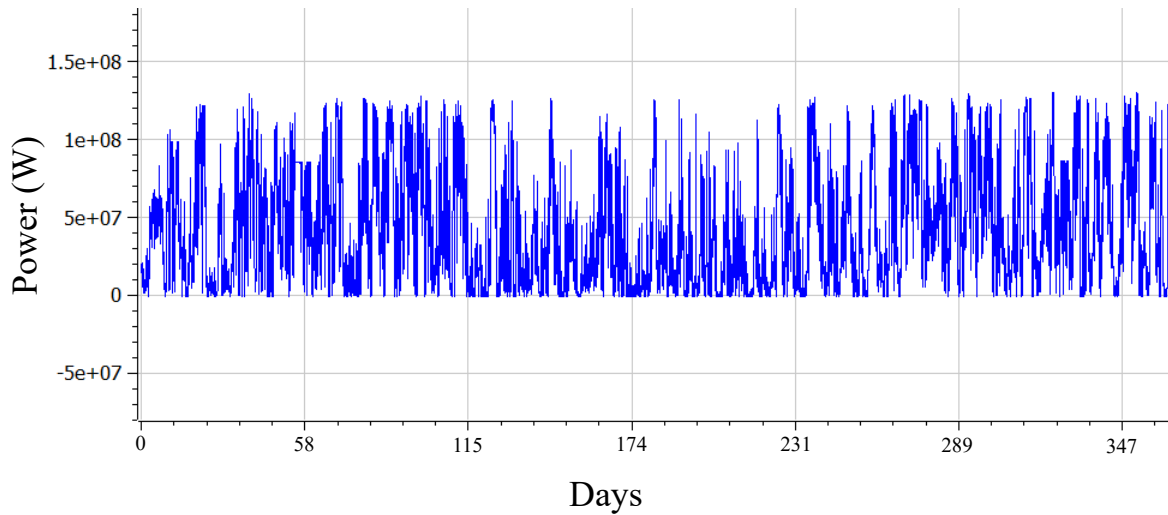
**Figure 3.1:** Annual production profile of the Bäckhammar WPP.

In Figure 3.2, the global irradiation profile from SMHI's measuring point in Karlstad can be seen. The solar irradiation profile is also in line with the literature presented in Section 2.3.2. The global irradiation is significantly higher during the solar months.
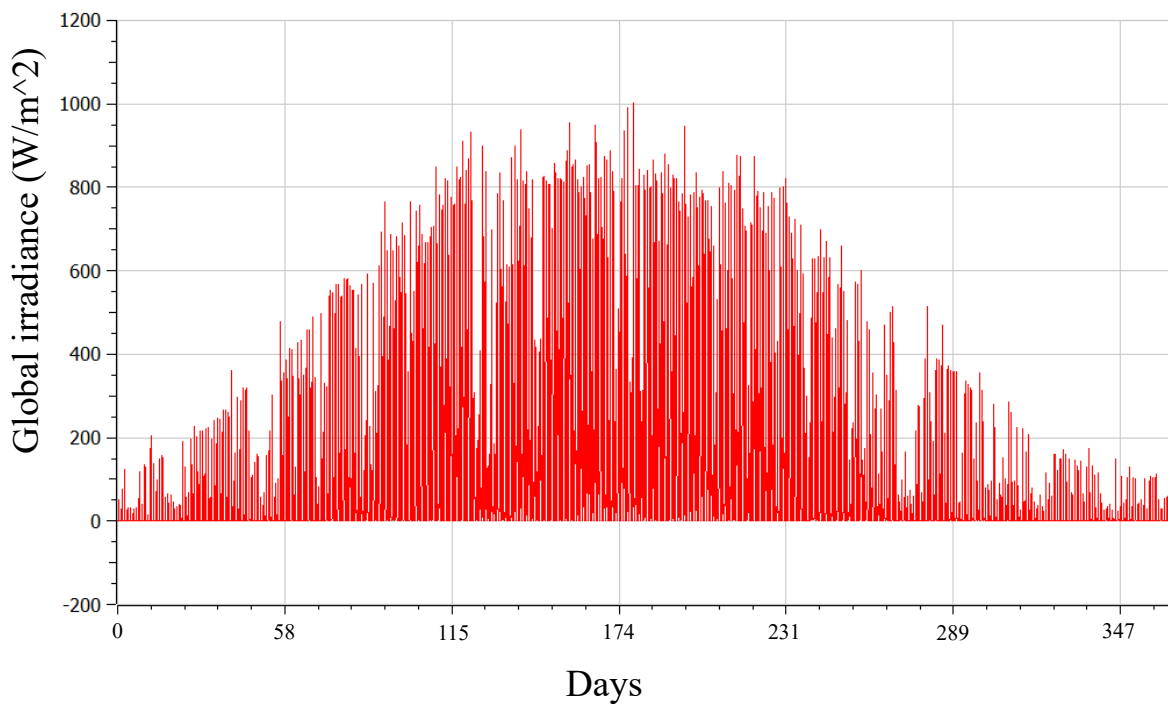


**Figure 3.2:** Annual global irradiation profile from the SMHI measuring point in Karlstad.

Figure 3.3 shows the price fluctuations for the day-ahead data in SE3 during 2021. The prices at the end of the year were significantly higher than at the beginning of the year.
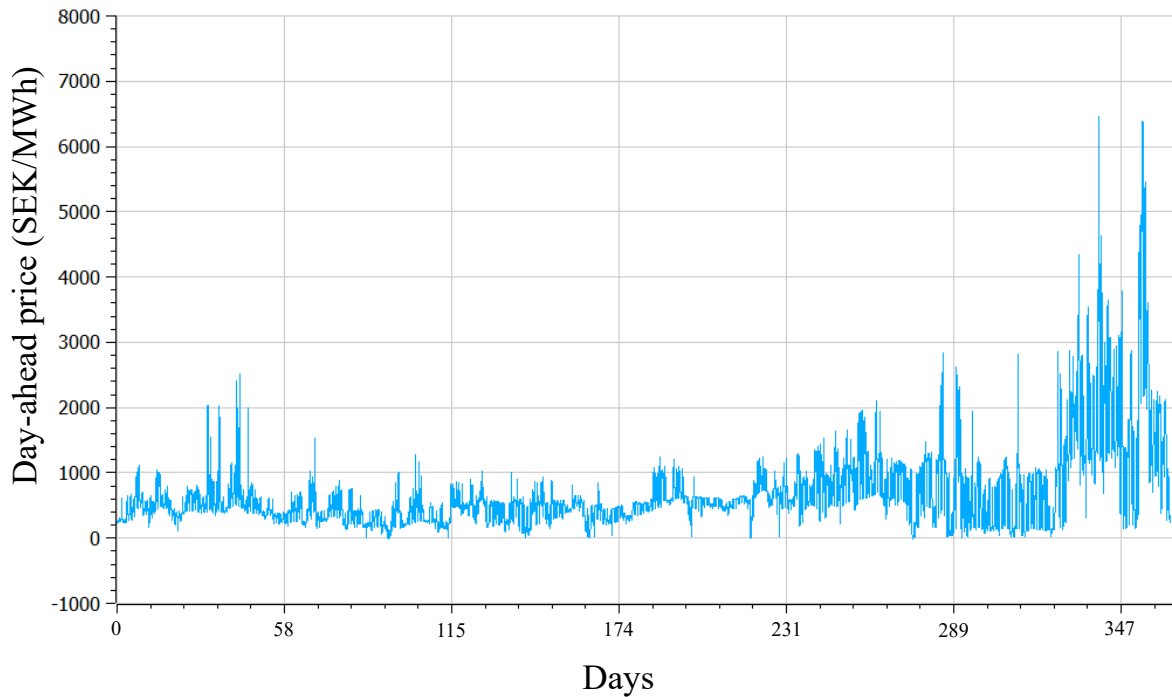
**Figure 3.3:** Annual price profile of day-ahead in SE3.

### Dimensioned components

There are several dimensions in the model that are not obtained through optimisation, but still need set dimensions. These dimensions include the WPP, SPP, and GCP power ratings as well as the efficiencies of the components in the ESS. The power ratings of the WPP and GCP are set by the existing site to 130 MW.

In order to estimate the annual production from a SPP placed close to the Bäckhammar WPP, solar irradiation data from SMHI's Karlstad measuring point will be used (SMHI [63]). This location is quite close to Bäckhammar, see Figure 3.4.
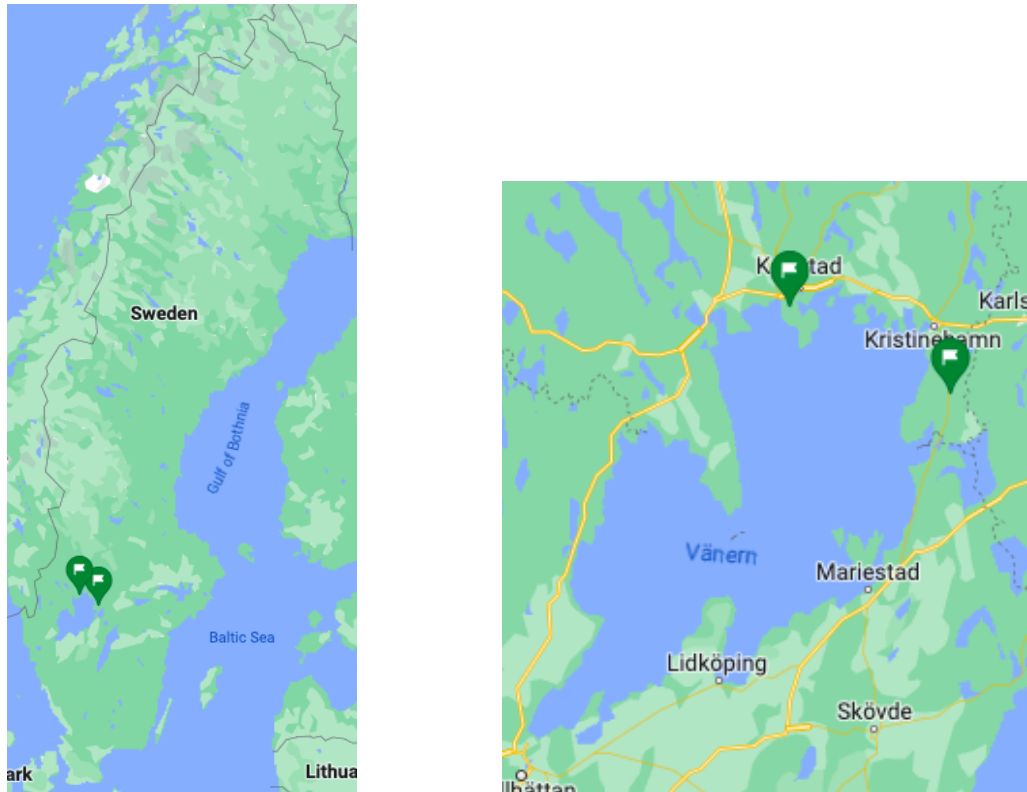
**Figure 3.4:** Map showing locations of Karlstad measuring point for solar irradiation (left) [63] and Bäckhammar wind power plant (right) [15], generated using Google Maps.

As mentioned in Section 2.3.2, it is common practice to oversize the peak power output of a solar park compared to its inverters to increase the number of full load hours. This will be done in Section 5.1.1.

## 3.2 Initial data analysis

The initial data analysis is performed by creating duration diagrams for wind, solar and combined power production and finding the correlation between wind and solar production. The total curtailment for different ratios of wind to solar power without an ESS is also calculated. A correlation between wind power output data and day-ahead price data is also generated to analyse if there are signs of the cannibalisation effect at this site.

## 3.3 System overview

This section will introduce the entire system, including the different parts included and the technical assumptions made. The system is made up of two parts, the model and the operational strategy, as can be seen in Figure 3.5. On the left, the data series used as inputs for the operational strategy are shown. Other inputs for the operational strategy include the outputs from the model, as shown by the arrows. The input data for the model corresponds to the output parameters of the operational strategy. The purpose of the model is to simulate

the energy flows of the electrical system, enable implementation of the operational strategy, and to output the relevant data to conduct a simple optimisation of system dimensions.
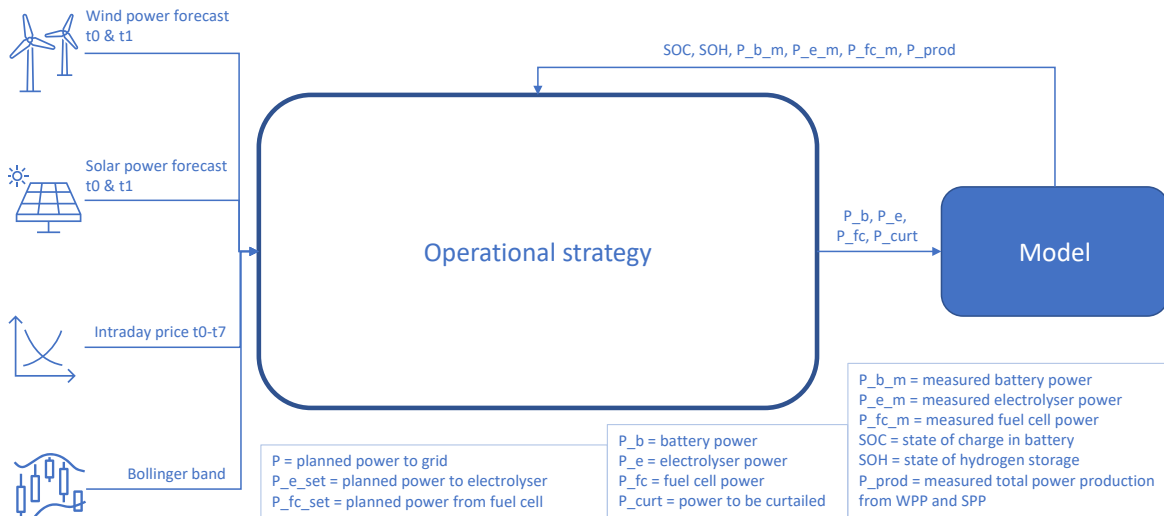


**Figure 3.5:** Functional system overview.

### 3.3.1 Model overview

Figure 3.6 demonstrates a simplified model overview. To clarify, the parts included in the solution are outlined in blue and called System.

The components, which will be analysed independently in the investment appraisal, are the SPP, BESS, FC, and H2ESS. Please note that the H2ESS refers to both the electrolyser and the hydrogen storage.
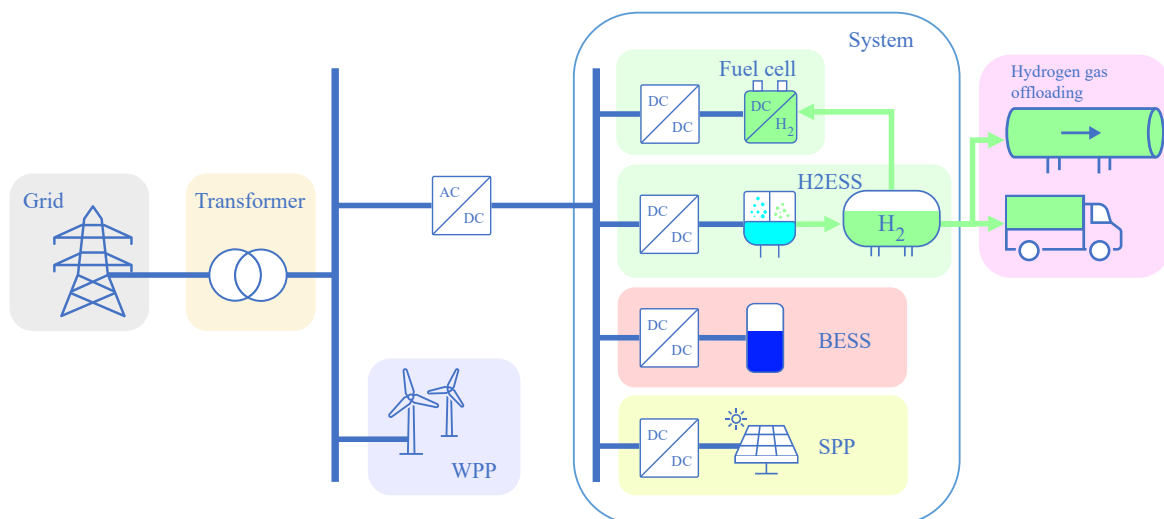


**Figure 3.6:** Simple model overview, including the definition of the system.

### 3.3.2 OpenModelica

The tool used for both creation and simulation of the model is OpenModelica. OpenModelica is a high-performance, open-source modeling and simulation environment based on the Modelica language (Modelica Association [50]). Modelica is a declarative, object-oriented, equation-based language used for modeling complex physical systems, including electrical, mechanical, hydraulic, and thermal systems. OpenModelica provides a powerful platform for designing and simulating dynamic systems, and its modular structure allows for the creation of reusable components. The version used in this thesis is OpenModelica v1.20. In addition to the standard Modelica library and its pre-made blocks, an electrical power library provided by Jörgen Svensson, senior lecturer at Industrial Electrical Engineering and Automation at Lund University, Faculty of Engineering, is in part used to construct the model.

### 3.3.3 Implemented OpenModelica model

As previously noted, the main parts included in the model are a WPP, SPP, BESS, H2ESS and a GCP connecting the site to the grid. The different parts can be seen in Figure 3.7 and will be discussed in more detail in the following sections.
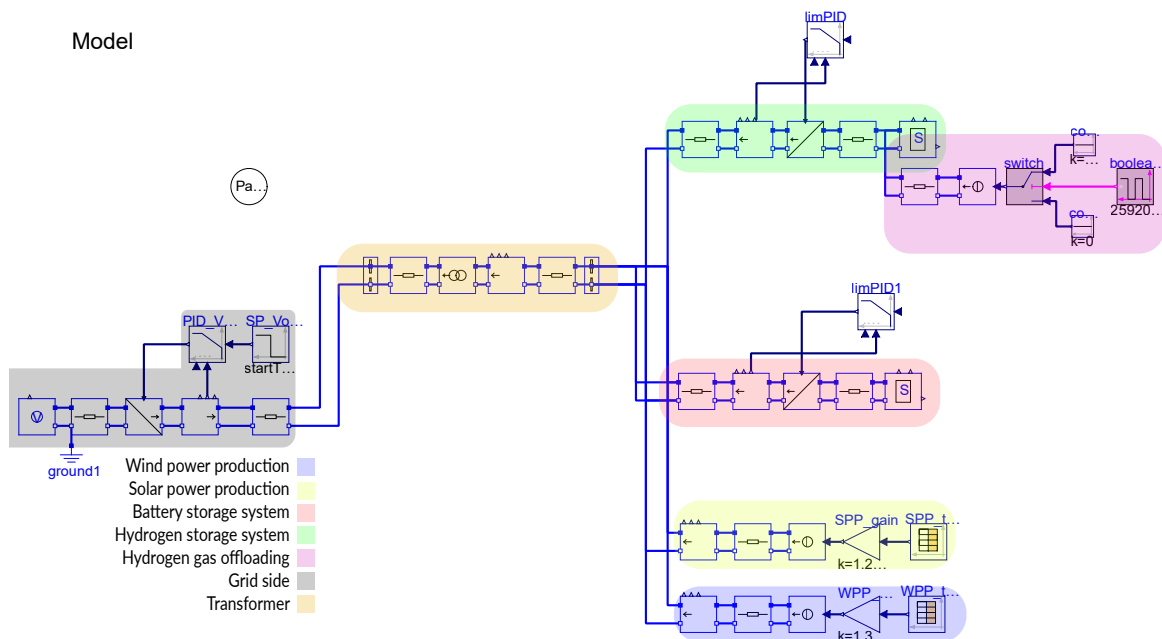


**Figure 3.7:** Model overview in OpenModelica interface.

### 3.3.4 Power generation

The two power generating components, the WPP and SPP, are modelled as generator units with the wind power output data and modified solar global irradiation data respectively. The generator units are connected to the site bus through a measuring unit and a resistor, simulating the resistance in the cables. The WPP and SPP implemented in OpenModelica can be seen in Figure 3.8.

50
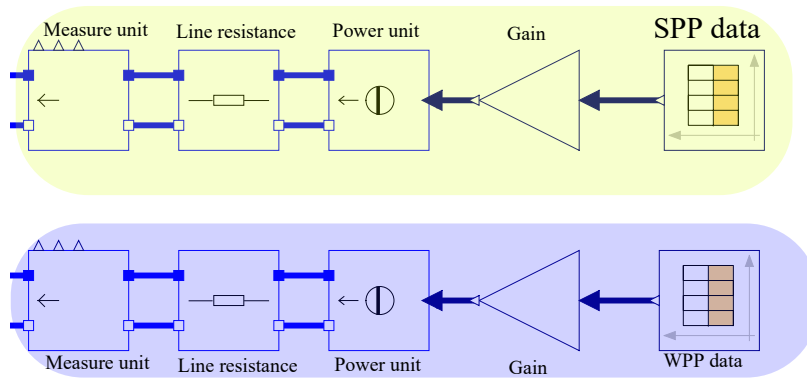
**Figure 3.8:** The power generating components (WPP and SPP) in OpenModelica interface.

### 3.3.5 Energy storage systems

Both the BESS and H2ESS are modelled as capacitors that are charged and discharged by DC/DC converters controlled by PI controllers, which in turn control the power of the converters. PI controllers are controllers which combine proportional and integral control to manage a system (Woolf [90]). To model the different behaviours of the ESSs, specifically the step responses of both storage solutions, the PI parameters are set up differently in each storage solution. Simply put, the step response of the electrolyser is significantly slower than the BESS. This difference in step response is set up mainly to mimic the effect that hydrogen storage is incapable of controlling the fast changing power level as well as the need of the faster responding battery.

The losses accumulated by charging and discharging the ESSs are modelled as efficiencies in the DC/DC converters. The BESS is simplified to the same efficiency for charging and discharging. The H2ESS has two different efficiencies for charging and discharging, representing the respective efficiencies of the electrolyser and fuel cell.

The H2ESS has an alternative way of discharging which is through the direct trade of compressed hydrogen gas. This is modelled as a load discharging the H2ESS with a constant power. The model representation of the BESS and H2ESS can be seen in Figure 3.9.
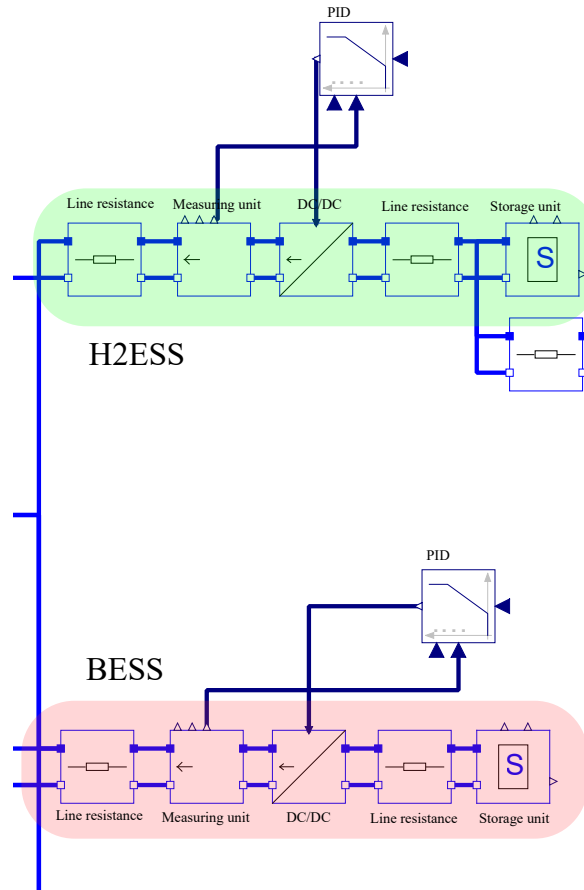
**Figure 3.9:** The HESS (H2ESS and BESS) in OpenModelica interface.

### 3.3.6 Grid and grid connection point

Similarly to the BESS and H2ESS, the grid side is modelled using a DC/DC converter controlled by a PI controller. However, instead of controlling the power of the DC/DC converter, the PI controls the voltage and therefore absorbs all energy the site produces. The constraining factor for how much power the site can export to the grid comes from the GCP, which has a rated power of 130 MW. The grid side and GCP implemented in OpenModelica can be seen in Figure 3.10.
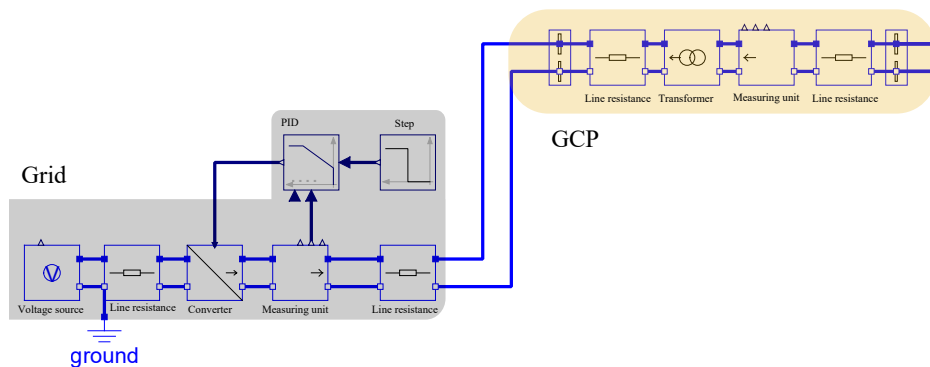


**Figure 3.10:** Grid and GCP in OpenModelica interface.

### 3.3.7 Technical assumptions

As this thesis mainly focuses on the energy flow between components and out to the grid, one simplification implemented in the model is that all components are assumed to be connected via DC and not three phase alternating current (AC). This simplification makes analysing energy flows in the system trivial.

Another assumption made is that the transmission network is never going to be fully saturated, e.g. that there is always the option to supply power to the GCP. The AC transformer is assumed to be only a DC/DC converter with a fixed ratio. The voltage in the system is set to 400 kV on the grid side of the transformer and 100 kV on the production side.

The assumed technical parameters are derived from both the literature review and other relevant sources conferred with. These can be seen in Table 3.2. Please note that sources marked as Confidential cannot be disclosed, but that these numbers are based on a budgetary offer from a relevant company working in the battery industry.

PEM technology is chosen for both the electrolyser and the fuel cell. In the case of the electrolyser, this is because this technology has both a higher efficiency and lower CAPEX in 2030 than the AEL (IEA [40]). The PEMFC, similarly, has a higher efficiency than the AFC. Even though the PEMFC is about twice as expensive as the AFC, this is outweighed by the PEMFC having a four times as long lifetime as the AFC.

The BESS is a modular battery system with 10MW/12MWh power rating and storage capacity. Scaling the BESS will always be done by adding or removing modules, therefore affecting both the power rating and storage capacity.

Also note that the efficiency of the SPP is not included. This is because the solar irradiation data has been scaled to correspond to the desired power output, and therefore, the efficiency is already included before this point.

**Table 3.2:** Technical assumptions for components.

| Component | Type | Amount | Unit | Year | Source |
|---|---|---|---|---|---|
| SPP | Lifetime | 25 | years | 2023 | Eolus. |
| Battery | Efficiency | 90 | % | 2023 | Confidential. |
| | Lifetime | 15 | years | 2023 | Confidential. |
| | Power for heating/cooling | 135 | kW/10 MW | 2023 | Confidential. |
| PEM electrolyser | Efficiency | 82 | % | 2030 | IEA [39]. |
| | Lifetime | 75 000 | hours | 2030 | IEA [39]. |
| Hydrogen storage | Efficiency | 92 | % | 2022 | Abdin et al. [1]. |
| | Lifetime | 30 | years | 2022 | Abdin et al. [1]. |
| | Energy consumption for compressed storage | 2.2 | kWh/kg | 2022 | Abdin et al. [1]. |
| | Energy consumption for compressor cooling | 0.68 | kWh/kg | 2022 | Abdin et al. [1]. |
| PEM fuel cell | Efficiency | 54 | % | 2030 | IEA [39]. |
| | Lifetime | 80 000 | hours | 2030 | IEA [39]. |

## 3.4 Energy storage strategy and operation

This section will present the two-part operational strategy as well as the operational logic behind the simulation.

### 3.4.1 Operational logic

The goal of the operational strategy in this thesis is to provide, through the use of energy storage systems, the ability to plan and control the power output of a hybrid wind and solar plant while facilitating the storage of excess power that the GCP cannot deliver. The additions of these abilities do not only allow the system to have a significantly higher peak power output than otherwise possible, but it also reduces or even eliminates the forecast error's effect on the site while guaranteeing constant power output within the hour. The ability to control power output also facilitates energy arbitrage.

Other possibilities of this operational strategy that are not within the scope are participation on ancillary service markets and the ability to guarantee a minimum power output at all times (baseload PPA).

### 3.4.2 Operational strategy

The operational strategy is divided into two algorithms, the Scheduler and Controller, which are shown in Figure 3.11.

The Scheduler plans what to do during the next hour based on market price, state of energy storage and forecasted power production of the coming two hours. After calculating the ideal electrolyser power (P_e_set), fuel cell power (P_fc_set) and power to grid (P) at the beginning of each hour it passes along the set points to the Controller.

The Controller's purpose is to keep the values provided by the Scheduler to the best of its ability while protecting the components from operating outside their specifications. The Scheduler makes qualified guesses based on forecasts, but if the requirements from the Scheduler are impossible to uphold, the Controller will act to protect the components.

To summarise, the Scheduler and Controller work on different time horizons to enable optimal technical and economical performance.
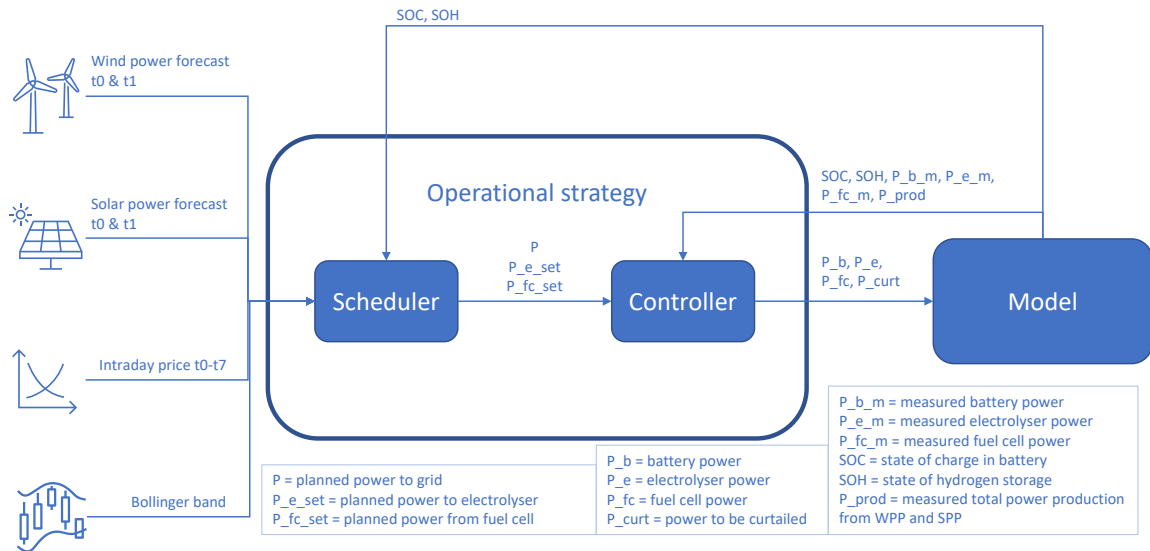
**Figure 3.11:** Functional system overview including the operational strategy.

### 3.4.3 Scheduler

As aforementioned, the Scheduler is tasked with setting the ideal electrolyser, fuel cell, and grid output powers. In order to do this, it makes price comparisons based on a moving average and the prices for the upcoming seven hours. The general operation of the Scheduler can be seen in Figure 3.12, and the full code is available in Appendix B. The state in which the Scheduler operates in is determined based on the forecast power production at the first hour, T0, and following hour, T1.
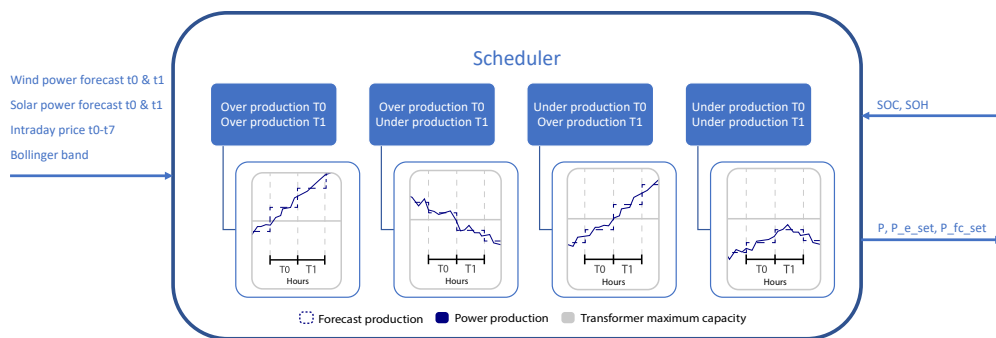


**Figure 3.12:** General operation of the Scheduler, including its inputs and outputs.

At the beginning of each hour, the Scheduler performs a comparison between two hours, the coming hour (T0) and the hour after that one (T1). When the production exceeds the maximum allowed power output of the GCP, 130 MW, the site is overproducing, and when

the production is lower than the maximum allowed power output of the GCP, the site is underproducing. Since each hour could be either underproducing or overproducing there are a total of four possible combinations. Underproduction this hour and underproduction next hour, underproduction this hour and overproduction next hour, overproduction this hour and overproduction next hour, and overproduction this hour and the next. The actions taken for each respective case are shown in Table 3.3.

The moving average comparison is made using Bollinger bands. Bollinger bands are a technical analysis tool typically used in investing to show whether a market is overbought or oversold based on moving average prices and standard deviations (Hayes [34]). As seen in Figure 3.13, Bollinger bands consist of three bands - the middle being the moving average, the upper being the moving average plus one standard deviation, and the lower being the moving average minus one standard deviation. In the typical use case, a price exceeding the upper level indicates that the market might be overbought and a price below the lower level means it might be oversold.
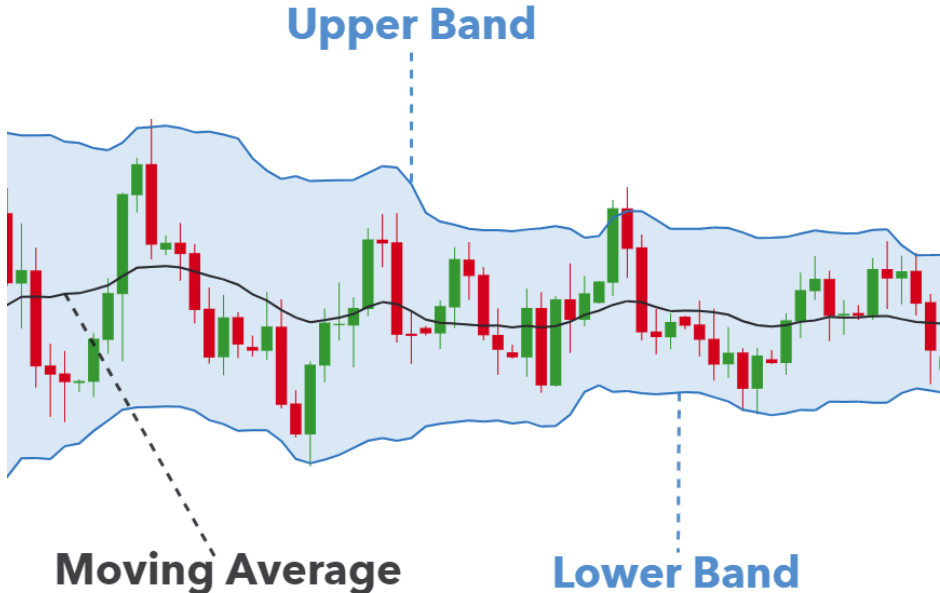


**Figure 3.13:** Example of Bollinger bands [86].

For our application however, the moving average is based on a 24 hour simple moving average (12 hours forwards and backwards in time). The upper and lower bands indicate that the current price is relatively low or relatively high.

Figure 3.14 shows how the Scheduler makes its decisions based on the Bollinger bands, intraday prices, and hydrogen price. The necessary fuel cell price and necessary electrolyser price are shown in Equations 3.2 and 3.1.
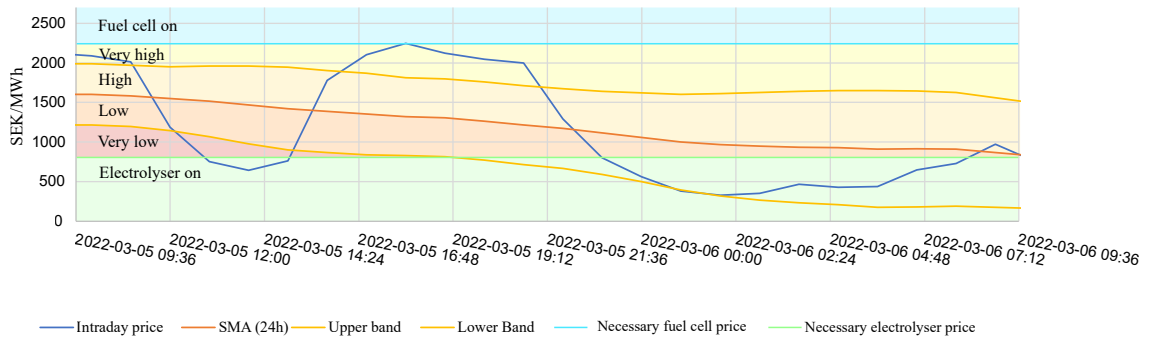
**Figure 3.14:** Illustration of how the Scheduler makes decisions based on Bollinger bands, intraday prices, necessary fuel cell price, and necessary electrolyser price.

Besides this, a seven hour comparison is also made to catch the highest possible bid hour. While a price may be relatively high, it might still be lower than another price in the near future. If this is the case, the algorithm waits for the hour with the highest price to make its sale and by doing so maximises the profit.

The different levels of SOC and SOH that the Scheduler plans with can be seen in Figure 3.15. Note that the BESS has a larger buffer until it operates outside of its operating range. This is because of the higher volatility that comes from it always having a high power-to-energy capacity ratio.
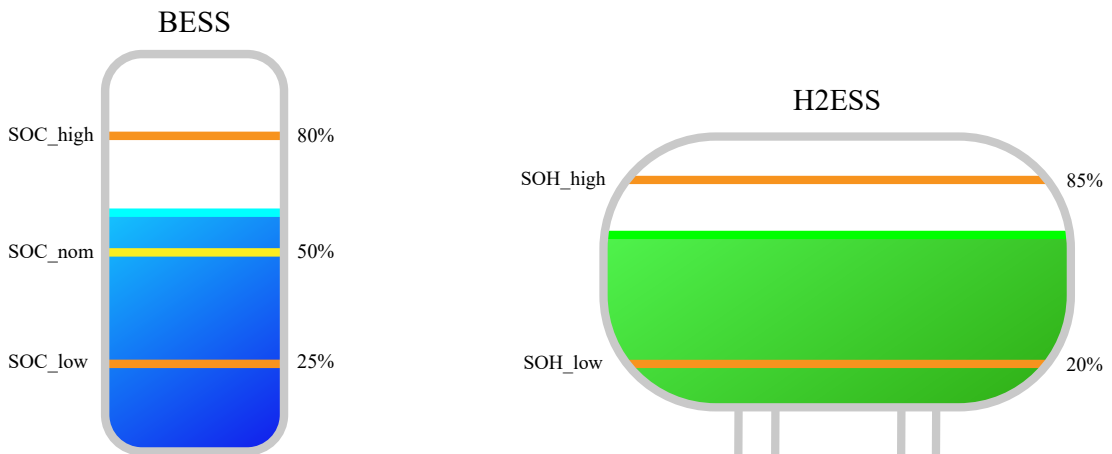


**(a)** The SOC levels the Scheduler plans for with the BESS.

**(b)** The SOH levels the Scheduler plans for with the H2ESS.

**Figure 3.15:** SOC and SOH levels used for planning in the Scheduler.

**Table 3.3:** Scheduler mapping production in relation to transformer capacity for the next two hours.

| | Overproduction T1 | Underproduction T1 |
|---|---|---|
| Overproduction T0 | If the battery's state of charge is expected to be too high in two hours, then the battery aims to not become too high in the next hour in order to prepare itself. If necessary, the electrolyser can be activated to help the battery with this. | If the state of charge in one hour will be higher than mid, then the goal is to steer the battery back to mid to have as much room for action as possible. This is done by activating the electrolyser to the power necessary.<br><br>If the state of charge in one hour will be lower than nominal state of charge, the electrolyser is not activated. |
| Underproduction T0 | If the state of charge in two hours is above the highest allowed level, then the goal is to steer the battery back to the high level. If the price is high enough, then hydrogen may be produced. If not, the battery will be used during this hour to better adapt the level in two hours.<br><br>If the state of charge in two hours is below the nominal level, then there is no need to act in this hour. | See Table 3.4. |

When the Scheduler discovers that there is underproduction in this hour and the next, it has the opportunity to make decisions to maximise profit by setting ideal values for P, P_e_set and P_fc_set, see Table 3.4. This is the most complicated case and the only time the Scheduler makes decisions based the market. In the other three cases, either one or both hours will experience overproduction, making decision-making easier and only based on momentary SOC and calculated future SOC based on the production forecast. In case of overproduction at T0, the ideal grid power output is always set to the GCP maximum capacity as this can never be exceeded. In that case, the fuel cell is also set to be deactivated since there is no need for an increased power output.

In Table 3.4, some new terms are introduced - necessary fuel cell price and necessary electrolyser price. These price levels are based on the efficiencies of the electrolyser and the fuel cell, as well as a profit margin. The profit margin is to make sure that there is no production of hydrogen or usage of the fuel cell when their operation would just result in a break-even. The profit margin is set to 20%. The necessary fuel cell price and electrolyser price are calculated according to Equations 3.1 and 3.2.

Necessary electrolyser price = selling price of hydrogen∗(electrolyser efficiency - profit margin)(3.1)

$$\text{Necessary fuel cell price} = \frac{\text{selling price of hydrogen}}{\text{fuel cell efficiency - profit margin}} \qquad (3.2)$$

**Table 3.4:** Scheduler state machine when underproduction occurs in the next hour.

| State | Cause | Action |
|-------|-------|--------|
| Very_high | The current electricity price is higher than the high level, higher than the necessary electrolyser price, and lower than the necessary fuel cell price. | If the current price is the highest out of the prices for the upcoming 7 hours, then the battery will be set to discharge to the lowest allowed level. The grid output power is set to the sum of the forecasted power output and the added power output from the battery.<br><br>If not, the grid output power is set to the production forecast in order to save battery power for the hour with the highest price. |
| High | The current electricity price is higher than the average level, higher than the necessary electrolyser price, and lower than the necessary fuel cell price. | If the current price is the highest out of the prices for the upcoming 7 hours, then the battery will be set to discharge to medium full. The grid output power is set to the sum of the forecasted power output and the added power output from the battery.<br><br>If not, the grid output power is set to the production forecast in order to save battery power for the hour with the highest price. |
| Low | The current electricity price is higher than the lower level, higher than the necessary electrolyser price, and lower than the necessary fuel cell price. | The battery will aim for a medium-high state of charge (60%). The power output to the grid is set to the sum of the forecasted power production and the battery output. |
| Very_low | The current electricity price is lower than the lower level, higher than the necessary electrolyser price, and lower than the necessary fuel cell price. | The battery will aim for a high state of charge in the next hour, in order to prepare for an hour with a higher price. The grid power output is set to the sum of the forecasted power production and the contribution from the battery. |
| Fuel_cell_on | The current electricity price is higher than the necessary price to activate the fuel cell. | If the current price is the highest out of the prices for the upcoming 7 hours, then the fuel cell will be set to discharge as much as possible, while not making the hydrogen storage too empty. Since the price is so high, the battery is also set to discharge as much as possible. The grid output power is set to the sum of the forecasted power output, the battery power output and the fuel cell power output.<br><br>If not, the grid output power is set to the sum of the production forecast and fuel cell power output. This way, the battery will be able to help more when a more expensive hour arrives. |
| Electrolyser on | The current electricity price is so low that producing hydrogen is more economically sustainable than providing energy to the grid. | The electrolyser is activated to its fullest potential, without exceeding the maximum capacity of the hydrogen storage. |

### 3.4.4 Controller

The Controller protects the components and facilitates the Scheduler's plans during operation by managing the energy flows in the system. It does this by controlling the battery power, electrolyser power, fuel cell power, and curtailment of solar power. The behaviour of the Controller is based on measurements of the system and inputs from the Scheduler.

The energy management strategy takes a similar approach to previous work by Phan Van et al., referred to in Section 2.9 (Phan Van et al. [57]). Inspiration was drawn by utilising a similar state machine that is controlled by the SOC of the battery, SOH of the hydrogen storage, and a relationship between electrical power generated and a wanted level of power to grid. This relationship is expressed in the parameter P_diff, which denotes the difference between the measured generated power (P_prod) and the wanted power set by the Scheduler (P). If P_diff is positive, the site is overproducing in relation to the wanted level, and if P_diff is negative, it is underproducing in relation to the wanted level.

The Controller has three states for each ESS dependent on their energy content. Combining these states gives a state machine consisting of nine main states. These states all corresond to a minimum, medium, or maximum SOC or SOH for each energy storage type. These states be seen in Figure 3.16.
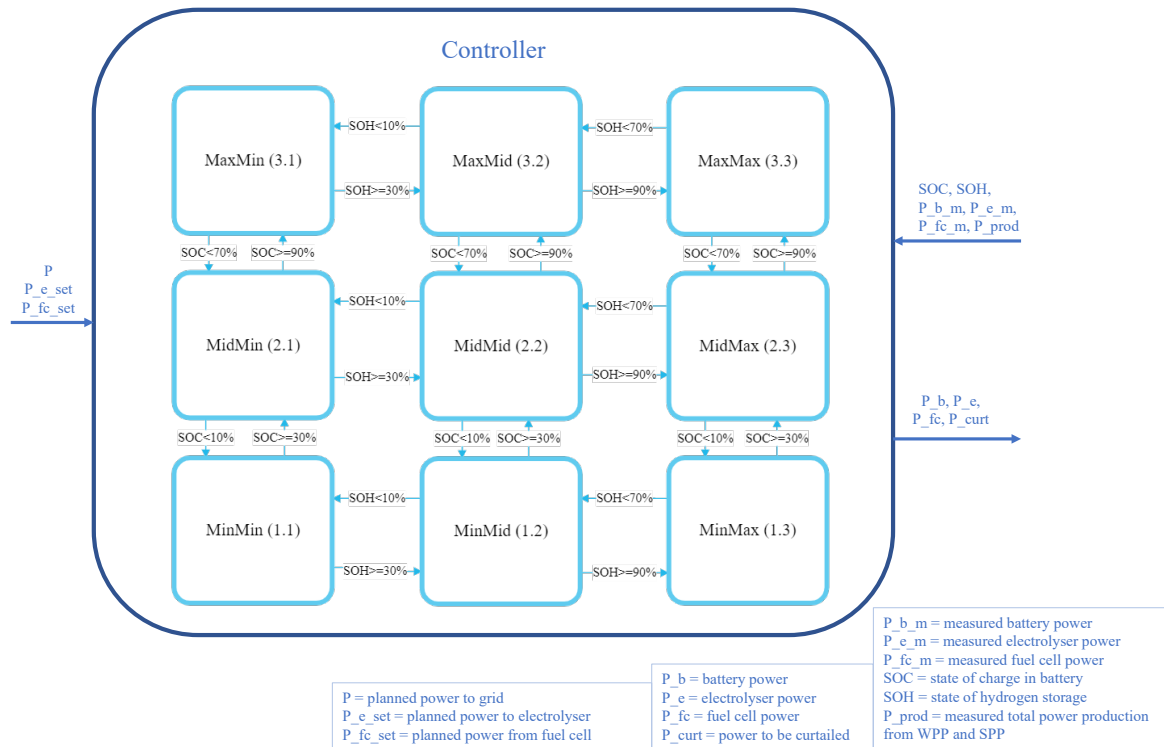


**Figure 3.16:** General operation of the Controller, including its inputs and outputs. Note that P_diff is the difference between P_prod and P.
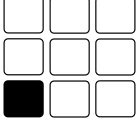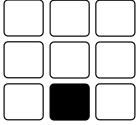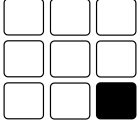
Each state has two sub-states based on whether P_diff is positive or negative. Inside these sub-states, the Controller will act differently depending on how large the P_diff parameter is and other measurement signals sent to the Controller.

The Scheduler plans ahead as to not reach the outer boundaries of the component operating ranges. If the Scheduler fails at this, or if a component for any reason is close to operating

outside its range, the Controller will stop following the Scheduler's set points and adjust the appropriate values. The logic behind this is shown in Tables 3.5, 3.6, and 3.7.
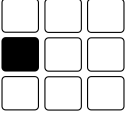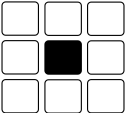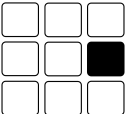
The goal state for both the Controller and Scheduler is the middle (mid) state for both energy storages, that is, the MidMid state. When in this state, the H2ESS and BESS are at their nominal operating ranges and the Controller will follow the set points P, P_e_set and P_fc_set sent by the Scheduler. The measurement signals P_b_m, P_e_m, and P_fc_m in the Controller are defined as positive when energy flows out of the component. For example, if the battery is active and charging, energy is flowing into the battery and out of the site bus. Therefore, P_b_m will be negative.

**Table 3.5:** Controller state machine used for strategic decisions (part 1).
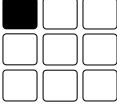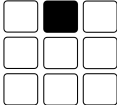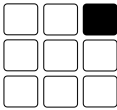
| State | P_diff >0 | P_diff <0 |
|---|---|---|
| MinMin | if P_diff <= P_b_max then<br>P_b = -P_diff;<br>P_e = 0;<br>P_fc = 0;<br>P_curt = 0;<br>elseif P_diff <= (P_b_max + 0.5*P_e_max) then<br>P_e = -0.5*P_e_max;<br>P_b = -(P_diff + 0.5*P_e_m);<br>P_fc = 0;<br>P_curt = 0;<br>else<br>P_b = -P_b_max;<br>P_e = -P_e_max;<br>P_fc = 0;<br>if P_prod >P_t_max + P_b_m + P_e_m then<br>P_curt = P_prod - P_t_max + P_b_m + P_e_m;<br>else<br>P_curt = 0;<br>end if;<br>end if; | P_b = 0<br>P_e = 0<br>P_fc = 0<br>P_curt = 0 |
| MinMid | if P_diff <= P_b_max then<br>P_b = -(P_diff + P_e_m);<br>P_e = 0;<br>P_fc = 0;<br>P_curt = 0;<br>elseif P_diff <= P_b_max + 0.5*P_e_max then<br>P_b = -(P_diff + P_e_m);<br>P_e = -0.5*P_e_max;<br>P_fc = 0;<br>if P_prod >P_t_max - P_e_m - P_b_m then<br>P_curt = P_prod - P_t_max + P_b_m + P_e_m;<br>else<br>P_curt = 0;<br>end if;<br>else // P_diff >P_b_max + P_e_max<br>P_b = -P_b_max;<br>P_e = -P_e_max;<br>P_fc = 0;<br>if P_prod >P_t_max - P_e_m - P_b_m then<br>P_curt = P_prod - P_t_max + P_b_m + P_e_m;<br>else<br>P_curt = 0;<br>end if;<br>end if; | if not P_fc_set == 0 and P_prod + P_fc_set <P_t_max then<br>P_b = 0;<br>P_e = 0;<br>P_fc = P_fc_set;<br>P_curt = 0;<br>elseif not P_fc_set == 0 and P_prod + P_fc_set >P_t_max then<br>P_b = P_prod + P_fc_m - P_t_max;<br>P_e = 0;<br>P_fc = P_fc_set;<br>P_curt = 0;<br>else<br>P_b = -P_e_m;<br>P_e = 0;<br>P_fc = 0;<br>P_curt = 0;<br>end if; |
| MinMax | if P_diff <= P_b_max then<br>P_b = -P_diff;<br>P_e = 0;<br>P_fc = 0;<br>P_curt = 0;<br>else //P_diff >P_b_max<br>P_b = -P_b_max;<br>P_e = 0;<br>P_fc = 0;<br>if P_prod >P_t_max - P_b_m - P_e_m then<br>P_curt = P_prod - P_t_max + P_b_m + P_e_m;<br>else<br>P_curt = 0;<br>end if;<br>end if; | if not P_fc_set == 0 and P_prod + P_fc_set <P_t_max then<br>P_b = 0;<br>P_e = 0;<br>P_fc = P_fc_set;<br>P_curt = 0;<br>elseif not P_fc_set == 0 and P_prod + P_fc_set >P_t_max then<br>P_b = P_prod + P_fc_m - P_t_max;<br>P_e = 0;<br>P_fc = P_fc_set;<br>P_curt = 0;<br>else<br>P_b = -P_e_m;<br>P_e = 0;<br>P_fc = 0;<br>P_curt = 0;<br>end if; |

**Table 3.6:** Controller state machine used for strategic decisions (part 2).

| State | | P_diff >0 | P_diff <0 |
|---|---|---|---|
| ▨ (left-mid cell filled) | MidMin | P_fc = 0;<br>if P_diff <= P_b_max + P_e_set then<br>P_b = -(P_diff + P_e_m);<br>P_e = -P_e_set;<br>P_curt = 0;<br>elseif P_diff <= P_b_max + P_e_max then<br>P_b = -(P_diff + P_e_m);<br>P_e = -P_e_max;<br>P_curt = 0;<br>else //P_diff >P_b_max + P_e_max<br>P_b = -P_b_max;<br>P_e = -P_e_max;<br>if P_prod >= P_t_max - P_b_m - P_e_m then<br>P_curt = P_prod - P_t_max + P_b_m + P_e_m;<br>else<br>P_curt = 0;<br>end if;<br>end if;<br>end if; | P_e = -P_e_set;<br>P_fc = 0;<br>P_curt = 0;<br>P_b = if -P_diff - P_e_m >P_b_max then P_b_max else -P_diff - P_e_m; |
| ▨ (center cell filled) | MidMid | P_fc = 0;<br>if P_diff <= P_b_max + P_e_set then<br>P_b = -(P_diff + P_e_m);<br>P_e = -P_e_set;<br>if P_prod >= P_t_max - P_b_m - P_e_m then<br>P_curt = P_prod - P_t_max + P_b_m + P_e_m;<br>else<br>P_curt = 0;<br>end if;<br>elseif P_diff <= P_b_max + P_e_max then<br>P_b = -(P_diff + P_e_m);<br>P_e = -P_e_max;<br>if P_prod >= P_t_max - P_b_m - P_e_m then<br>P_curt = P_prod - P_t_max + P_b_m + P_e_m;<br>else<br>P_curt = 0;<br>end if;<br>else //P_diff >P_b_max + P_e_max<br>P_b = -P_b_max;<br>P_e = -P_e_max;<br>if P_prod >= P_t_max - P_b_m - P_e_m then<br>P_curt = P_prod - P_t_max + P_b_m + P_e_m;<br>else<br>P_curt = 0;<br>end if;<br>end if;<br>end if; | P_e = -P_e_set;<br>P_fc = P_fc_set;<br>P_curt = 0;<br>P_b = if -(P_diff + P_e_m) >P_b_max then P_b_max else -(P_diff + P_e_m); |
| ▨ (right-mid cell filled) | MidMax | if P_diff <= P_b_max then<br>P_b = -P_diff - P_e_m;<br>P_e = 0;<br>P_fc = 0;<br>P_curt = 0;<br>else //P_diff >P_b_max<br>P_b = -P_b_max - P_e_m;<br>P_e = 0;<br>P_fc = 0;<br>if P_prod >P_t_max - P_b_m - P_e_m then<br>P_curt = P_prod - P_t_max + P_b_m + P_e_m;<br>else<br>P_curt = 0;<br>end if;<br>end if; | if -P_diff <= P_b_max and P_fc_set == 0 then<br>P_b = -P_diff - P_e_m;<br>P_e = 0;<br>P_fc = 0;<br>P_curt = 0;<br>elseif -P_diff >P_b_max and P_fc_set == 0 then<br>P_b = P_b_max - P_e_m;<br>P_e = 0;<br>P_fc = 0;<br>P_curt = 0;<br>else // not P_fc_set == 0<br>P_e = 0;<br>P_curt = 0;<br>if -P_diff <= P_b_max + P_fc_max then<br>P_fc = P_fc_max;<br>P_b = -P_diff - P_fc_m;<br>else //-P_diff >P_b_max + P_fc_max<br>P_b = P_b_max;<br>P_fc = P_fc_max;<br>end if;<br>end if; |

**Table 3.7:** Controller state machine used for strategic decisions (part 3).

| State | P_diff >0 | P_diff <0 |
|---|---|---|
| [grid icon] MaxMin | if P_diff <= 0.5*P_e_max and P_diff <P_e_m then<br>P_b = -(P_diff + P_e_m);<br>P_e = -0.5*P_e_max;<br>P_fc = 0;<br>P_curt = 0;<br>elseif P_diff <= P_e_max and P_diff <P_e_m then<br>P_b = -(P_diff + P_e_m);<br>P_e = -P_e_max;<br>P_fc = 0;<br>P_curt = 0;<br>else // P_diff >P_e_max<br>if P_diff + P_e_m <0 then<br>P_b = -(P_diff + P_e_m);<br>else<br>P_b = 0;<br>end if;<br>P_e = -P_e_max;<br>P_fc = 0;<br>if P_prod >P_t_max - P_e_m - P_b_m then<br>P_curt = P_prod - P_t_max + P_e_m + P_b_m;<br>else<br>P_curt = 0;<br>end if;<br>end if; | if -P_diff <= P_b_max then<br>if -P_diff + P_e_m <0 then<br>P_b = -(-P_diff + P_e_m);<br>else<br>P_b = 0;<br>end if;<br>P_e = 0;<br>P_fc = 0;<br>P_curt = 0;<br>else<br>// -P_diff >P_b_max<br>P_b = P_b_max;<br>P_e = 0;<br>P_fc = 0;<br>P_curt = 0;<br>end if; |
| [grid icon] MaxMid | if P_diff <= 0.5*P_e_max and P_diff <P_e_m then<br>P_b = -(P_diff + P_e_m);<br>P_e = -0.5*P_e_max;<br>P_fc = 0;<br>P_curt = 0;<br>elseif P_diff <= P_e_max and P_diff <P_e_m then<br>P_b = -(P_diff + P_e_m);<br>P_e = -P_e_max;<br>P_fc = 0;<br>P_curt = 0;<br>else // P_diff >P_e_max<br>if P_diff + P_e_m <0 then<br>P_b = -(P_diff + P_e_m);<br>else<br>P_b = 0;<br>end if;<br>P_e = -P_e_max;<br>P_fc = 0;<br>if P_prod >P_t_max -P_b_m - P_e_m then<br>P_curt = P_prod - P_t_max +P_b_m + P_e_m;<br>else<br>P_curt = 0;<br>end if;<br>end if; | if -P_diff <= P_b_max and P_fc_set == 0 then<br>P_b = -P_diff - P_e_m;<br>P_e = 0;<br>P_fc = 0;<br>P_curt = 0;<br>elseif -P_diff >P_b_max and P_fc_set == 0 then<br>P_b = P_b_max;<br>P_e = 0;<br>P_fc = 0;<br>P_curt = 0;<br>else // P_fc_set != 0<br>P_e = 0;<br>P_curt = 0;<br>if -P_diff <= P_b_max + 0.5*P_fc_max then<br>P_fc = 0.5*P_fc_max;<br>P_b = -P_diff - P_fc_m;<br>else //-P_diff <= P_b_max + P_fc_max<br>P_fc = P_fc_max;<br>P_b = -P_diff - P_fc_m;<br>end if;<br>end if; |
| [grid icon] MaxMax | if P_diff + P_e_m <0 then<br>P_b = -(P_diff + P_e_m);<br>else<br>P_b = 0;<br>end if;<br>P_e = 0;<br>P_fc = 0;<br>if P_prod >= P_t_max - P_e_m - P_b_m then<br>P_curt = P_prod - P_t_max + P_e_m + P_b_m;<br>else<br>P_curt = 0;<br>end if;<br>end if; | if -P_diff <= P_b_max and P_fc_set == 0 then<br>if P_diff + P_e_m <0 then<br>P_b = -(P_diff + P_e_m);<br>else<br>P_b = 0;<br>end if;<br>P_e = 0;<br>P_fc = 0;<br>P_curt = 0;<br>elseif -P_diff >P_b_max and P_fc_set == 0 then<br>P_b = P_b_max;<br>P_e = 0;<br>P_fc = 0;<br>P_curt = 0;<br>else // P_fc_set != 0<br>P_e = 0;<br>P_curt = 0;<br>if -P_diff <= P_b_max + 0.5*P_fc_max then<br>P_fc = 0.5*P_fc_max;<br>P_b = -(P_diff + P_fc_m);<br>else //-P_diff <= P_b_max + P_fc_max<br>P_fc = P_fc_max;<br>P_b = - (P_diff + P_fc_m);<br>end if;<br>end if; |

### 3.4.5 Operational strategy example case

To better explain how the Scheduler and Controller are supposed to collaborate, two scenarios of ideal behaviour will be presented. Note that these figures are illustrations of how the operational strategy is intended to work, not directs outputs after strategy implementation.

In Figure 3.17, a scenario of overproduction is showcased. To clarify, overproduction in this case means that the power production exceeds the maximum power that can pass through the GCP. When there is no storage and operational strategy (far left), underproduction means that there is no control over how the power is delivered to the grid, and all excess power during overproduction is curtailed.

When the energy storage has been implemented and the Controller is active, seen in the middle of Figure 3.17, the power delivered to the grid is aligned with the forecasted power output. No curtailment occurs until the battery is full. Once the battery is full, curtailment begins while the electrolyser remains active to reduce the amount of power that is curtailed.

When the Scheduler has also been activated, seen on the far right in Figure 3.17, the strategy can plan ahead for overproduction. In this case, the planning works by making sure the electrolyser is activated at hour T0 in order to reduce the SOC ahead of overproduction. That way, the battery has a greater capacity to absorb the excess energy.
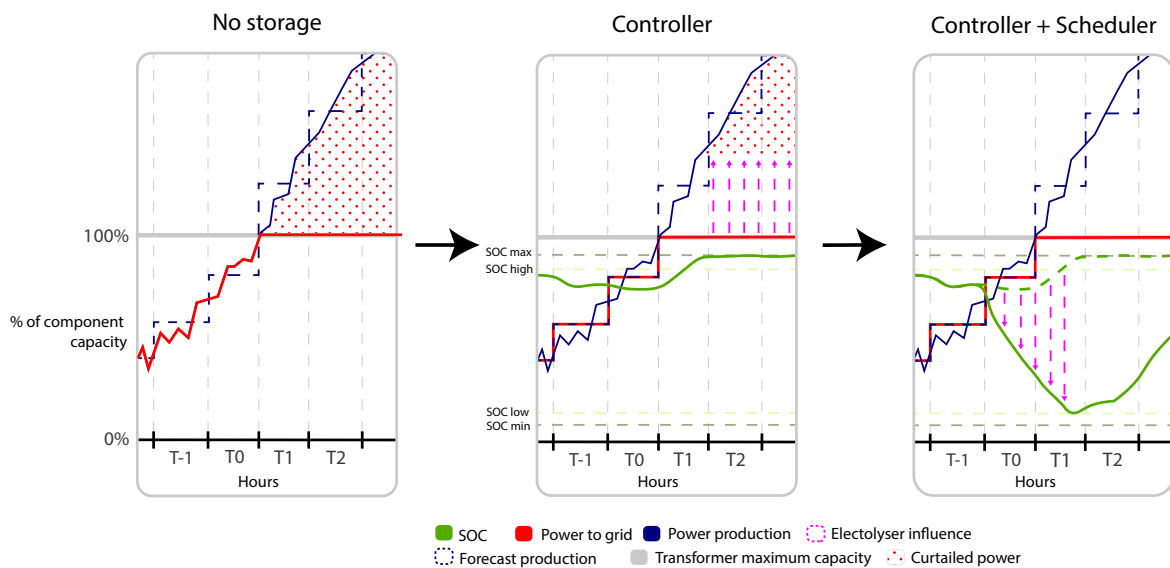


**Figure 3.17:** The wanted behaviour of the Controller and Scheduler in an overproduction scenario.

In Figure 3.18, an energy arbitrage scenario is showcased. Since it is only the relationship between prices that matters for the strategy, the intraday price has been shifted on the y-axis for increased legibility.

The far right subfigure in Figure 3.18 will now be studied. At hour T-1, the price is the lowest it will be for the given period while hour T1 has the highest price for the given period. The Controller and Scheduler reduce the power to grid at T-1 in order to charge the battery (increasing the SOC). At hour T1, the power to grid is instead increased to discharge the battery (which is evident, since the SOC significantly reduces in this case). This means more energy could be sold to the intraday market.
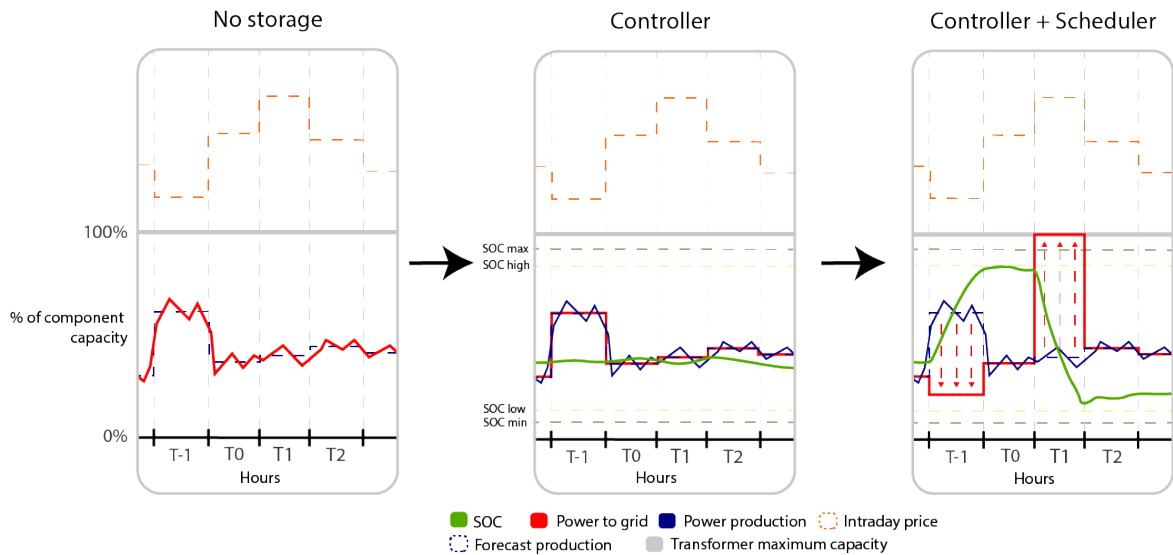
**Figure 3.18:** The wanted behaviour of the Controller and Scheduler in a energy arbitrage scenario.

# 3.5 Implemented OpenModelica system

The system, complete with the model and operational strategy, can now be implemented in OpenModelica, as seen in Figure 3.19.
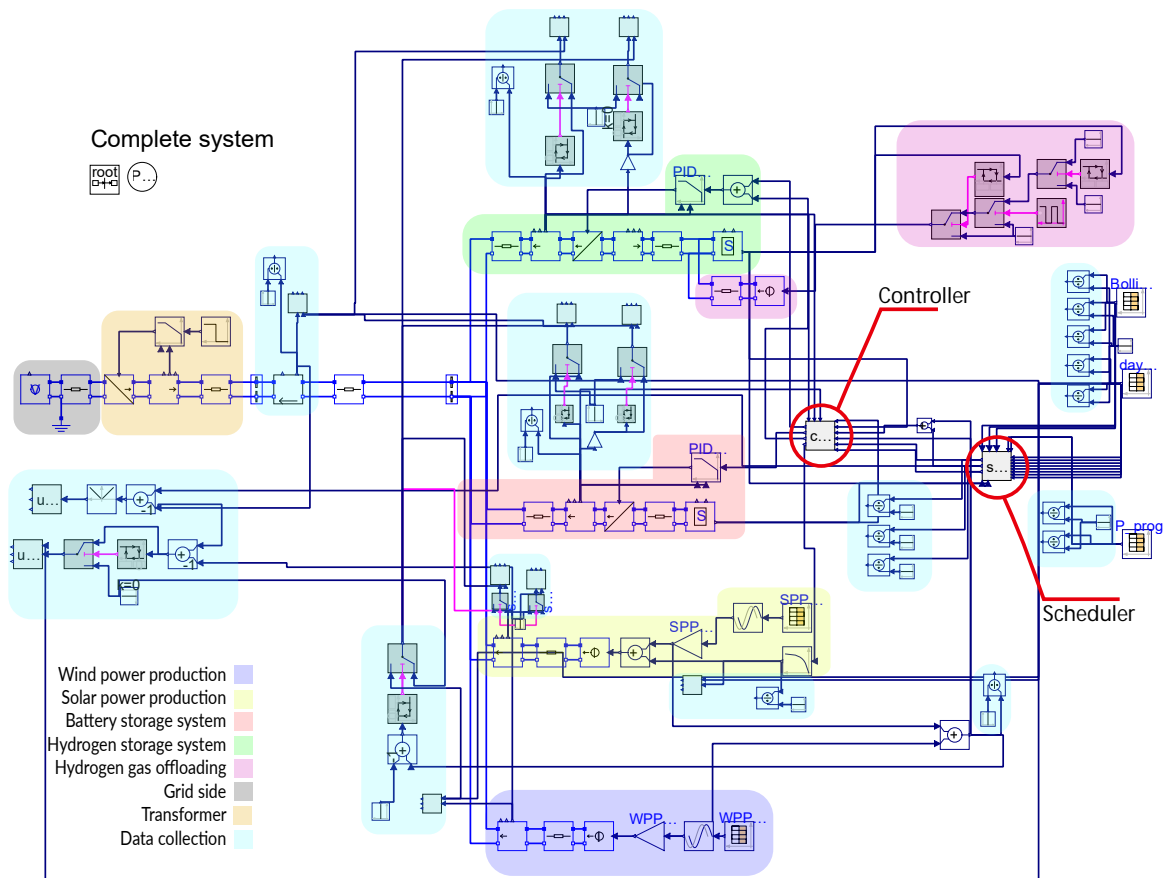


**Figure 3.19:** Complete system, including model and operational strategy, implemented in OpenModelica.

# 4 Techno-economic dimensioning method

The techno-economic dimensioning uses simulation outputs together with key economic values and a simple optimisation process to determine the best dimensions for the system. This chapter will present the different parts included in the techno-economic dimensioning and explain the investment appraisal used to evaluate each scenario of dimensions. The economic assumptions used in the investment appraisal will also be presented as well as explanations of the key economic values used.

## 4.1 Economic overview

The investment appraisal consists in part of key economic values, detailed in the following section, derived from economic assumptions. This analysis will in part contribute to the dimensioning of the system, the method for which is detailed in Section 3.1.

### 4.1.1 Key economic values

**Internal Rate of Return**

The Internal Rate of Return (IRR) is a financial metric that estimates the profitability of a potential investment while taking into account the time value of money (Fernando [29]). This is done by identifying the discount rate that makes the net present value (NPV) of all cash flows equal zero in a discounted cash flow analysis (analysis of current and future available cash). The equation for NPV is Equation 4.1 (Fernando [30]).

$$NPV = \sum_{t=0}^{T} \frac{C_t}{(1+i)^t} - C_0 \qquad (4.1)$$

Where:

- $T$ represents the final time period

- $t$ represents the number of time periods

- $C_t$ represents the net cash flow at time $t$

- $i$ represents the required return or discount rate

- $C_0$ represents the total initial investment cost

The IRR can be seen as the annual growth rate that an investment is anticipated to generate. Generally, a higher IRR value is positive for investments. IRR is given by solving Equation 4.2.

$$NPV = \sum_{t=0}^{T} \frac{C_t}{(1 + IRR)^t} - C_0 = 0 \qquad (4.2)$$

Where:

- $NPV$ represents the NPV

- $T$ represents the final time period

- $t$ represents the number of time periods

- $C_t$ represents the net cash flow at time $t$

- $i$ represents the required return or discount rate

- $C_0$ represents the total initial investment cost

It is important to note that there are some limitations to using IRR to compare different investments. These can be avoided by using several different metrics to determine profitability. The IRR value is only as useful as its estimates are correct. Also, analysing IRR values can be misleading when comparing projects of different lifetimes, as shorter projects can obtain a higher IRR value and therefore appear to be better investments. Furthermore, a mix of positive and negative cash flows can generate multiple IRR values.

**Levelised Cost of Energy**

LCOE is a metric representing the cost of producing one unit of energy over the lifetime of a energy generating asset (Schmidt [60]). It is calculated by dividing the NPV of the total cost of building and operating the asset by the total electricity generation over its lifetime, see Equation 4.3 (Stehly and Duffy [65]). The metric includes all associated expenses, such as fuel and maintenance costs as well as financing. By factoring in as many costs as possible, LCOE becomes a more reliable metric to compare different types of power generating technologies.

$$LCOE = \frac{(CAPEX * FCR) + OPEX}{\frac{AEP_{net}}{1000}} \qquad (4.3)$$

Where:

- $CAPEX$ represents the capital expenditure

- $FCR$ represents the fixed change rate

- $OPEX$ represents the operational expenditure

- $AEP_{net}$ represents the net average annual energy production [MWh/MW/year]

**Capacity factor**

Capacity factor denotes the ratio of energy produced by a generating unit for a unit of time to the energy the unit could have produced at its full operating potential for the same time period (U.S Energy Information Administration [85]). Therefore, it is more of a techno-economic metric rather than a purely economic one. The capacity factor can be useful to analyse how much of an initial investment is utilised during its lifetime. Generally, a higher capacity factor is better. The capacity factor is given by Equation 4.4.

$$\text{Capacity factor} = \frac{E_t}{P * t} \tag{4.4}$$

Where:

- $E_t$ represents energy produced during the period $t$ (MWh)

- $P$ represents the unit's power rating (MW)

- $t$ represents the time period (h)

### 4.1.2   Economic assumptions

A number of economic assumptions are made for the simulation, both based on the literature review and other information collected.

**Capital expenditures**

The CAPEX assumed for the components of the system are given in Table 4.1.

**Table 4.1:** Capital expenditures of components.

| Component | Type | Cost | Unit | Year | Source |
|---|---|---|---|---|---|
| SPP | Installation cost | 6936 | SEK/kW | 2023 | Eolus. |
| Battery | Module CAPEX | 80 | MSEK/(10MW/12MWh) | 2023 | Confidential. |
| Electrolyser | Installation cost | 5073 | SEK/kW | 2030 | Clean Hydrogen Europe [7]. |
| Hydrogen storage | Installation cost | 123 | SEK/kWh | 2030 | Abdin et Al. [1]. |
| Fuel cell | Installation cost | 9132 | SEK/kW | 2030 | Clean Hydrogen Europe [7]. |

The CAPEX need to be repeated after each component lifetime. The component lifetimes are estimated based on their respective capacity factors from the simulation as follows.

- Battery lifetime in years = lifetime in cycles / (energy to battery * battery size per year)

- Electrolyser lifetime in years = lifetime in hours * capacity factor / hours per year

- Fuel cell lifetime in years = lifetime in hours * capacity factor / hours per year

**Maintenance and operational expenditures**

The costs for maintenance and OPEX for the components in the system are given in Table 4.2.

**Table 4.2:** Operational expenditures of components.

| | Type | Amount | Unit | Year | Source |
|---|---|---|---|---|---|
| SPP | Service and maintenance | 9 | SEK/MWh | 2023 | Eolus. |
| | Replacement of inverters (1x/15 years) | 283 | kSEK/MW | 2023 | Eolus. |
| BESS | Servicing contract (1x/5 years) | 5581 | kSEK/10MW | 2023 | Confidential. |
| Electrolyser | OPEX | 213 | SEK/(kg/d)/yr | 2030 | Clean Hydrogen Europe [7]. |
| Hydrogen storage | Fixed OPEX | 40 | SEK/kWh | 2030 | Abdin et al. [1]. |
| Fuel cell | OPEX | 0.20 | SEK/kWh | 2030 | Clean Hydrogen Europe [7]. |

**Revenues and tariffs**

The following items are the revenues and tariffs assumed in the economic analysis. Please note that uncited numbers are market standards disclosed in discussions with relevant parties and companies.

- Company tax for 2021 is 20,6% (Skatteverket [62]).

- The cost for the land lease is assumed to be 4% of gross revenue per year.

- The grid benefit (compensation for energy supplied to grid) is 3 SEK/MWh.

- The assumed compensation for Guarantees of Origin (compensation for supplying renewable energy) is 25 SEK/MWh.

- The selling price for hydrogen gas is assumed to be 4,45 EUR/kg or 1344 SEK/MWh (Aurora Energy Research [6]).

- The volume fee for production by the TSO (Svenska kraftnät) is 1,2 EUR/MWh (Svenska Kraftnät [71]).

- The fee for imbalance volume by Svenska kraftnät is 1,15 EUR/MWh (Svenska Kraftnät [71]).

- The Nord Pool fee is 0,046 EUR/MWh (shared by Eolus).

Another assumption made relates to how imbalance costs are dealt with in the investment appraisal. Normally, wind power producers enter a contract with a BRP, who takes on the imbalance risk, in exchange for a fee depending on the amount of imbalance caused by the producer (Eickhoff [10]). In this thesis, the algorithm will be able to minimise the effects of forecast errors, and therefore, an assumption made is that a different type of agreement could be entered with the BRP where all imbalance costs are dealt with by the power producer. This is not an uncommon type of agreement among plannable power producers.

**Operational parameters**

Other assumptions are made impacting the function of the simulation.

One major assumption is that the day-ahead prices are used in the simulation, but that these are assumed to be intraday prices. This impacts the simulation because it allows for decisions to be made one hour before an event, which is not possible in the case of day-ahead prices.

This assumption is made based on trends in markets similar to the position Sweden may be in in the future with continued expansion of VRES. Intraday markets are attractive to VRES because they offer much-needed flexibility by allowing trade closer to the point of purchase than the day-ahead market (EPEX Spot [19]). A well-functioning intraday market

can lower costs associated with VRES by reducing their need to use balancing strategies or pay expensive imbalance costs (Hu et al. [38]).

One market with a higher share of intraday trading is the German/Luxembourg market. Figures 4.1 and 4.2 are based on data from EPEX ([17], [18], [20]) and demonstrate this ratio. The Nordic market includes Sweden, Denmark, Finland, and Norway. The German power market has a high share of VRES compared to Sweden. This, along with the knowledge that an increase in VRES leads to a more prominent intraday market, is the foundation for the assumption that in the future, the volume of bids on the intraday market should be comparable to that of the present-day day-ahead market.
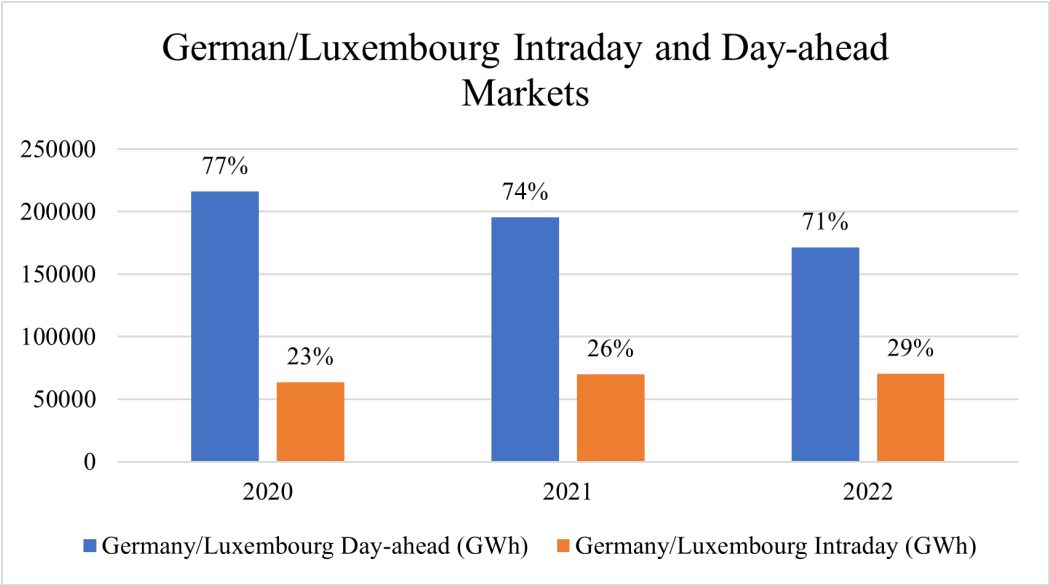


**Figure 4.1:** Trading volumes for the German/Luxembourg intraday and day-ahead markets 2020-2022.
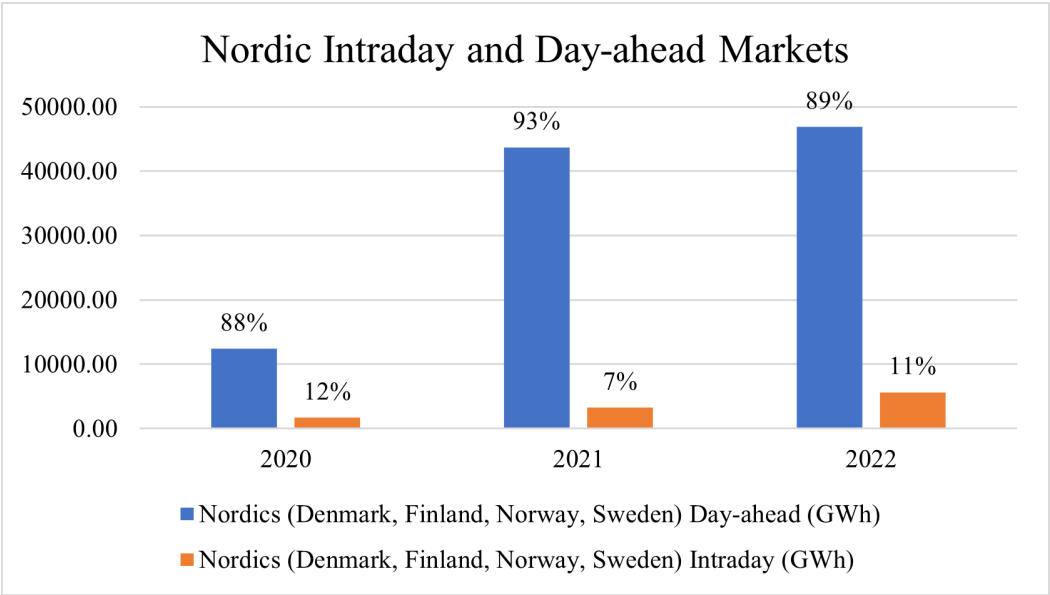


**Figure 4.2:** Trading volumes for the Nordic intraday and day-ahead markets 2020-2022.

74

A forecast error is to be introduced in order to make the simulation more realistic. David Eickhoff, Originator at Axpo Nordic, informed in an interview that the average onshore wind forecast error is 20-30% (Eickhoff [10]). For this reason, a forecast error of 25% is introduced, corresponding to a delay of 15 minutes per hour. To clarify, this means that the production is shifted by 15 minutes in each instance compared to the forecast. Alas, the forecast error is only a shift of production in time and not a shift in production volume.

An assumption relating to hydrogen is that the demand will be high in the future. As detailed in Section 2.1.4, policies set by both Europe and the USA push for an increased integration of hydrogen in the energy system. For this reason, the hydrogen storage tank will be unloaded regularly in the simulation.

To determine the right amount of hydrogen gas to be exported from the site, the maximum capacity factor for the electrolyser will be extracted from the simulation. This is done by running the simulation with a very large hydrogen storage and low electrolyser power so that the electrolyser gets utilised the maximum amount. An estimate of how much hydrogen gas a given electrolyser size will produce can then be calculated, by multiplying the maximum capacity factor by hours in a year and the electrolyser power rating. This estimated hydrogen production is then distributed over a year to acquire the average export over a day.

The rate of export is chosen to have three modes, one when SOH is above 55% with a high export rate, one when SOH is below 45% with a low export rate, and one when the hydrogen storage is empty to stop the export of hydrogen gas. The high and low export rates are set to be 17% above and below the estimated daily export rate, respectively.

To demonstrate how this works, a short example will be explained excluding efficiencies. For a 60 MW electrolyser with a maximum capacity factor of 0.5, the estimated annual production would be 262 800 MWh each year. This would mean that there would be an export 720 MWh each day, corresponding to 30 MWh each hour. The high export rate would be 35 MWh/h and the low export rate would be 25 MWh/h. If a compressed hydrogen truck with a capacity of 1.1 tonnes at 500 bar is used, this would equate to an export of 20 trucks per day.

**Template constants**

The inflation is set to 2% as is typically the case for investment calculations.

The exchange rates for USD and EUR to SEK are based on the annual average of 2021, see Table 4.3.

**Table 4.3:** Average exchange rates for 2021 (USD, EUR, SEK).

|          | Factor                    | Source                        |
|----------|---------------------------|-------------------------------|
| USD-EUR  | 1,1827                    | European Central Bank [23].   |
| EUR-SEK  | 10,1465                   | European Central Bank [22].   |
| USD-SEK  | 10,1465/1,1827 = 8,5791   | See calculation.              |

## 4.2 Investment appraisal

### 4.2.1 System level

A simple diagram of the system energy and cash flows can be seen in Figure 4.3. The calculations made to determine the cash flow of the system for each year of the economic lifetime are given by Tables 4.4 and 4.5. To clarify, the system level denotes the components: BESS, H2ESS, FC, and SPP. Please note that for the economic calculations, the revenues, costs and OPEX associated with the WPP is not included. This is because the aim of this report is to determine the economic and technical viability of the system that is added to an existing power plant.
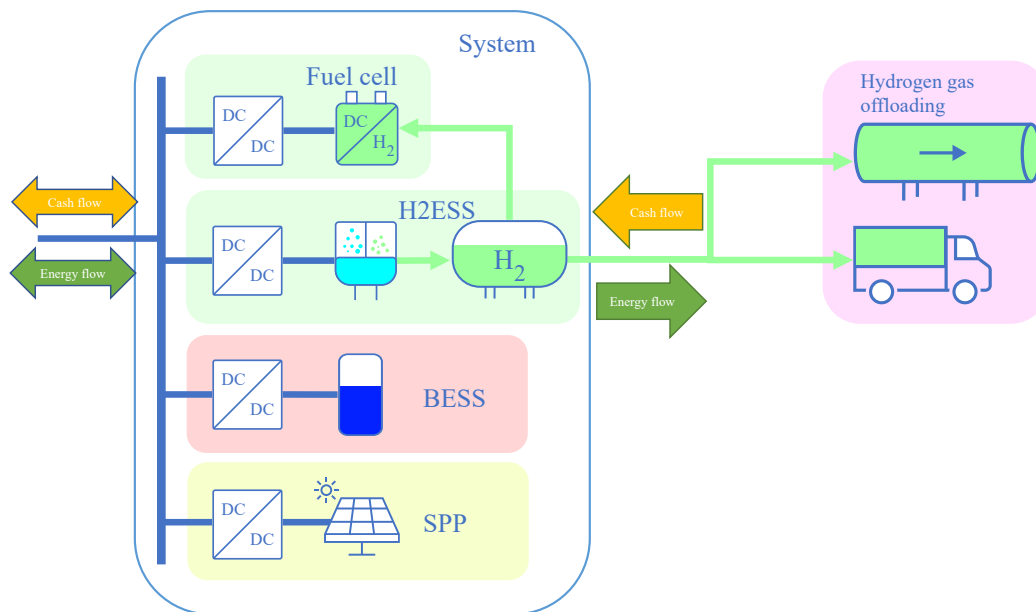


**Figure 4.3:** The system energy and cash flows.

**Table 4.4:** System revenues and costs.

| Revenue / Cost | Description | Formula | Notes |
|---|---|---|---|
| Revenue of intraday sales | All revenues from electricity sales to grid. | Delivered electricity * intraday price | Given by simulation. |
| Revenue of hydrogen gas sales | Revenues of sold hydrogen gas. | Delivered hydrogen * hydrogen price | |
| Revenue of grid benefit | Compensation for energy supplied to the grid. | Delivered electricity * grid benefit | |
| Revenue of balancing cost reduction | Cost reduction by battery for reducing forecasting error. | Forecast error reduction * imbalance fee | Reduction of forecast error = standalone WPP forecast error - system forecast error. |
| Revenue of guarantees of origin | Contractual revenue from supplying renewable energy. | Delivered electricity * guarantees of origin | |
| Cost of sales incl. balancing resp. | TSO and Nord Pool fee. | - Delivered electricity * cost of sales incl. balancing resp. | |
| Cost of imbalance | TSO imbalance volume fee. | - Forecast error * imbalance fee | Forecast error = sum of all production deviation from forecast. |

Investment calculations are also made on component-level to determine economic values of the different components. These are given in the following subsections.

**Table 4.5:** System operational expenditures.

| Operational expenditures | Description | Formula | Notes |
|---|---|---|---|
| Service and maintenance of SPP | Continuous costs associated with operation. | Solar energy produced * service and maintenance cost | |
| Replacement of SPP inverters (1x/15 years) | Cost of replacing SPP inverters. | SPP capacity * inverter replacement cost | |
| OPEX of electrolyser | Operational expenditure of electrolyser. | Electrolyser capacity * OPEX cost | Stack replacement is included. |
| OPEX of fuel cell | Operational expenditure of fuel cell. | Fuel cell capacity * OPEX cost | Stack replacement is included. |
| Annual battery OPEX | Cost for cooling and heating battery. | Power to cool and heat battery * avg. annual electricity price | |
| Servicing contract of battery | Service contract paid once per 5 years. | Battery capacity * service contract cost | |
| Fixed OPEX of hydrogen storage | Fixed operational expenditure of hydrogen storage. | Hydrogen storage capacity * fixed OPEX | |
| Variable OPEX of hydrogen storage | Cost of energy consumption and cooling of compressor. | Produced hydrogen * hydrogen storage energy consumption per kg * average electricity price | |
| Land lease | Cost of leasing land for system. | Land lease factor * gross revenues | |

Please note that some revenues on one component are costs for another. This is because there is an internal energy flow, and therefore cash flow, that needs to be accounted for in the system. Some costs and revenues are internally discounted to appropriately assign them to the right component. For example, the value of hydrogen gas delivered to the fuel cell is a cost for the fuel cell, as it "buys" hydrogen from the hydrogen storage system, while this is a revenue for the hydrogen storage system as it "sells" hydrogen to the fuel cell.

## 4.2.2   Solar power plant level without energy storage

The following is a base case that can be used to compare the system with hydrogen storage with. It consists of a separate simulation with just wind and solar power, with the same dimensions as for the case with the energy storage, but without any energy storage whatsoever. Costs and revenues for this stand-alone system can be seen in Table 4.6, while Table 4.7 lists the OPEX.

**Table 4.6:** Costs and revenues for base case with only a solar power plant.

| Revenue / Cost | Description | Formula | Notes |
|---|---|---|---|
| Revenue of intraday sales | All revenues from SPP electricity sales to grid. | Delivered electricity * intraday price | Given by simulation. |
| Revenue of grid benefit | Compensation for energy supplied to the grid. | Delivered electricity * grid benefit | |
| Revenue of guarantees of origin | Contractual revenue from supplying renewable energy. | Delivered electricity * guarantees of origin | |
| Cost of sales incl. balancing resp. | TSO and Nord Pool fee. | - Delivered electricity * cost of sales incl. balancing resp. | |
| Cost of imbalance | TSO imbalance volume fee. | - Forecast error * imbalance fee | Forecast error = sum of all production deviation from forecast. |

**Table 4.7:** Operational expenditures for base case with only a solar power plant.

| Operational expenditures | Description | Formula | Notes |
|---|---|---|---|
| Service and maintenance of SPP | Continuous costs associated with operation. | Solar energy produced * service and maintenance cost | |
| Replacement of SPP inverters (1x/15 years) | Cost of replacing SPP inverters. | SPP capacity * inverter replacement cost | |
| Land lease | Cost of leasing land for system. | Land lease factor * gross revenues | |

## 4.2.3   Solar power plant level with energy storage

Figure 4.4 shows a simple diagram of the SPP energy and cash flows. The costs and revenues for the SPP component of the system are given in Table 4.8. Please note that the OPEX associated with the SPP component consists of the same costs as the system with just wind and solar power without energy storage, see Table 4.7.
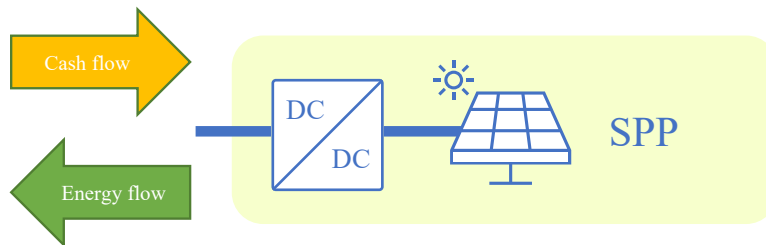


**Figure 4.4:** The SPP energy and cash flows.

**Table 4.8:** Costs and revenues solar power plant in system.

| Revenue / Cost | Description | Formula | Notes |
|---|---|---|---|
| Revenue of intraday sales | All revenues from SPP electricity sales to grid. | Delivered electricity * intraday price | Given by simulation. |
| Revenue of grid benefit | Compensation for energy supplied to the grid. | Delivered electricity * grid benefit | |
| Revenue of guarantees of origin | Contractual revenue from supplying renewable energy. | Delivered electricity * guarantees of origin | |
| Internal revenue from battery | Revenue from battery "buying" electricity from SPP | Electricity to battery from SPP * electricity price | Given by simulation. |
| Internal revenue from electrolyser | Revenue from electrolyser "buying" electricity from SPP | Electricity to electrolyser from SPP * electricity price | Given by simulation. |
| Cost of sales incl. balancing resp. | TSO and Nord Pool fee. | - Delivered electricity * cost of sales incl. balancing resp. | |
| Cost of imbalance | TSO imbalance volume fee. | - Forecast error * imbalance fee | Forecast error = sum of all production deviation from forecast. |

## 4.2.4 Battery level

A simple diagram of the BESS energy and cash flows can be seen in Figure 4.5. The costs and revenues for the BESS component of the system are given in Table 4.9. OPEX for this component are given in Table 4.10.
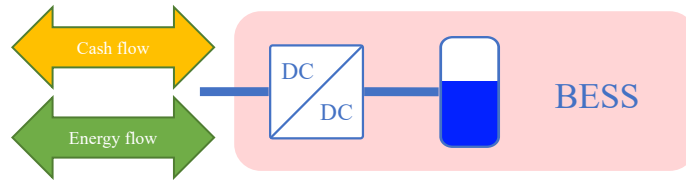


**Figure 4.5:** The BESS energy and cash flows.

**Table 4.9:** Costs and revenues for battery in system.

| Revenue / Cost | Description | Formula | Notes |
|---|---|---|---|
| Revenue of sold electricity by battery | All revenues from battery electricity sales to grid. | Delivered electricity * intraday price | Given by simulation. |
| Revenue of grid benefit | Compensation for energy supplied to the grid. | Delivered electricity * grid benefit | |
| Revenue of guarantees of origin | Contractual revenue from supplying renewable energy. | Delivered electricity * guarantees of origin | |
| Revenue of balancing cost reduction | Cost reduction by battery for reducing forecasting error. | Forecast error reduction * imbalance fee | Reduction of forecast error = standalone WPP forecast error - system forecast error. |
| Cost of sales incl. balancing resp. | TSO and Nord Pool fee. | - Delivered electricity * cost of sales incl. balancing resp. | |
| Cost of bought electricity by battery | Cost from battery "buying" electricity from SPP | - Electricity to battery from SPP * electricity price | Given by simulation. |

**Table 4.10:** Operational expenditures for battery in system.

| Operational expenditures | Description | Formula | Notes |
|---|---|---|---|
| Annual battery OPEX | Cost for cooling and heating battery. | Power to cool and heat battery * avg. annual electricity price | |
| Servicing contract of battery | Service contract paid once per 5 years. | Battery capacity * service contract cost | |
| Land lease | Cost of leasing land for system. | Land lease factor * gross revenues | |

## 4.2.5 Electrolyser and hydrogen storage level

The electrolyser and hydrogen storage are evaluated collectively as the H2ESS component in the system, a simple diagram for which can be seen in Figure 4.6. The costs and revenues for the H2ESS are given in Table 4.11, while the OPEX for the component is given in Table 4.12.
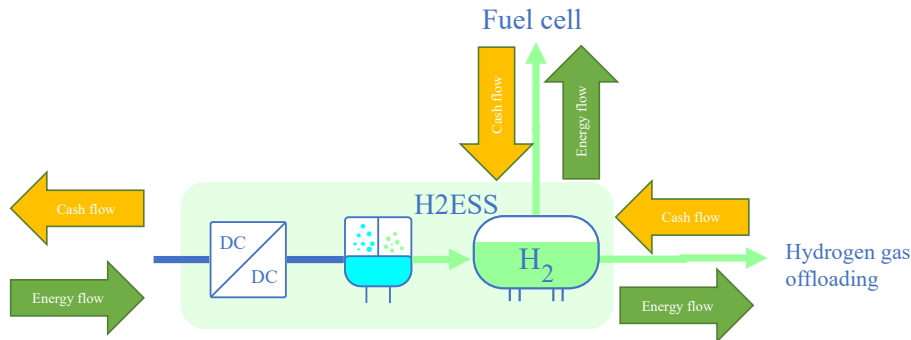


**Figure 4.6:** The H2ESS energy and cash flows.

**Table 4.11:** Costs and revenues for electrolyser and hydrogen storage in system.

| Revenue / Cost | Description | Formula | Notes |
|---|---|---|---|
| Revenue of hydrogen gas sales | Revenues of sold hydrogen gas. | Delivered hydrogen * hydrogen price | Given by simulation. |
| Revenue of hydrogen gas to fuel cell | Revenue from fuel cell "buying" hydrogen gas from storage | Hydrogen delivered to fuel cell * hydrogen price | Given by simulation. |
| Cost of bought electricity by electrolyser | Cost from electrolyser "buying" electricity from SPP | - Electricity to electrolyser from SPP * electricity price | Given by simulation. |

**Table 4.12:** Operational expenditures for electrolyser and hydrogen storage in system.

| Operational expenditures | Description | Formula | Notes |
|---|---|---|---|
| OPEX of electrolyser | Operational expenditure of electrolyser. | Electrolyser capacity * OPEX cost | Stack replacement is included. |
| Fixed OPEX of hydrogen storage | Fixed operational expenditure of hydrogen storage. | Hydrogen storage capacity * fixed OPEX | |
| Variable OPEX of hydrogen storage | Cost of energy consumption and cooling of compressor. | Hydrogen storage capacity * variable OPEX | |
| Land lease | Cost of leasing land for system. | Land lease factor * gross revenues | |

## 4.2.6 Fuel cell level

A simple diagram of the FC energy and cash flows can be seen in Figure 4.7. Tables 4.13 and 4.14 give the costs and revenues as well as OPEX for the FC in the system.
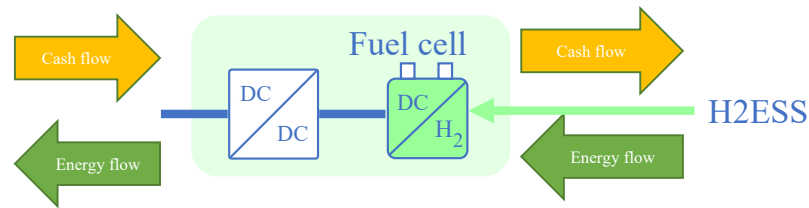


**Figure 4.7:** The fuel cell energy and cash flows.

**Table 4.13:** Costs and revenues for fuel cell in system.

| Revenue / Cost | Description | Formula | Notes |
|---|---|---|---|
| Revenue of sold electricity from fuel cell | Revenues of electricity delivered by fuel cell | Delivered electricity by fuel cell * intraday price | Given by simulation. |
| Revenue of grid benefit | Compensation for energy supplied to the grid. | Delivered electricity * grid benefit | |
| Revenue of guarantees of origin | Contractual revenue from supplying renewable energy. | Delivered electricity * guarantees of origin | |
| Cost of hydrogen gas to fuel cell | Cost from fuel cell "buying" hydrogen gas from storage | - Hydrogen delivered to fuel cell * hydrogen price | Given by simulation. |

**Table 4.14:** Operational expenditures for fuel cell in system.

| Operational expenditures | Description | Formula | Notes |
|---|---|---|---|
| OPEX of fuel cell | Operational expenditure of fuel cell. | Fuel cell capacity * OPEX cost | Stack replacement is included. |
| Land lease | Cost of leasing land for system. | Land lease factor * gross revenues | |

## 4.3 Optimising energy storage

### 4.3.1 System evaluation

In order to evaluate the system created, a number of parameters are considered. The following technical numbers are extracted from the simulation.

- Total power delivered to grid excluding wind power production [MWh]

- Electricity from the battery [MWh]

- Electricity to the battery [MWh]

- Electricity delivered to the grid by the fuel cell [MWh]

- Solar power exceeding transformer capacity [MWh]

- Solar power not exceeding transformer capacity [MWh]

- Hydrogen gas delivered to fuel cell [MWh]

- Energy sold by hydrogen storage (hydrogen gas exported) [MWh]

- Electricity to the electrolyser [MWh]

The economic numbers extracted are as follows. Please note that "bought" and "sold" does not only refer to exchanges with the grid, but also to the internal discounting between components.

- Total intraday revenues [$10^3$ SEK]

- Cost of electricity bought by battery [$10^3$ SEK]

- Revenue of sold electricity by battery [$10^3$ SEK]

- Cost of electricity bought by electrolyser [$10^3$ SEK]

- Revenue of sold hydrogen gas [$10^3$ SEK]

- Value of hydrogen gas used by fuel cell [$10^3$ SEK]

- Revenue of sold electricity from fuel cell [$10^3$ SEK]

- Revenue of sold solar electricity [$10^3$ SEK]

The total energy flows are calculated inside the simulation by integrating the power over the year. The total total cash flows are calculated by multiplying the energy flows in each instance by the instantaneous intraday price, and integrating this over the year. The different energy and cash flows by components are calculated by doing this for different power

sources. The energy storage systems only "pays" for the electricity when the site is under-producing in relation to the GCP. This is because the SPP cannot deliver power that exceeds the maximum GCP capacity, so that energy would have been curtailed had it not been for the ESS. This "free electricity" which is supplied to the ESS is included by setting the intraday price to zero when the site is overproducing in relation to the GCP.

In order to optimise the system, the energy storage will be dimensioned to make the project as economically and technically feasible as possible. The economic dimensioning will be done by comparing the IRR and LCOE of the different dimensioning attempts to each other.

To evaluate the technical features of the project, controllability and curtailment will be studied. The definition of controllability in this scenario is the system's ability to deliver a near-constant power output within the hour. This is evaluated using an average forecasting error parameter. This parameter sums the forecasting error (absolute value of the deviations from the forecast power output for each hour) and divides it by the number of hours in a year. The larger this number is, the higher the average forecast error. The curtailment should also not become too high, as this would indicate that the energy storage is not succeeding in moving the energy sufficiently in time. Of course, the system's ability to not deliver more power than the maximum capacity of the GCP will also be ensured.

Both with regards to economical and technical feasibility, the system will be compared to a system with wind power and solar power without energy storage.

### 4.3.2 Simple optimisation process

To optimise the economics of the system, the energy storage is dimensioned to maximise the IRR and minimise the LCOE without compromising the technical features of the system. This is done in an iterative process consisting of several steps.

1. The production is based on initial data analysis, and is kept at a set level from the start. The starting point for the energy storage components are set so that the operational strategy functions as intended at maximum power production, prior to reducing component sizes.

2. The battery and electrolyser powers (MW) are minimised first, as they have significant costs associated with them. Please note that the battery storage size (MWh) is always altered according to the battery power (MW), as the BESS is modular.

3. Then, the hydrogen storage size (MWh) is altered. This is associated with a lower cost to the system than the electrolyser power. However, it needs to be reduced both to enable controllability of the system and to reduce its cost.

4. The fuel cell does not play a significant role for the controllability of the system. Therefore, it is the last one to be altered.

5. The process is repeated until a stable system with the best possible IRR, lowest possible LCOE, and acceptable technical functionality has been established.

# 5 Results

This chapter will present the results of the simulation and techno-economic dimensioning. As part of the simulation results, the initial data analysis, pre-set component dimensions, operational strategy, and model performance will be reviewed. In the results of the techno-economic analysis, the outputs of the simple optimisation process as well as the dimensions and results of the optimsed model will be offered.

## 5.1 Simulation results

### 5.1.1 Initial data analysis and dimensioned components

Wind and solar power correlation is shown for a sample period in Figure 5.1. This correlation is about -20.9%. The negative correlation signifies that increased wind power relates to decreased solar power and vice versa. Because of this correlation, it can be deduced that adding a SPP to this existing WPP could be a wise choice, as it would help keep a more regular power output through the transformer.
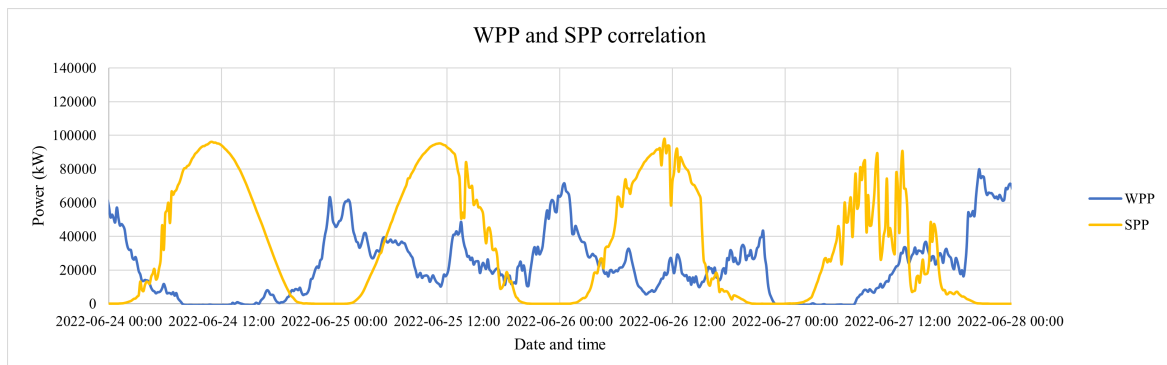


**Figure 5.1:** Wind and solar power production for a sample time period.

A natural consequence of adding more production capacity without altering the transformer is that there is an increase in curtailment. The curtailment percentages for different ratios of wind to solar power are given in Table 5.1. The ratio of 1:1 signifies the wind:solar ratio being 130:130 MW. The GCP capacity factor for the different ratios are also presented. To compare, the GCP capacity factor of the system with only the Bäckhammar WPP was 31.2% for 2021.

**Table 5.1:** Curtailment and GCP capacity factors for different wind-solar ratios.

| Ratio of wind power:solar power | Solar curtailment (%) | GCP capacity factor (%) |
| --- | --- | --- |
| 1:1 | 7.4% | 44.3% |
| 1:1.5 | 21.8% | 48.6% |
| 1:2 | 36.4% | 51.3% |

Duration curves have been generated to show how often a given amount of power is being produced by the wind and solar units during 2021 and 2022, see Figure 5.3a. The maximum capacity of the GCP is also shown, all power above this capacity would normally be curtailed. It is evident that as the solar production increases its ratio, the amount of curtailment increases, as seen in Table 5.1. This is the amount of energy that could potentially be stored by the energy storage system.

To allow an ESS, with an emphasis on bulk energy storage, to actually be used, there needs to be sufficient excess power produced. Therefore, the ratio of wind to solar power production that is chosen is 1:2 (130:260 MW).

However, as mentioned in Section 3.1, it is commonplace to oversize the solar power output in relation to its inverters in order to increase the amount of full load hours. Since the output will be oversized by 30%, the total DC-capacity of the SPP will become 260 * 1.3 = 338 MW, while the capacity of the inverters remain 260 MW. The annual production profile for such a SPP can be seen in Figure 5.2. The duration curves after implementing the oversized SPP can be seen in Figure 5.3b.
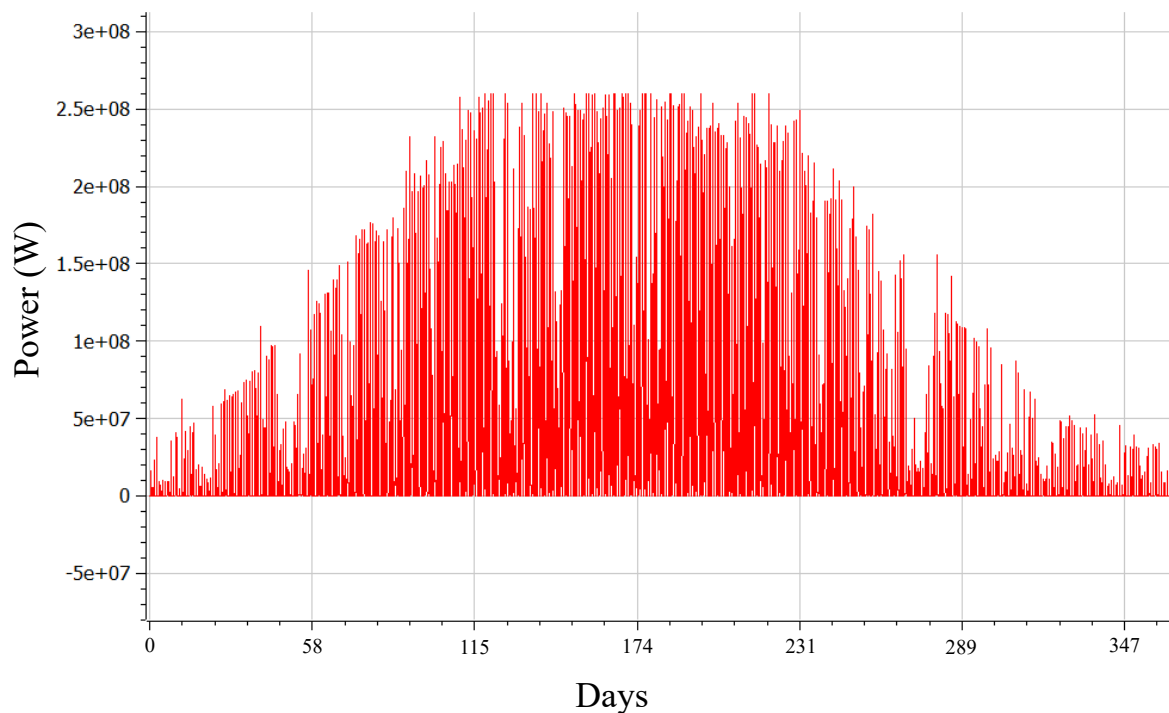


**Figure 5.2:** Annual production pattern of a SPP which has been overdimensioned by 30% compared to its converters, and capped at 260 MW.
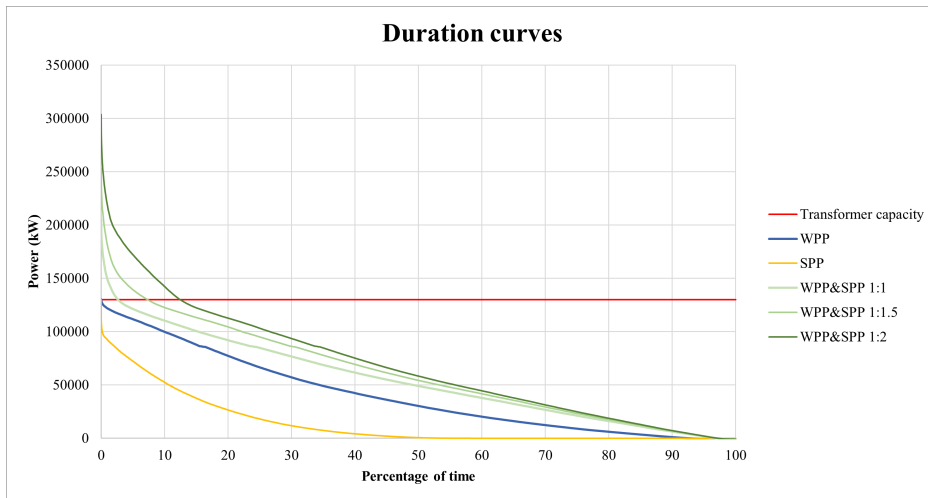
**(a)** Duration curves without oversizing the SPP.
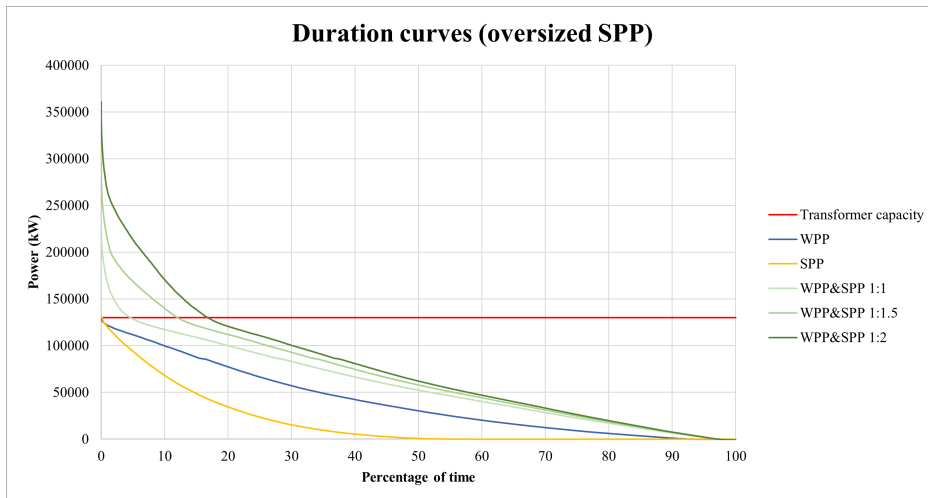


**(b)** Duration curves after oversizing the SPP by 30% and capping production at 260 MW.

**Figure 5.3:** Duration curves for different ratios of wind and solar power, with and without oversizing and capping.

The annual production profile for the Bäckhammar WPP in 2021 can be seen in Figure 5.4.
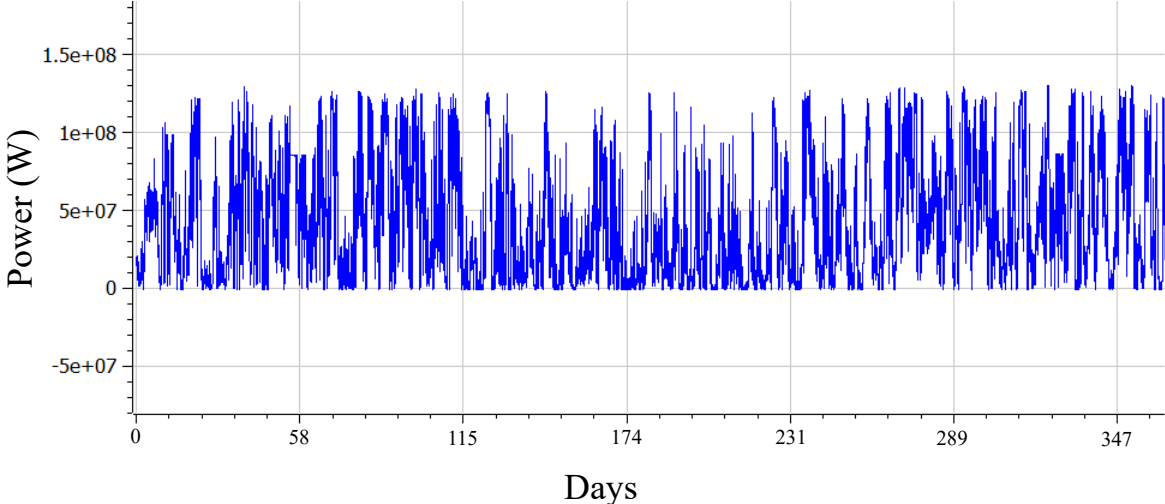


**Figure 5.4:** Annual production pattern of the Bäckhammar WPP.

The result of combining the SPP and WPP production for the year can be seen in Figure 5.5.
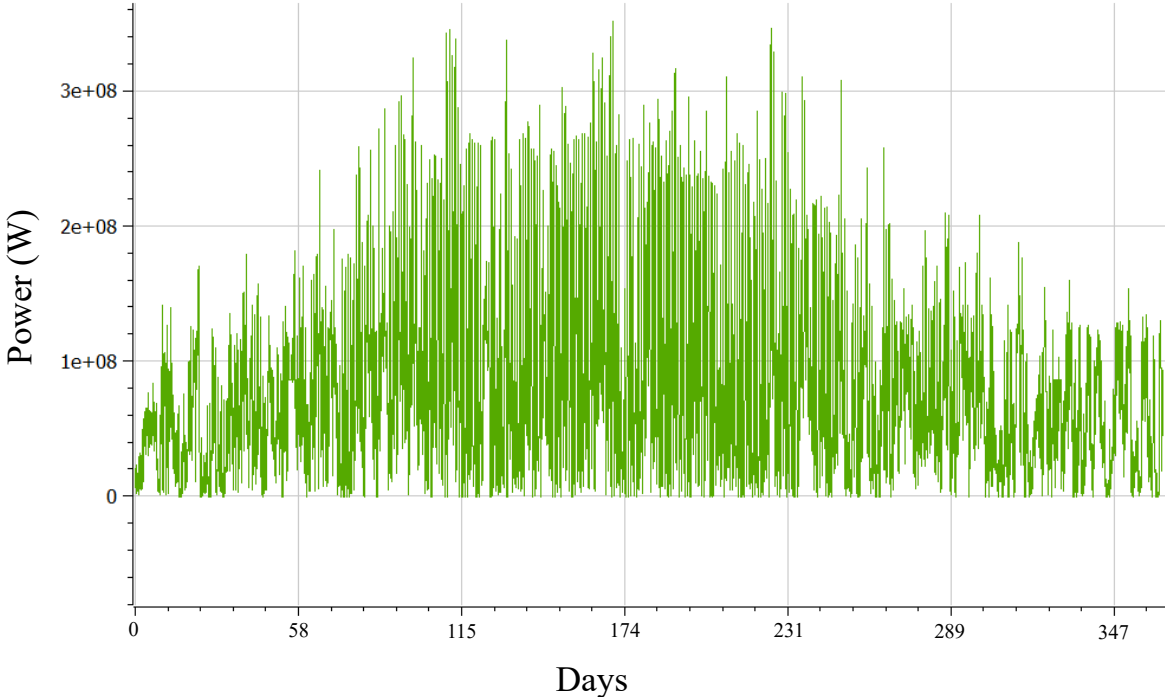


**Figure 5.5:** Annual production pattern of the combined Bäckhammar WPP and SPP.

A graph showing wind power production and spot price is created to show the impact of the cannibalisation effect of wind power, see Figure 5.6. The cannibalisation effect is a term used to describe how increased wind power penetration results in lower electricity prices, therefore making wind power less profitable at times of high production (Prol et al. [58]). By observing the graph, it is clear that effects of cannibalisation are prevalent in this scenario.

This effect is one reason why utilising energy storage could make a lot of sense for wind power. Since wind power production often negatively correlates with the spot price, moving
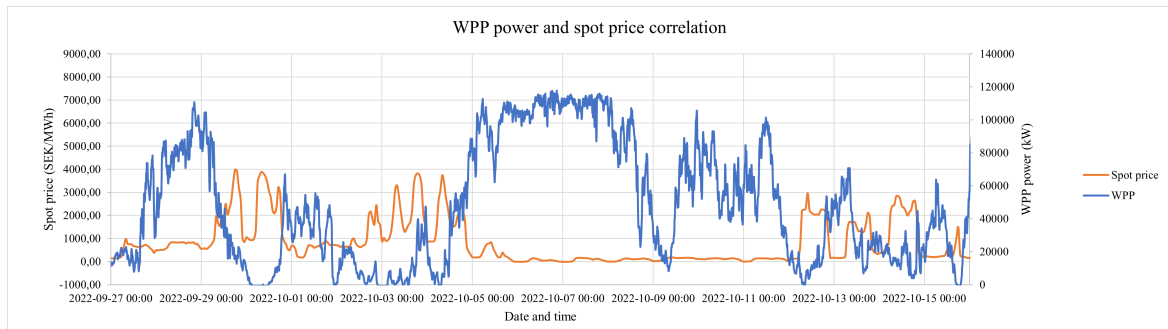
**Figure 5.6:** Relationship between spot price and wind power production at the Bäckhammar site.

the power distribution through time or producing hydrogen to sell instead is an efficient way to increase profitability.

## 5.1.2 Operational strategy

A three-day period of the simulated year is chosen to present the results of the system's operational strategy. Various values will be presented to explain the behaviour of the model, Scheduler and Controller. The following figures show that the operational strategy presented satisfies the conditions outlined in Section 2.9.

The features of the Scheduler and Controller will be presented using specific events in the figures. The power to grid, forecast production, actual production and curtailed solar power are all normalised in relation to the GCP's maximum capacity of 130 MW. The power to electrolyser and fuel cell are normalised to their respective maximum capacities. The state of the battery (expressed as SOC) and hydrogen storage (expressed as SOH) are also normalised, i.e 0 signifies an empty storage while 1 signifies a full storage. The intraday price and Bollinger bands are normalised to the highest occuring price of the year. A graph with all values included can be viewed in Appendix C.

Figure 5.7 shows power to grid, forecast power production, real power production, and curtailed power. Events A, B and C are examples of the Controller protecting the GCP during times of overproduction. Despite the power production exceeding the GCP maximum capacity, the power to grid does not exceed the maximum limit. The Figure also shows that the power to grid is kept constant during all hours of the three-day period.
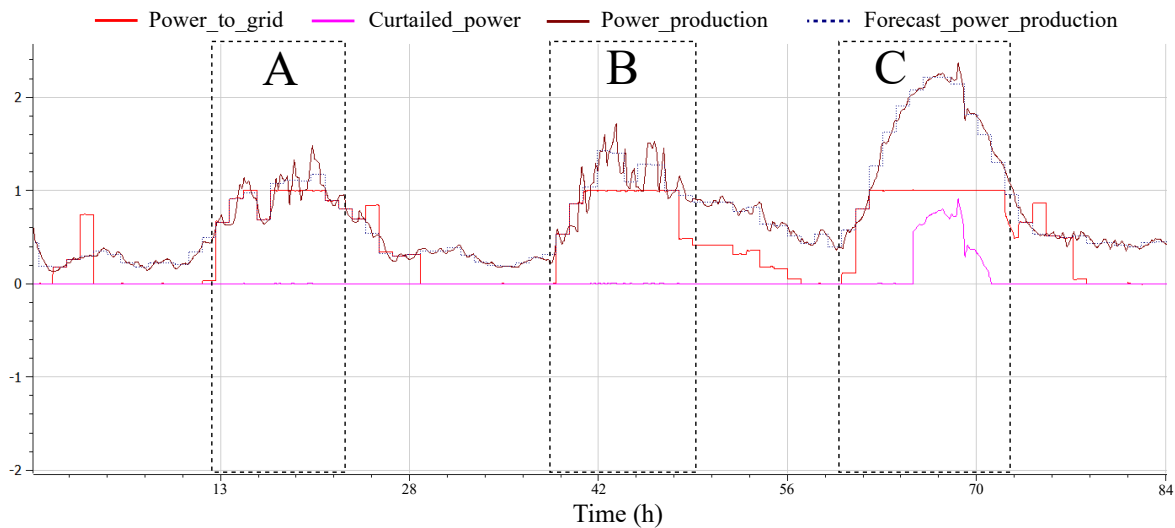
**Figure 5.7:** Simulation plot of power to grid, forecast production, real production, and curtailed solar power.

Figure 5.8 shows power to grid, SOC, and forecast power production. The events D and E show the feature of energy arbitrage. During event D, the power to grid surpasses the forecast power production while the SOC is lowered significantly. In event E, the opposite effect takes place. The SOC increases while the power to grid is lower than the forecast power production. However, these two events on their own do not signify that energy arbitrage is achieved, so more information is needed.

The Scheduler often prepares for overproduction, one clear example of this is event F. The Scheduler has signalled to the Controller that the battery should be discharged. In this case, the electrolyser is used to discharge the battery. This is evident since the power to grid and forecast power remain the same while the SOC decreases.

By discharging the battery ahead of overproduction, the system is capable of absorbing as much excess power as possible. This worked well at event D, but at event G, overproduction is particularly high. This results in the battery becoming fully charged. Now that the battery is full, it cannot absorb any more energy. Therefore, the Controller stops charging the battery and begins curtailing energy. This curtailment can be seen during event C in Figure 5.7. Note that event C encompasses event G.
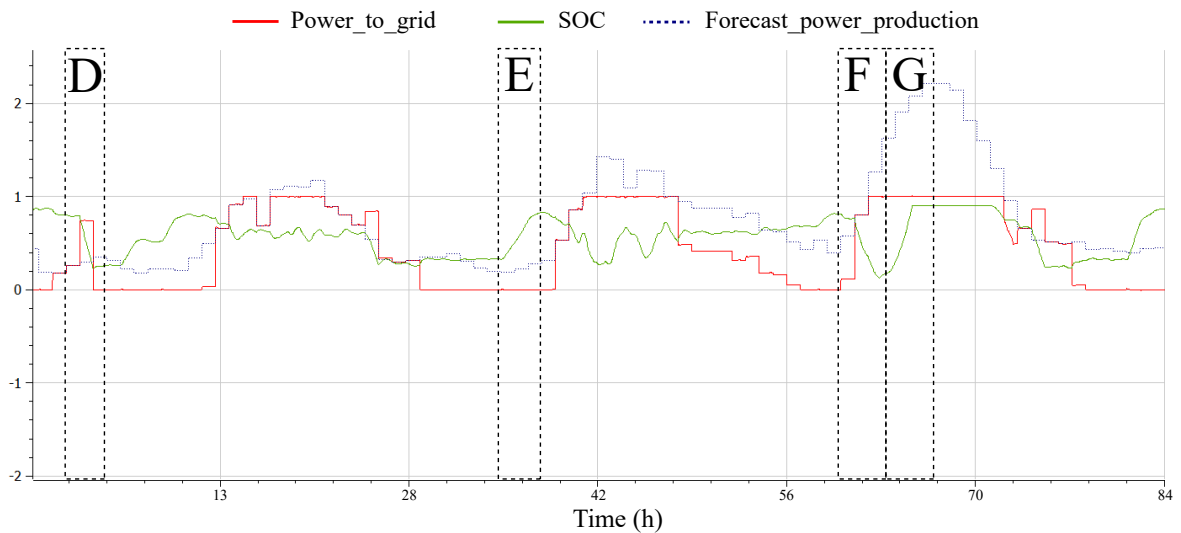
**Figure 5.8:** Simulation plot of power to grid, forecast production, and battery state of charge.

In Figure 5.9 the power to grid, forecast power production and intraday price are shown be seen. The events H and I correspond directly to events D and E in Figure 5.8. By comparing these events to eachother, the Scheduler's ability to set the HESS to discharge at high prices and charge at low prices can be confirmed. At event H, the intraday price is seen to be at a local high and at event D, it can be observed that power is sold as the battery is discharging. At event I, the intraday price is at a local low, which corresponds to the battery charging at event E.
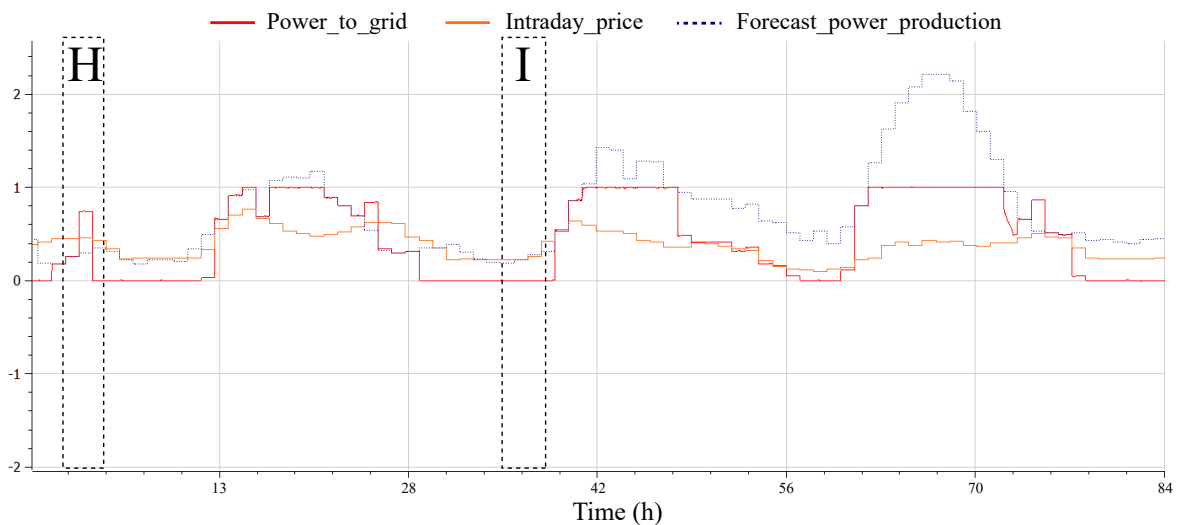


**Figure 5.9:** Simulation plot of power to grid, forecast production, and intraday price.

The power to grid, forecast power production, SOH, and electrolyser power are showcased in Figure 5.10. At event J, another example of preparation for overproduction can be seen. The electrolyser is activated prior to overproduction in order to lower SOC, giving the battery room to absorb energy during overproduction. This lowered SOC can be seen when inspecting Figure 5.8 at the same time period as event J.
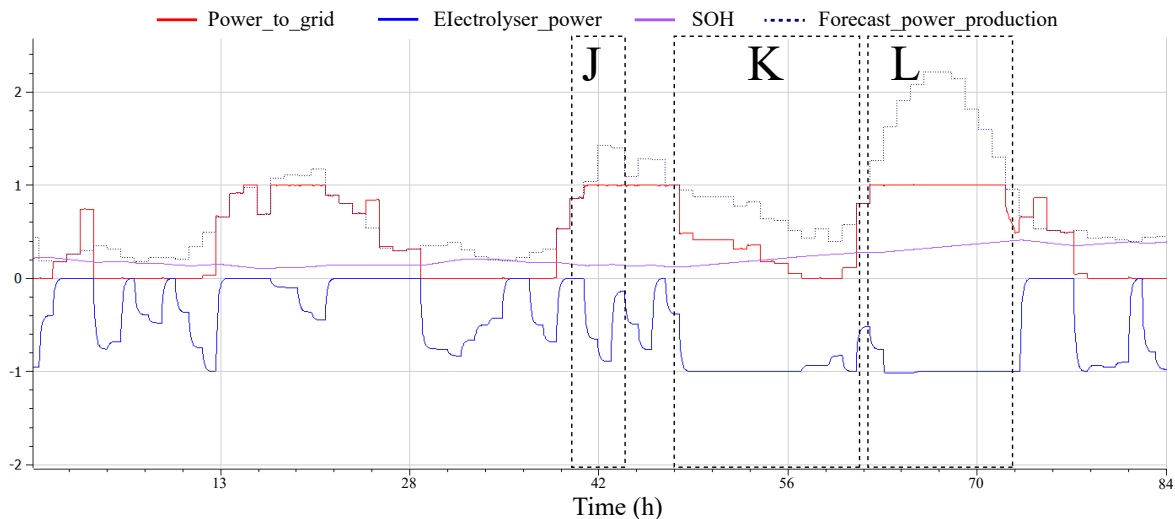
**Figure 5.10:** Simulation plot of power to grid, forecast production, state of hydrogen storage, and electrolyser power.

Event K constitutes as an example of when the intraday price is lower than the acceptable price to produce hydrogen. During event K, the power being produced exceeds the electrolyser's maximum capacity. This means that the electrolyser can be fully active to produce hydrogen, lowering the power to grid by a constant amount compared to the forecast power. When the next hour's forecast power production no longer exceeds the electrolyser's maximum power output, the electrolyser lowers its output so it only absorbs the amount necessary.

Event L occurs at the same time as events F and G, and it presents the attempt to prepare for overproduction using the electrolyser. The preparation by the Scheduler was not sufficient in this case, so the battery SOC is increasing. Instead of curtailing all excess power, the electrolyser stays active to recover as much energy as possible.

### 5.1.3 Model performance

The simulation of the model has overall been successful. Despite the model being quite complex, all necessary components could be implemented and could interact with each other without presenting with issues. Also, the two-part operational strategy could successfully be implemented, and could work well together despite having many moving parts.

As the component sizes decreased, the simulation became more prone to crashing. This made it difficult to further decrease the size of components, especially the battery. The results of the operational strategy are unaffected by this. The only results affected by crashing are the chosen dimensions, as not all combinations could be evaluated.

## 5.2 Techno-economic dimensioning results

### 5.2.1 Simple optimisation process

The results of the economic dimensioning will be presented in this section. Section 4.3.2 outlines the process followed for the economic dimensioning. As previously explained, the initial component dimensions are generous in order to ensure the system works as intended (i.e. the operational strategy is successful) prior to reducing their sizes.

The economic results of the original dimensions are called 1A, as a reference to it being part of the first step of the process outlined in Section 4.3.2. The naming of the other dimensioning attempts will be done in the same way, with a number denoting which step it is part of and a letter to denote which attempt it is. Please note that dimensions that caused the simulation to crash are not presented in this section, so plenty more attempts were carried out besides those listed in the tables.

Trend lines are used in Figures 5.11 and 5.12 to clarify how parameters are altered between attempts. The red colour is associated with a negative trend (reduction between the first and final number), the yellow colour means a parameter has been unchanged, and the green colour means that there is a positive trend (increase between the first and final number). The colours do not indicate a good or bad result, only a change in the size of a number between attempts.

The factors being considered when deciding in what way parameters should change for the following dimensioning attempt are IRR, average forecast error and energy curtailed. Please note that both pre- and post-tax IRR are presented. This is because attempts that have more years with a positive cash flow are more heavily taxed than those with fewer years with a positive cash flow.

Throughout all attempts, the FC capacity factor always ended up being 0. Therefore, this component was eliminated for all attempts as it always negatively impacted the IRR of the system.

In the first step, the battery and electrolyser powers are decreased, see Figure 5.11. First, the electrolyser power was decreased, see attempt 2A. The system remained stable but the IRR became very low. Then, the battery power was decreased, see attempt 2B. This is the lowest battery power possible with the other dimensions being used. This generated a better IRR than attempt 2A, and will therefore be the starting point for step 3. Note that despite having a lower IRR than attempt 1A, this attempt is chosen as the next starting point since the goal for step 2 is merely to minimise the electrolyser and battery powers as much as possible.

| Step 2 | 1A | 2A | 2B | Trend line |
|---|---|---|---|---|
| Battery power (MW) | 110 | 110 | 90 | |
| Battery storage (MWh) | 132 | 132 | 108 | |
| Electrolyser power (MW) | 110 | 60 | 60 | |
| Hydrogen storage (MWh) | 7000 | 7000 | 7000 | |
| Battery capacity factor (%) | 11.59% | 9.34% | 10.71% | |
| Electrolyser capacity factor (%) | 52.89% | 55.38% | 55.33% | |
| SPP capacity factor (%) | 13.60% | 13.05% | 12.99% | |
| GCP capacity factor (%) | 26.45% | 32.05% | 31.99% | |
| Average hourly forecast error (MWh/h) | 0.24 | 0.31 | 0.33 | |
| Solar curtailment (%) | 0.46% | 4.48% | 4.93% | |
| **LCOE (SEK/MWh)** | **1070** | **1164** | **1141** | |
| **Pre-tax IRR (%)** | **3.37%** | **0.86%** | **1.53%** | |
| **Post-tax IRR (%)** | **2.38%** | **0.13%** | **0.81%** | |

**Figure 5.11:** Dimensions and outputs from step 2 of dimensioning.

Then, attempts were made to decrease the size of the hydrogen storage, see Figure 5.12. Attempts 3A, 3B, and 3C show that decreasing the hydrogen storage has a positive effect on the investment IRR. However, attempt 3D decreased the hydrogen storage too much, resulting in a lower IRR than in attempt 3C. In attempt 3D, the curtailment also increased while the electrolyser capacity factor decreased, making it clear that the electrolyser had less room for action. Therefore, a hydrogen storage of 500 MWh is chosen.

| Step 3 | 2B | 3A | 3B | 3C | 3D | Trend line |
|---|---|---|---|---|---|---|
| Battery power (MW) | 90 | 90 | 90 | 90 | 90 | |
| Battery storage (MWh) | 108 | 108 | 108 | 108 | 108 | |
| Electrolyser power (MW) | 60 | 60 | 60 | 60 | 60 | |
| Hydrogen storage (MWh) | 7000 | 2000 | 1000 | 500 | 200 | |
| Battery capacity factor (%) | 10.71% | 10.73% | 10.78% | 10.96% | 11.59% | |
| Electrolyser capacity factor (%) | 55.33% | 55.24% | 54.79% | 53.53% | 47.41% | |
| SPP capacity factor (%) | 12.99% | 12.99% | 12.99% | 12.99% | 12.95% | |
| GCP capacity factor (%) | 31.99% | 32.03% | 32.23% | 32.81% | 35.53% | |
| Average hourly forecast error (MWh/h) | 0.327 | 0.328 | 0.328 | 0.331 | 0.331 | |
| Solar curtailment (%) | 4.93% | 4.93% | 4.93% | 4.93% | 5.25% | |
| **LCOE (SEK/MWh)** | **1141** | **594** | **486** | **433** | **406** | |
| **Pre-tax IRR (%)** | **1.53%** | **12.42%** | **14.89%** | **15.89%** | **15.54%** | |
| **Post-tax IRR (%)** | **0.81%** | **10.17%** | **12.23%** | **13.04%** | **12.74%** | |

**Figure 5.12:** Dimensions and outputs from step 3 of dimensioning.

## 5.2.2 Dimensions and results of optimised model

The final dimensions chosen after optimisation can be observed in Figure 5.12 as attempt 3C. These dimensions generate the best IRR out of all evaluated dimensions, with a 15,9% pre-tax IRR and a 13,0% post-tax IRR. Besides this, the dimensions result in the model having a low average forecast error and low percentage of energy curtailed. In the following section, other metrics of interest such as individual IRR and LCOE for components will be presented. The results given by the optimised model will be compared to the results of a model without energy storage curtailing all excess power.

The system and individual component energy flows, cash flows, IRR, LCOE, and capacity factors can be seen in Figure 5.13. The energy and cash flows are summations of all yearly contributions to costs and revenues presented in Section 4.2.1. The system refers to the combined appraisal of adding the BESS, H2ESS and SPP while excluding the existing WPP from energy and cash flows.

| Optimised model results | Direction | Energy flow (MWh/year) | Cash flow (kSEK/year) | Pre-tax IRR (%) | Post-tax IRR (%) | LCOE (SEK/MWh) | Capacity factor (%) | Initial invesmtment (kSEK) |
|---|---|---|---|---|---|---|---|---|
| System | in | - | 410 601 | 15.89% | 13.04% | 433 | 32.81% | 2 247 259 |
|  | out | 177 239 | 63 384 | | | | | |
| H2ESS | in | 280 967 | 184 264 | 40.33% | 33.08% | 286 | 53.53% | 365 674 |
|  | out | 209 427 | 44 524 | | | | | |
| BESS | in | 45 372 | 14 003 | - | - | 1371 | 10.96% | 711 585 |
|  | out | 36 813 | 7 708 | | | | | |
| SPP | in | - | 180 739 | 15.95% | 13.41% | 617 | 12.99% | 1 170 000 |
|  | out | 295 480 | 9 889 | | | | | |

**Figure 5.13:** Key values for system and components of the chosen model.

Please note that energy and cash flows in and out do not strictly relate to the grid. As aforementioned, an internal discounting is performed on component-level in order to appropriately place costs and revenues. For example, the BESS has an energy flow in from the SPP, and an energy flow out both to the H2ESS and GCP. This means that its cash flow in consists of revenues both from the H2ESS "buying" power from it, but also from electricity sales to the grid. Its cash flow out only consists of the cost of electricity it pays to the SPP.

In the figure, it is apparent that the system never imports energy from the grid. The LCOE of the system is 433 SEK/MWh. To put this into perspective, the LCOE of onshore wind in the EU in 2018 which was about 670 SEK/MWh, see Section 2.2.2. This number for Sweden in 2021 was in a range between 240 and 260 SEK/MWh (Elmqvist et al. [11]). The capacity factor of the GCP is 32.8%. The total initial investment amounts to about 2.25 billion SEK.

The H2ESS has the highest pre-tax IRR (40.3%) and lowest LCOE (286 SEK/MWh) of all components in the system, indicating that it could be a very good investment. The capacity factor of the electrolyser is 53.5%, indicating that it is active the majority of the time. Figure 5.13 also shows that about 209 GWh of hydrogen gas are exported per year. With the energy density of hydrogen gas being 33.33 kWh/kg (U.S Department of Energy [82]), this corresponds to an export of about 6 300 tonnes per year and an average of about 17 tonnes per day. It is worth noting that the initial investment for the H2ESS is about half of the initial investment for the BESS.

The BESS is the only component which has a non-applicable IRR since it is never profitable in the system. It also has a very high LCOE and the lowest capacity factor out of all the

components in the system. One interesting revenue it brings is the revenue from balancing cost reduction, at a value of 545 thousand SEK. This is shown in Appendix D. As previously noted in Section 4.2.4, this value is not calculated in a completely realistic way, as the average forecast error is estimated as the sum of all energy deviations during the year, divided by the hours per year (MWh/year). This value for the stand-alone WPP system is then subtracted by this value for the implemented HESS system. The difference is then multiplied by the imbalance fee to get an indication of how much money could be saved on fees by reducing the error.

The SPP naturally does not have an energy flow in, but delivers all of its energy to the remaining system. Its pre-tax IRR of 16% indicates that it is a positive investment. In this system, the capacity factor of the SPP is lower than the initial data analysis for the system with wind and solar power without energy storage (13% vs. 13.9%). The LCOE for the SPP in this system is much lower than the LCOE for most EU countries in 2018, being 617 SEK/MWh as opposed to 1136.8 SEK/MWh, see Section 2.3.2. However, it is slightly higher than the LCOE for new utility-scale SPPs in Sweden in 2021, which sits between 290 and 520 SEK/MWh (Elmqvist et al. [11]). The initial investment for the SPP makes up about half of the total initial investment.

The investment appraisal in its entirety is located in Appendix D.

A comparison of the results to the model without energy storage can be seen in Figure 5.14. As aforementioned, this model consists of a WPP and SPP with the same dimensions as those in the final model, but without the ESS. The addition of energy storage and operational strategy presents a 26% higher pre-tax IRR, a 92% reduction in average hourly forecast error, a 65% higher LCOE, and a 36% lower GCP capacity factor. The capacity factor for the SPP is understandably lower for the system without the energy storage since it has a significant curtailment of 28%, compared to the 5% after implementing the ESS.

| Comparison to no storage | No storage | Final model | Percentage change |
|---|---|---|---|
| Initial investment (kSEK) | 1 170 000 | 2 247 259 | 92% |
| Pre-tax IRR (%) | 12.64% | 15.89% | 26% |
| Post-tax IRR (%) | 10.64% | 13.04% | 23% |
| LCOE (SEK/MWh) | 262 | 433 | 65% |
| GCP capacity factor (%) | 51.63% | 32.81% | -36% |
| SPP capacity factor (%) | 9.89% | 12.99% | 31% |
| Average hourly forecast error (MWh/h) | 4.27 | 0.33 | -92% |
| Solar curtailment (%) | 27.62% | 4.93% | -82% |

**Figure 5.14:** Comparison of key values between model with no storage and the chosen model.

# 6 Discussion

The following chapter constitutes a discussion based on the results previously presented. Among other things, operational strategy, model performance, investment appraisal, implications for future investments, and further research suggestions will be examined.

## 6.1 Initial data analysis

The initial data analysis shows that by adding a solar capacity of 130 MW to the system, only 7.4 % of the total solar production would be curtailed. This is fairly low, and therefore indicates that the wind and solar production profiles are quite well-adapted to each other in this location.

To have a useful energy storage solution for bulk storage, a ratio of wind to solar power of 1:2 (130:260 MW) was chosen. A ratio of 1:1.5 could also have been chosen if the goal was to curtail as little as possible or to achieve even smaller component sizes. By oversizing and capping the solar power, more energy can also be stored, since this allows for more full load hours to occur during the year.

Because of the cannibalisation effect, a lot of money can be made off of wind power. By producing hydrogen at times of low electricity price, when wind production is high, the profit margin of hydrogen gas becomes higher than when it is produced at times with high electricity price. Because this is so profitable, energy storages could work to counteract the cannibalisation effect in the long run.

## 6.2 Operational strategy

In the simulation, it could be observed that the Controller switches states appropriately and at the right time. It is also robust, in the sense that it can continue to operate as intended despite switching cases often. One room for improvement in the Controller relates to market behaviour. In real life, forecast errors are not accounted for instantaneously, but rather as an average for one hour. For this reason, it is a bit excessive to require that the Controller keeps the power output constant during the hour. Keeping the power constant requires that the battery operates even at times where the errors would have ended up cancelling each other out at the end of the hour.

One approach that could reduce the unnecessary work the battery carries out, and the losses this entails, is to calculate the expected delivered energy for the next hour and adjust the battery accordingly so that at the end of the hour, the correct amount of energy has been delivered. This solution is better adapted to how the market is designed today, but the solution presented in this thesis may be better adapted for future markets. If the system is

able to keep the power output constant during the hour, this also suggests that it will be more than capable to operate on the intraday markets with shorter time spans that are under development (such as 15- and 30-minute intraday markets).

The results demonstrate that the operational strategy makes the correct decisions at the right times and that most bugs seem to have been eliminated. The Scheduler exhibits the correct behavior as it correctly prepares the battery for future hours of overproduction, recharges the energy storage at low prices, and discharges it at high prices.

One aspect that was not investigated extensively in this thesis is whether the chosen levels at which the Scheduler plans to keep the battery SOC at are the optimal ones. Since the solar power heavily affects the total power production and because of its periodic nature, if overproduction ends, it is not likely to be followed by another hour of overproduction. Therefore, it might have been better to plan the highest possible SOC after periods of overproduction to be able to sell as much energy as possible during the next highest price incoming in the next afternoon and night.

Sometimes, as can be noted in the beginning and end of Figure 5.10, the decision to use all energy to produce hydrogen is made as opposed to delivering power to the grid. This is because if producing hydrogen is more lucrative than delivering power to the grid, the Scheduler will try to produce as much hydrogen as possible while neglecting the grid. Combined with the fact that the assumed hydrogen price is often above the intraday price, this is likely one of the reasons why the capacity factor of the GCP only increases marginally after implementing the HESS.

## 6.3   Model performance

Some sources of error occur due to operational assumptions, parameter assumptions, and the chosen simulation program.

One assumption made for the operation of the model is that the forecast error is a constant shift in time of production, as described in Section 4.1.2. This is simplified compared to the real case, as a forecast error can both consist of a shift in amount of energy or a shift in time. Also, forecast errors are not constant and do not necessarily occur for each hour of operation. This assumption is likely a disadvantage to the system, and might impact the result by challenging the controllability of the system.

Parameter assumptions also make for sources of error. The biggest source of error might be that, for the techno-economic parameters in the simulation, sources stating costs for both 2023 and 2030 are included. Preferably, one would only include sources predicting costs for 2030. However, sources deemed to be very reliable, such as budgetary offers, were prioritised over cost and technical projections for certain components when these projections varied significantly. This is the case for both the BESS and the SPP.

Furthermore, the degradation rates of the components are not taken into account besides their effect on component lifetimes. This has an advantageous effect on the results as degradation normally has a negative impact on the efficient power yield of each component.

Finally, the simulation software used could be a cause for some errors. For instance, the step response in the PI regulators of the electrolyser and battery are not in line with reality. The step response of the electrolyser is about 40 minutes, which is significantly higher than the 10 seconds estimated for 2030 by Clean Hydrogen Europe, the source used for the remaining response times (Clean Hydrogen Europe [7]). This was overlooked because the system became unstable when the electrolyser responded too quickly. Also, the hysteresis used in the simulation can cause output data inaccuracies since components do not activate and deactivate at precise values.

In general, the implementation in OpenModelica presented some instability issues. The simulations were quite sensitive and prone to crashing which limited the ability to exhaust all combinations of component dimensions. If possible, it would have been particularly interesting to reduce the battery power further.

## 6.4 Dimensions and results of optimised model

The results of the dimensioning indicates that for the constructed system, with the chosen operational strategy and assumptions made, this investment would be very profitable. The pre-tax IRR of 15.9% is exceptionally high for pilot projects using cutting-edge technology.

The results of the system show that the components of the energy storage system can be made significantly smaller than the added production capacity (260 MW), yet still provide the intended features discussed in Section 3.4.1. However, the component sizes are still very large, especially the electrolyser which has a power capacity amongst the largest in the world, even compared to future electrolyser projects. The size of the battery storage is also large, but within the limits of existing battery storage sites today. The total initial investment is large, but not larger than other projects of similar magnitude (SSAB [64], Patel [53]).

The H2ESS, made up of the electrolyser and hydrogen storage, is by far the most profitable component of the system, as can be seen Figure 6.1. Since the FC was deemed to be un-profitable in this system, none of the revenue generated by the H2ESS can be attributed to electricity delivery to the grid. This indicates that hydrogen gas may be more suitable as a means for energy storage, as opposed to electricity storage. To aid in the green transition, hydrogen gas will likely play an important role in many different sectors in the future.
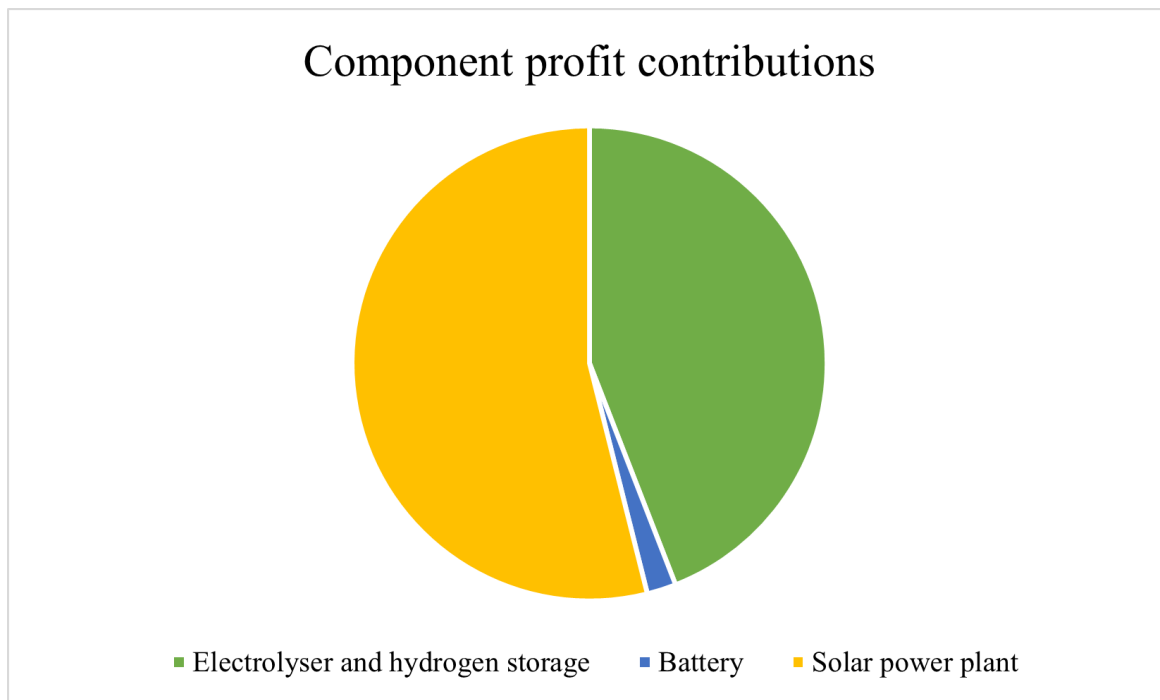
**Figure 6.1:** Profit contributions to the system by different components.

The average daily amount of hydrogen that needs to be exported is 17.6 tonnes. This amount would best be handled by distribution pipelines (IRENA [42]). If compressed hydrogen trucks at 500 bars with a capacity of 1.1 tonnes were be to used instead to export the hydrogen, about 16 trucks per day would be required. The high and low rate of export presented would amount to about 19 and 13 trucks per day respectively.

While the FC is not economically self-sufficient in this simulation, it is worth noting that this is based on the electricity prices of 2021, and hydrogen price projections for 2030, while the component costs are based on predictions for 2030. It is difficult to predict future electricity and hydrogen prices, but it is possible that the electricity prices in 2030 will be high enough or that the hydrogen price will be low enough to make FCs economically worthwhile. Also, the possible future increase in Baseload PPAs (detailed in Section 2.8) could make the FC more profitable in the future. FCs could also potentially participate on some ancillary service markets.

The investment appraisal for the battery indicates that it makes for a very unprofitable investment in all scenarios. This could be a result of the many indirect effects the battery has on the system that go unaccounted for in the investment appraisal. The effect of controlling the energy flows in real time does not contribute significantly to the battery revenues. However, it enables the entire system to function. Another revenue stream that goes unaccounted for is the internal revenue of when the battery supplied the electrolyser with electricity. This should result in a revenue to the battery and a cost for the electrolyser. Without this revenue, the battery provides free electricity to the electrolyser, resulting in a better investment appraisal for the electrolyser and a worse one for the battery. One stream of revenue not investigated in this thesis is the battery's participation on the ancillary service markets. The Scheduler could be altered to allow for these markets to be integrated. Another cause for the poor profitability of the BESS can be attributed to the initial investment costs being out of proportion in relation to the costs of other components. Costs for other components are

based on projections for 2030, while costs for the BESS are not.

One way to make the investment appraisal more accurately reflect the profitability of the system is by setting up a separate investment appraisal for the HESS which includes both the BESS and H2ESS. This would make a lot of sense because, as previously noted, the BESS is a necessary component in order for the HESS to fulfil its technical features.

The results indicate that the SPP also is very profitable in this system. Since the contributions from wind power are ignored for both the system with and without energy storage, the parameters for the SPP in the storage system and the no storage system are easily compared, see Figures 5.13 and 5.14. The pre-tax IRR for the system without storage is 12.6% while the same number for the SPP in the energy storage system in 16%. It is clear that integrating the SPP in the system with hydrogen and battery storage makes it an even better investment.

It is worth noting that the future predictions used for many parts of the economic analysis are unsure, as technology and politics are both in constant motion. This could for example impact the hydrogen price, hydrogen demand, and the electrolyser and FC costs.

There are some expenditures such as the variable OPEX of the battery and hydrogen storage that are caused by energy consumption. These expenditures are simplified by multiplying the energy handled by these components by the average electricity price for the entire year. By instead including the energy consumption of the components inside the model, a more accurate representation of the costs aggregated by consumption could be shown.

## 6.5 Implications for investments

This thesis shows that investing in a hybrid energy storage system for wind and solar production at an existing onshore wind power site is, based on electricity prices for 2021 as well as investment and hydrogen price projections for 2030, very economically sustainable. Although this does not appear to apply to all parts of the system, it is worth noting that the battery is a necessary component to support the functions of this system.

One alternative investment to the provided system in this thesis is to simply increase the capacity of the GCP in order to install more solar power at the same site. Although this might be a cheaper alternative upfront, it does not offer the ability to partake on the growing hydrogen market. Also, it does not to the same extent provide easier access to both the ancillary service and intraday markets. Furthermore, the system in this thesis makes renewable energy completely controllable within the hour, which is unique and could be a step in the right direction for an increased penetration of VRES in the power grid.

There are some requirements that need to be fulfilled in order to make this solution happen. For example, there needs to be opportunities to transport large amounts of hydrogen, which requires access to infrastructure and technology development. Also, there needs to be plenty of land surrounding existing onshore wind sites to make room for the new components and infrastructure.

This thesis also underlines that, with the correct dimensions, HESS can help mitigate the need to expand GCPs or increase transformer capacity before installing more variable re-

newable capacity on a given site. Since GCPs and transformers account for substantial investments and lead times when expanding energy production, this conclusion makes expanding renewable energy production rapidly seem more optimistic.

# 6.6 Future development

## 6.6.1 Market development

The future development of the hydrogen market is a large contributor to the viability of this system. Not only does the system quite heavily rely on hydrogen gas as a means to generate revenue; it also relies on it to actually be able to handle all the excess power that is installed on-site. If the market is saturated with hydrogen gas, the hydrogen storage would fill up and the ability to produce hydrogen at hours of high production would be lost.

Developments in the electricity markets also have a significant impact on the solution presented in this thesis. The intraday market is currently not that big in Sweden compared to the day-ahead market. In order for the solution to work as presented in this thesis, the development of the intraday market is crucial.

However, there are some modifications that could quite easily be made to the model to allow it to participate on the day-ahead market instead. The changes would be to either change the Scheduler, so that it never plans to deliver electricity below the forecast output, or to introduce a hybrid market participation on both the day-ahead and intraday markets. If participating on both markets, the Scheduler can plan to deliver electricity according to the production forecast, but adapt the power output to grid if intraday bids are present in the coming hours. That way, the strategy could both satisfy the intraday bids and meet the production forecast. The deployment of faster intraday markets would also present many possibilities, as it would allow the Scheduler to make more decisions in the same amount of time.

## 6.6.2 Technological development

Future technological developments that could benefit this system are first and foremost component developments, which could lower costs and increase efficiencies. While batteries have been used as energy storage for a long time, the components relating to hydrogen storage and FCs are not as well-developed. Hydrogen conversion and storage technologies still face challenges that require cost-effective solutions. With more cost-effective hydrogen conversion and storage technologies, the market penetration rate of hydrogen could increase.

Learning rate is a term that denotes the rate at which production costs reduce as deployment increases because of improvements in manufacturing and technology (Taibi et al. [75]). The expected learning rate for PEMELs between 2020 and 2030 is 13%, while the learning rate for PEMFCs based on proprietary data is 15%.

## 6.7    Further research

There are several areas of further research that could add to the results of this thesis. The main areas are stability improvements or model rebuild, integration of more markets, a more in-depth economic analysis with better behind-the-meter appraisal and a more sophisticated optimisation of dimensions.

The simulated system had some stability issues when component sizes was significantly reduced. These instabilities could likely be eliminated through a more thorough investigation. With the instabilities eliminated, a more effective optimisation could be achieved and a better system could be dimensioned.

As for the model rebuild, it would be interesting to implement the ability for the system to buy energy from the grid at times of low or no local production. The strategy would still be able to find the right times to buy energy, and the right times to sell it, in order to maximise profit.

It would also be very interesting to integrate more markets into the simulation, especially the ancillary service markets and intraday market. This would change how parts of the control strategy works. For example, having a constant power output through the GCP during the hour would perhaps not be necessary.

Finally, it would be interesting to further integrate the investment appraisal inside the model. By doing so, all costs and revenue streams could be guaranteed to reflect their time of creation thus generating a more reliable result.

For future projects, it woulds also be interesting to see this strategy implemented at other locations, with other electricity and hydrogen prices, using other combinations of energy storage technologies as well as different types of renewable energy. Hopefully, the strategy constructed is robust enough to complement other constellations of both storage and production.

# 7 Conclusion

In conclusion, this thesis presents a hybrid hydrogen and battery storage which can successfully be implemented together with solar and wind power at an existing onshore wind power site. The combination of hydrogen and batteries does not only offer substantial economic possibilities, but also enables plannable renewable production.

The operational strategy that is introduced combines the hourly economic decision-making of a Scheduler with a robust Controller which ensures the technical functionality of the HESS in real-time. The strategy is proven robust and makes decisions at the right times to maximise energy conversion and profit. However, improvements can be made to improve this strategy and include more markets in the future.

The profitability analysis indicates that the H2ESS is the most profitable component of the system, while the battery is unprofitable in all scenarios. However, the unprofitability of the battery should not be taken as an indicator that this part of the system is unnecessary, as it enables the functioning of the rest of the system. While a great driver of profitability, this thesis indicates that hydrogen will most likely not be used as a means of electricity storage, but rather as energy storage. The green hydrogen produced by renewable sources can enable the transition to a sustainable future within transportation and industry. The system with energy storage proves to be a much better investment compared to a similar system without storage.

Solutions like the one presented in this thesis can enable the expansion of VRES without contributing to the destabilisation of the power grid with the help of flexible, reliable power. This thesis indicates that a system with a HESS is better than alternative investments. The system opens doors to new streams of revenue, including the hydrogen market and potentially other markets in the future.

Further research is suggested to address stability issues, integrate more markets, conduct a more in-depth economic analysis, and further optimise system dimensions. As with all future projections, changing markets, technological development, and geopolitical circumstances render the outcomes uncertain.

Overall, this thesis provides valuable insights into the economic sustainability and potential of a HESS for renewable energy integration, contributing to the acceleration of the green transition.

# Bibliography

[1] Zainul Abdin, Kaveh Khalilpour and Kylie Catchpole. "Projecting the levelized cost of large scale hydrogen storage for stationary applications". In: *Energy Conversion and Management* 270 (2022). ISSN: 0196-8904. DOI: https://doi.org/10.1016/j.enconman.2022.116241. URL: https://www.sciencedirect.com/science/article/pii/S0196890422010184.

[2] Monika Agrawal, Bharat Kumar Saxena and K. V. S. Rao. "Feasibility of establishing solar photovoltaic power plants at existing wind farms". In: *2017 International Conference On Smart Technologies For Smart Nation (SmartTechCon)* (2017). DOI: 10.1109/SmartTechCon.2017.8358378.

[3] Abdullah Alshahrani, Siddig Omer, Yuehong Su, Elamin Mohamed and Saleh Alotaibi. "The Technical Challenges Facing the Integration of Small-Scale and Large-scale PV Systems into the Grid: A Critical Review". In: *Electronics* 8 (2019). DOI: 10.3390/electronics8121443.

[4] Arechkik Ameur, Asmae Berrada, Khalid Loudiyi and Raymond Adomatis. "Chapter 6 - Performance and energetic modeling of hybrid PV systems coupled with battery energy storage". In: *Hybrid Energy System Models*. Ed. by Asmae Berrada and Rachid El Mrabet. Academic Press, 2021, pp. 195–238. ISBN: 978-0-12-821403-9. DOI: https://doi.org/10.1016/B978-0-12-821403-9.00008-1. URL: https://www.sciencedirect.com/science/article/pii/B9780128214039000081.

[5] Ibrahem E. Atawi, Ali Q. Al-Shetwi, Amer M. Magableh and Omar H. Albalawi. "Recent Advances in Hybrid Energy Storage System Integrated Renewable Power Generation: Configuration, Control, Applications, and Future Directions". In: *Batteries 2023* (2023). DOI: 10.3390/batteries9010029. URL: https://www.mdpi.com/2313-0105/9/1/29.

[6] Aurora Energy Research. *Renewable Hydrogen Imports Could Compete with EU Production by 2030*. 2023. URL: https://auroraer.com/media/renewable-hydrogen-imports-could-compete-with-eu-production-by-2030/. Accessed 2023-05-04.

[7] Clean Hydrogen Europe. *Strategic Research and Innovation Agenda 2021 – 2027*. 2022. URL: https://www.clean-hydrogen.europa.eu/system/files/2022-02/Clean%20Hydrogen%20JU%20SRIA%20-%20approved%20by%20GB%20-%20clean%20for%20publication%20%28ID%2013246486%29.pdf. Accessed 2023-05-17.

[8] Paul Denholm. "Energy storage to reduce renewable energy curtailment". In: *Proc. IEEE Power and Energy Soc. GeneralMeeting* (2012). DOI: 10.1109/PESGM.2012.6345450.

[9] Boucar Diouf and Ramchandra Pode. "Potential of lithium-ion batteries in renewable energy". In: *Renewable Energy* (2015). ISSN: 0960-1481. DOI: https://doi.org/10.1016/j.renene.2014.11.058. URL: https://www.sciencedirect.com/science/article/pii/S0960148114007885.

[10] David Eickhoff. *Interview with David Eickhoff, originator at Axpo (28-04-2023)*. 2023.

[11] Åsa Elmqvist, Mattias Wondollek and Marie Kofod-Hansen. *El från nya anläggningar: Rapport 2021:714*. 2021. URL: https://energiforsk.se/media/30735/el-fran-nya-anlaggningar-energiforskrapport-2021-714.pdf. Accessed 2023-05-21.

[12] Enercon. *E-126*. URL: https://www.enercon.de/en/products/ep-8/e-126/. Accessed 2023-02-22.

[13] Energimarknadsinspektionen. *Så här fungerar elmarknaden*. 2021. URL: https://ei.se/konsument/el/sa-har-fungerar-elmarknaden. Accessed 2023-05-17.

[14] Environmental and Energy Study Institute. *Fact Sheet — Energy Storage (2019)*. 2019. URL: https://www.eesi.org/papers/view/energy-storage-2019. Accessed 2023-05-11.

[15] Eolus Vind AB. *Vindpark Bäckhammar uppförd och överlämnad till KGAL*. URL: https://www.globenewswire.com/news-release/2020/08/31/2086346/0/sv/Vindpark-B%C3%A4ckhammar-uppf%C3%B6rd-och-%C3%B6verl%C3%A4mnad-till-KGAL.html. Accessed 2023-02-22.

[16] Eolus Vind AB. *Pionjäranda, kompetens och affärssinne har tagit oss långt*. 2023. URL: https://www.eolusvind.com/om-eolus/. Accessed 2023-03-14.

[17] EPEX Spot. *EPEX SPOT Annual Market Review 2020: New record volume traded on EPEX SPOT in 2020*. 2021. URL: https://www.epexspot.com/sites/default/files/download_center_files/2021-01-14_EPEX%20SPOT_Annual%20Press%20Release-2020_final.pdf. Accessed 2023-05-17.

[18] EPEX Spot. *EPEX SPOT Annual Market Review 2021: Dynamic year for European power markets*. 2022. URL: https://www.epexspot.com/sites/default/files/download_center_files/2022-01-19_EPEX%20SPOT_Annual%20Press%20Release-2021_final_clean.pdf. Accessed 2023-05-17.

[19] EPEX Spot. *Basics of the Power Market*. 2023. URL: https://www.epexspot.com/en/basicspowermarket. Accessed 2023-05-04.

[20] EPEX Spot. *EPEX SPOT Annual Market Review 2022: Power markets deliver transparent price signals under increased supply pressure*. 2023. URL: https://www.epexspot.com/sites/default/files/download_center_files/2023-01-19%20%20EPEX%20SPOT_Annual%20Press%20Release-2022_final.pdf. Accessed 2023-05-17.

[21] eSett Oy. *15 min Imbalance Settlement Period in Norway and Sweden*. 2023. URL: https://www.esett.com/news/15-min-imbalance-settlement-period-in-norway-and-sweden/. Accessed 2023-05-17.

[22] European Central Bank. *Swedish krona (SEK)*. 2023. URL: `https://www.ecb.europa.eu/stats/policy_and_exchange_rates/euro_reference_exchange_rates/html/eurofxref-graph-sek.en.html`. Accessed 2023-04-20.

[23] European Central Bank. *US dollar (USD)*. 2023. URL: `https://www.ecb.europa.eu/stats/policy_and_exchange_rates/euro_reference_exchange_rates/html/eurofxref-graph-usd.en.html`. Accessed 2023-04-20.

[24] European Commission. *Roadmap for Stationary Applications for Batteries*. 2018. URL: `https://energy.ec.europa.eu/system/files/2022-01/vol-6-009.pdf`. Accessed 2023-05-17.

[25] European Commission. *Communication from the Comission to the European Parliament, the European Council, the Council, the Eurpean Economic and Social Committee and the Committee of the Regions: The European Green Deal*. 2019. URL: `https://eur-lex.europa.eu/resource.html?uri=cellar:b828d165-1c22-11ea-8c1f-01aa75ed71a1.0002.02/DOC_1&format=PDF`. Accessed 2023-05-17.

[26] European Commission. *Communication from the Comission to the European Parliament, the European Council, the Council, the Eurpean Economic and Social Committee and the Committee of the Regions: A hydrogen strategy for a climate-neutral Europe*. 2020. URL: `https://eur-lex.europa.eu/legal-content/EN/TXT/PDF/?uri=CELEX:52020DC0301&from=EN`. Accessed 2023-05-17.

[27] European Commission. *Commission Staff Working Document: Energy Storage - Underpinning a decarbonised and secure EU energy system*. 2023. URL: `https://energy.ec.europa.eu/system/files/2023-03/SWD_2023_57_1_EN_document_travail_service_part1_v6.pdf`. Accessed 2023-05-17.

[28] European Commission. *Energy storage*. 2023. URL: `https://energy.ec.europa.eu/topics/research-and-technology/energy-storage_en`. Accessed 14-04-2023.

[29] Jason Fernando. *Internal Rate of Return (IRR) Rule: Definition and Example*. 2022. URL: `https://www.investopedia.com/terms/i/irr.asp`. Accessed 2023-02-28.

[30] Jason Fernando. *Net Present Value (NPV): What It Means and Steps to Calculate It*. 2022. URL: `https://www.investopedia.com/terms/n/npv.asp`. Accessed 2023-02-28.

[31] Dolf Gielen and Martina Lyons. *Critical Materials for the Energy Transition: Lithium*. 2022. URL: `https://www.irena.org/-/media/Irena/Files/Technical-papers/IRENA_Critical_Materials_Lithium_2022.pdf?rev=acb7d0a37ec748758054920dc82dbc0a`. Accessed 2023-05-17.

[32] Ing Habil Agata Godula-Jopek and Andreas Friedrich Westenberger. "Fuel Cell Types: PEMFC/DMFC/AFC/PAFC//MCFC/SOFC/". In: *Encyclopedia of Energy Storage*. Oxford: Elsevier, 2022. DOI: `https://doi.org/10.1016/B978-0-12-819723-3.00056-1`.

[33] Fatemeh Hajeforosh, Math Bollen and Zunaira nazir ahmad. "Reliability Aspects of Battery Energy Storage in the Power Grid". In: Nov. 2020. DOI: `10.1109/ISGT-Europe47291.2020.9248757`.

[34] Adam Hayes. *Bollinger Bands®: What They Are, and What They Tell Investors*. 2023. URL: `https://www.investopedia.com/terms/b/bollingerbands.asp#:~:text=Bollinger%20Bands%C2%AE%20gives%20traders,the%20market%20may%20be%20overbought`. Accessed 2023-03-16.

[35] Hazim Imad Hazim, Kyairul Azmi Baharin, Chin Kim Gan, Ahmad H. Sabry and Amjad J. Humaidi. "Review on Optimization Techniques of PV/Inverter Ratio for Grid-Tie PV Systems". In: *Applied Sciences* 13.5 (2023). ISSN: 2076-3417. DOI: `10.3390/app13053155`. URL: `https://www.mdpi.com/2076-3417/13/5/3155`.

[36] Dominik Heide, Lueder von Bremen, Martin Greiner, Clemens Hoffmann, Markus Speckmann and Stefan Bofinger. "Seasonal optimal mix of wind and solar power in a future, highly renewable Europe". In: *Renewable Energy* 35.11 (2010), pp. 2483–2489. ISSN: 0960-1481. DOI: `https://doi.org/10.1016/j.renene.2010.03.012`. URL: `https://www.sciencedirect.com/science/article/pii/S0960148110001291`.

[37] Veronika Henze. *Corporate Clean Energy Buying Tops 30GW Mark in Record Year*. 2022. URL: `https://about.bnef.com/blog/corporate-clean-energy-buying-tops-30gw-mark-in-record-year/`. Accessed 2023-05-17.

[38] Xiao Hu, Jūratė Jaraitė and Andrius Kažukauskas. "The effects of wind power on electricity markets: A case study of the Swedish intraday market". In: *Energy Economics* (2021). DOI: `https://doi.org/10.1016/j.eneco.2021.105159`. URL: `https://www.sciencedirect.com/science/article/pii/S0140988321000645`.

[39] IEA. *Technology Roadmap: Hydrogen and Fuel Cells*. 2015. URL: `https://iea.blob.core.windows.net/assets/e669e0b6-148c-4d5c-816b-a7661301fa96/TechnologyRoadmapHydrogenandFuelCells.pdf`.

[40] IEA. *Electrolysers*. 2022. URL: `https://www.iea.org/reports/electrolysers`. Accessed 2023-01-26.

[41] IRENA. *Global Hydrogen Trade to Meet the 1.5°C Climate Goal: Part I - Trade Outlook for 2050 and Way Forward*. 2022. URL: `https://www.irena.org/-/media/Files/IRENA/Agency/Publication/2022/Jul/IRENA_Global_hydrogen_trade_part_1_2022_.pdf`. Accessed 2023-05-17.

[42] IRENA. *Global Hydrogen Trade to Meet the 1.5°C Climate Goal: Part II - Technology Review of Hydrogen Carriers*. 2022. URL: `https://www.irena.org/-/media/Files/IRENA/Agency/Publication/2022/Apr/IRENA_Global_Trade_Hydrogen_2022.pdf?rev=3d707c37462842ac89246f48add670ba`. Accessed 2023-05-17.

[43] IRENA. *Solar energy*. 2023. URL: `https://www.irena.org/Energy-Transition/Technology/Solar-energy`. Accessed 2023-02-22.

[44] IRENA. *Wind energy*. 2023. URL: `https://www.irena.org/Energy-Transition/Technology/Wind-energy`. Accessed 2023-02-22.

[45]  Kungl. Ingenjörsvetenskapsakademien (IVA). *Om vätgas och dess roll i elsystemet.*
      2022. URL: `https://www.iva.se/contentassets/62a4c0d2e21e4b289541377c29`
      `202205-iva-vatgasprojektet-syntesrapport.pdf`. Accessed 2023-
      05-17.

[46]  Anna Lejestrand. *Energiföretagen förklarar: Därför ser vi nu högre elpriser.* 2022.
      URL: `https://www.energiforetagen.se/pressrum/nyheter/`
      `2022/juli/energiforetagen-forklarar-darfor-ser-vi-hogre-`
      `elpriser/`. Accessed 2023-02-01.

[47]  Anna Lindgren. *Ekonomisk kartläggning av teknologier som potentiellt skulle kunna
      leverera reserverna FCR och aFRR.* 2019. URL: `https://www.svk.se/`
      `siteassets/5.jobba-har/dokument-exjobb/2019_ekonomisk_`
      `kartlaggning_teknologier_som_skulle_kunna_leverera_reserverna.`
      `pdf`. Accessed 2023-05-17.

[48]  J. F. Manwell, J. G. McGowan and A. L. Rogers. *WIND ENERGY EXPLAINED: The-
      ory, Design and Application. Second Edition.* West Sussex, United Kingdom: John
      Wiley  Sons Ltd., 2009.

[49]  J. Mitali, S. Dhinakaran and A.A. Mohamad. "Energy storage systems: a review". In:
      *Energy Storage and Saving* 1.3 (2022), pp. 166–216. ISSN: 2772-6835. DOI: `https:`
      `//doi.org/10.1016/j.enss.2022.07.002`. URL: `https://www.`
      `sciencedirect.com/science/article/pii/S277268352200022X`.

[50]  Modelica Association. *Modelica – A Unified Object-Oriented Language for Systems
      Modeling.* 2023. URL: `https://modelica.org/documents/MLS.pdf`.
      Accessed 2023-05-17.

[51]  Andreas Möser. *Interview with Andreas Möser, originator at Eolus Vind AB (13-04-
      2023).* 2023.

[52]  National Renewable Energy Laboratory (NREL). *Utility-Scale Battery Storage.* 2022.
      URL: `https://atb.nrel.gov/electricity/2022/utility-scale_`
      `battery_storage`. Accessed 2023-02-20.

[53]  Sonal Patel. *Pioneering 10-MW Baseload Hydrogen Power Plant Breaks Ground in
      French Guiana.* 2021. URL: `https://www.powermag.com/pioneering-`
      `10-mw-baseload-hydrogen-power-plant-breaks-ground-in-`
      `french-guiana/`. Accessed 2023-05-24.

[54]  Stefan Pfenninger and Iain Staffell. "Long-term patterns of European PV output using
      30 years of validated hourly reanalysis and satellite data". In: *Energy* 114 (2016),
      pp. 1251–1265. ISSN: 0360-5442. DOI: `https://doi.org/10.1016/j.`
      `energy.2016.08.060`. URL: `https://www.sciencedirect.com/`
      `science/article/pii/S0360544216311744`.

[55]  Stefan Pfenninger and Iain Staffell. "Using bias-corrected reanalysis to simulate cur-
      rent and future wind power output". In: *Energy* 114 (2016), pp. 1224–1239. ISSN:
      0360-5442. DOI: `https://doi.org/10.1016/j.energy.2016.08.068`.
      URL: `https://www.sciencedirect.com/science/article/pii/`
      `S0360544216311811`.

[56]  Stefan Pfenninger and Iain Staffell. *Renewables.ninja.* 2023. URL: `renwables.`
      `ninja`. Accessed 2023-05-23.

[57] Long Phan Van, Long Hoang Hieu, Kien Do Chi, Hirotaka Takano and Tuyen Nguyen Duc. "An improved state machine-based energy management strategy for renewable energy microgrid with hydrogen storage system". In: *Energy Reports* (2023). ISSN: 2352-4847. DOI: `https://doi.org/10.1016/j.egyr.2022.10.385`. URL: `https://www.sciencedirect.com/science/article/pii/S2352484722023204`.

[58] Javier Prol, Karl Steininger and David Zilberman. "The cannibalization effect of wind and solar in the California wholesale electricity market". In: *Energy Economics 85* (2019). DOI: `10.1016/j.eneco.2019.104552`. URL: `https://www.researchgate.net/publication/337054146_The_Cannibalization_Effect_of_Wind_and_Solar_in_the_California_WholesaleElectricity_Market#fullTextFileContent`.

[59] Regeringskansliet. *Det klimatpolitiska ramverket*. 2017. URL: `https://www.regeringen.se/artiklar/2017/06/det-klimatpolitiska-ramverket/`. Accessed 2023-05-17.

[60] Jeff Schmidt. *Levelized Cost of Energy (LCOE)*. 2023. URL: `https://corporatefinanceinsti com/resources/valuation/levelized-cost-of-energy-lcoe/`. Accessed 2023-03-14.

[61] S. Shiva Kumar and V. Himabindu. "Hydrogen production by PEM water electrolysis – A review". In: *Materials Science for Energy Technologies* 2.3 (2019), pp. 442–454. DOI: `https://doi.org/10.1016/j.mset.2019.03.002`. URL: `https://www.sciencedirect.com/science/article/pii/S2589299119300035`.

[62] Skatteverket. *Aktiebolag*. 2023. URL: `https://www.skatteverket.se/foretag/drivaforetag/foretagsformer/aktiebolag.4.5c13cb6b1198121ee858 html`. Accessed 2023-05-04.

[63] SMHI. *Ladda ner meteorlogiska observationer*. URL: `https://www.smhi.se/data/meteorologi/ladda-ner-meteorologiska-observationer/#param=globalIrradians,stations=core,stationid=93235`. Accessed: 2023-01-22.

[64] SSAB. *HYBRIT: SSAB, LKAB and Vattenfall building unique pilot project in Luleå for large-scale hydrogen storage investing a quarter of a billion Swedish kronor*. 2021. URL: `https://www.ssab.com/en/news/2021/04/hybrit-ssab-lkab-and-vattenfall-building-unique-pilot-project-in-lule-for-largescale-hydrogen-storag`. Accessed 2023-05-24.

[65] Tyler Stehly and Patrick Duffy. *2021 Cost of Wind Energy Review*. 2022. URL: `https://www.nrel.gov/docs/fy23osti/84774.pdf`. Accessed 2023-03-14.

[66] Katherine Stene Bakke and Sergiu Maznic. *Profit in peril? Correctly valuing Baseload PPAs in the Nordic market*. 2021. URL: `https://afry.com/en/insight/profit-in-peril-correctly-valuing-baseload-ppas-in-nordic-market`. Accessed 2023-05-17.

[67] Svensk Vindkraft. *Frågor och svar om vindkraft, juni 2021*. 2021. URL: `https://svenskvindkraft.com/fragor-och-svar-om-vindkraft-juni-2021/#:~:text=Utfallet%20l%C3%A4r%20bli%20b%C3%A4ttre%20och,en%20kapacitetsfaktor%20p%C3%A5%20ca%2037%25`. Accessed 2023-05-21.

[68] Svenska Kraftnät. *Handel med el*. 2021. URL: `https://www.svk.se/om-kraftsystemet/om-elmarknaden/handel-med-el/`. Accessed 2023-01-30.

[69] Svenska Kraftnät. *Om elmarknaden*. 2021. URL: `https://www.svk.se/om-kraftsystemet/om-elmarknaden/`. Accessed: 2023-01-30.

[70] Svenska kraftnät. *Elområden*. 2022. URL: `https://www.svk.se/om-kraftsystemet/om-elmarknaden/elomraden/`. Accessed 2023-03-16.

[71] Svenska Kraftnät. *Det här betalar du*. 2023. URL: `https://www.svk.se/aktorsportalen/balansansvarig/det-har-betalar-du/`. Accessed 2023-04-17.

[72] Svenska Kraftnät. *Om olika reserver*. 2023. URL: `https://www.svk.se/aktorsportalen/bidra-med-reserver/om-olika-reserver/`. Accessed 2023-05-23.

[73] Svenska Kraftnät. *Procurement and pricing of ancillary services*. 2023. URL: `https://www.svk.se/en/stakeholders-portal/electricity-market/provision-of-ancillary-services/procurement-and-pricing-of-ancillary-services/`. Accessed 2023-05-23.

[74] Swedish Energy Agency. *Energy in Sweden 2022 - An Overview*. 2022. URL: `https://energimyndigheten.a-w2m.se/Home.mvc?ResourceId=208766`. Accessed 2023-05-17.

[75] Emanuele Taibi, Herib Blanco, Raul Miranda (IRENA) and Marcelo Carmo (Forschungszentrum Jülich). *Green Hydrogen Cost Reduction: Scaling Up Electrolysers to Meet the 1.5°C Climate Goal*. 2020. URL: `https://www.irena.org/-/media/Files/IRENA/Agency/Publication/2020/Dec/IRENA_Green_hydrogen_cost_2020.pdf`. Accessed 2023-05-17.

[76] TenneT Holding B.V. *What kind of markets are there and how do they work?* 2023. URL: `https://netztransparenz.tennet.eu/electricity-market/about-the-electricity-market/what-kind-of-markets-are-there-and-how-do-they-work/`. Accessed 2023-05-20.

[77] J. Trinh, F. Harahap, A. Fagerström and J. Hansson. "What Are the Policy Impacts on Renewable Jet Fuel in Sweden?" In: *Energies 2021* (2021). DOI: `https://doi.org/10.3390/en14217194`.

[78] Trinomics for the European Commission. *Final Report Cost of Energy (LCOE): Energy costs, taxes and the impact of government interventions on investments*. 2020. URL: `https://op.europa.eu/en/publication-detail/-/publication/e2783d72-1752-11eb-b57e-01aa75ed71a1/language-en`. Accessed 2023-05-17.

[79] Salah Ud-Din Khan, Irfan Wazeer, Zeyad Almutairi and Meshari Alanazi. "Techno-economic analysis of solar photovoltaic powered electrical energy storage (EES) system". In: *Alexandria Engineering Journal* (2022). ISSN: 1110-0168. DOI: `https://doi.org/10.1016/j.aej.2021.12.025`. URL: `https://www.sciencedirect.com/science/article/pii/S1110016821008334`.

[80] U.S Department of Energy. *Hydrogen Fuel Basics*. URL: `https://www.energy.gov/eere/fuelcells/hydrogen-fuel-basics`. Accessed 2023-01-23.

[81] U.S Department of Energy. *Hydrogen Production: Electrolysis*. URL: `https://www.energy.gov/eere/fuelcells/hydrogen-production-electrolysis`. Accessed 2023-05-10.

[82] U.S Department of Energy. *Hydrogen Storage - Hydrogen and Fuel Cell Technologies Office*. URL: `https://www.energy.gov/eere/fuelcells/hydrogen-storage`. Accessed 2023-05-12).

[83] U.S Department of Energy. *DOE National Clean Hydrogen Strategy and Roadmap*. 2022. URL: `https://www.hydrogen.energy.gov/pdfs/clean-hydrogen-strategy-roadmap.pdf`. Accessed 2023-05-17.

[84] U.S Department of Energy: Fuel Cell Technologies Office. *Comparison of Fuel Cell Technologies*. URL: `https://www.energy.gov/sites/default/files/2016/06/f32/fcto_fuel_cells_comparison_chart_apr2016.pdf`. Accessed 2023-02-03.

[85] U.S Energy Information Administration. *Capacity factor*. 2023. URL: `https://www.eia.gov/tools/glossary/index.php?id=Capacity_factor`. Accessed 2023-03-14.

[86] Warren Venketas. *How to Use Bollinger Bands® in Forex Trading*. 2019. URL: `https://www.dailyfx.com/education/bollinger-bands/forex-trading.html`. Accessed 2023-05-24.

[87] Vestas. *V136-4.2 MW™*. 2023. URL: `https://www.vestas.com/en/products/4-mw-platform/V136-4-2-MW`. Accessed 2023-05-22.

[88] Vestas. *V150-4.2 MW™*. 2023. URL: `https://www.vestas.com/en/products/4-mw-platform/V150-4-2-MW`. Accessed 2023-05-22.

[89] Vätgas Sverige. *FAQ*. 2023. URL: `https://vatgas.se/fakta/faq/`. Accessed 2023-05-23.

[90] Peter J. Woolf. *Chemical Process Dynamics and Controls*. Michigan, United States of America: University of Michigan, 2009, pp. 635–639.

[91] Xinjing Zhang, Chao (Chris) Qin, Eric Loth, Yujie Xu, Xuezhi Zhou and Haisheng Chen. "Arbitrage analysis for different energy storage technologies and strategies". In: *Energy Reports* 7 (2021). ISSN: 2352-4847. DOI: `https://doi.org/10.1016/j.egyr.2021.09.009`. URL: `https://www.sciencedirect.com/science/article/pii/S2352484721008143`.

[92] Harald Åkesson. *Battery energy storage design and operation in an HVDC system with WPP clusters*. 2019. URL: `https://www.lunduniversity.lu.se/lup/publication/8974958`. Accessed 2023-05-17.
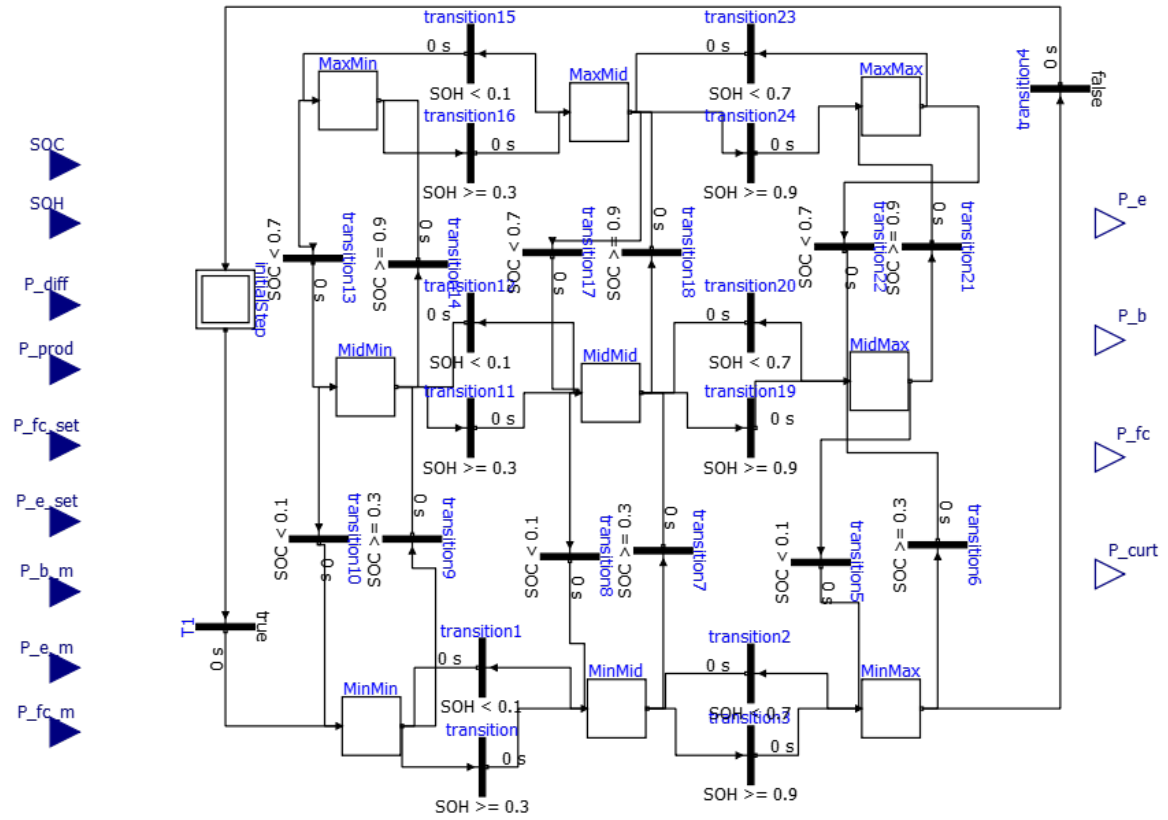
# Appendix A

# Controller



**Figure A.1:** Controller state machine implemented in OpenModelica.

```
model Controller
  parameter Real P_t_max = 130e+06 "in watts";
 parameter Real P_e_max = 70e+06 "maximum electrolyser power in watts";
 parameter Real P_fc_max = 10e+06 "maximum fuel cell power in watts";
 parameter Real SOC_max = 0.9;
 parameter Real SOC_min = 0.1;
 parameter Real SOH_max = 0.9;
 parameter Real SOH_min = 0.1;
 parameter Real P_b_max = 80e+06;
  Modelica.StateGraph.Transition T1(condition = true) annotation(
    Placement(visible = true, transformation(origin = {-138, -58}, extent =
{{-50, 50}, {-30, 30}}, rotation = -90)));
 Modelica.StateGraph.Step MinMax(nIn = 2, nOut = 3) annotation(
    Placement(visible = true, transformation(origin = {130, -46}, extent =
{{-10, -10}, {10, 10}}, rotation = 0)));
 Modelica.StateGraph.Step MinMid(nIn = 3, nOut = 3) annotation(
    Placement(visible = true, transformation(origin = {36, -46}, extent =
{{-10, -10}, {10, 10}}, rotation = 0)));
 Modelica.StateGraph.InitialStep initialStep annotation(
    Placement(visible = true, transformation(origin = {-98, 94}, extent =
{{-10, -10}, {10, 10}}, rotation = -90)));
 Modelica.StateGraph.Transition transition4(condition = false) annotation(
    Placement(visible = true, transformation(origin = {148, 206}, extent =
{{-50, -50}, {-30, -30}}, rotation = 90)));
 Modelica.StateGraph.Step MinMin(nIn = 3, nOut = 2) annotation(
    Placement(visible = true, transformation(origin = {-48, -52}, extent =
{{-10, -10}, {10, 10}}, rotation = 0)));
 Modelica.StateGraph.Transition transition3(condition = SOH >= 0.9)
annotation(
    Placement(visible = true, transformation(origin = {82, -62}, extent =
{{-10, -10}, {10, 10}}, rotation = 0)));
 /*Modelica.Blocks.Interfaces.RealInput P_diff annotation(
    Placement(visible = true, transformation(origin = {-158, 80}, extent =
{{-10, -10}, {10, 10}}, rotation = 0), iconTransformation(origin = {-110,
60}, extent = {{-10, -10}, {10, 10}}, rotation = 0)));
 */Modelica.StateGraph.Transition transition(condition = SOH >= 0.3)
annotation(
    Placement(visible = true, transformation(origin = {-10, -66}, extent =
{{-10, -10}, {10, 10}}, rotation = 0)));
 Modelica.StateGraph.Transition transition1(condition = SOH < 0.1)
annotation(
    Placement(visible = true, transformation(origin = {-10, -32}, extent =
{{10, -10}, {-10, 10}}, rotation = 0)));
 Modelica.StateGraph.Transition transition2(condition = SOH < 0.7)
annotation(
    Placement(visible = true, transformation(origin = {82, -34}, extent =
{{10, -10}, {-10, 10}}, rotation = 0)));
 Modelica.StateGraph.Step MidMax(nIn = 3, nOut = 3) annotation(
    Placement(visible = true, transformation(origin = {126, 66}, extent =
{{-10, -10}, {10, 10}}, rotation = 0)));
 Modelica.StateGraph.Transition transition5(condition = SOC < 0.1)
annotation(
```

**Figure A.2:** OpenModelica code for Controller (1/13).

```
      Placement(visible = true, transformation(origin = {106, 4}, extent =
   {{-10, -10}, {10, 10}}, rotation = -90)));
    Modelica.StateGraph.Transition transition6(condition = SOC >= 0.3)
   annotation(
      Placement(visible = true, transformation(origin = {146, 10}, extent =
   {{10, -10}, {-10, 10}}, rotation = -90)));
    Modelica.StateGraph.Transition transition7(condition = SOC >= 0.3)
   annotation(
      Placement(visible = true, transformation(origin = {52, 8}, extent = {{10,
   -10}, {-10, 10}}, rotation = -90)));
    Modelica.StateGraph.Transition transition8(condition = SOC < 0.1)
   annotation(
      Placement(visible = true, transformation(origin = {20, 6}, extent = {{-10,
   -10}, {10, 10}}, rotation = -90)));
    Modelica.StateGraph.Step MidMid(nIn = 4, nOut = 4) annotation(
      Placement(visible = true, transformation(origin = {34, 62}, extent =
   {{-10, -10}, {10, 10}}, rotation = 0)));
    Modelica.StateGraph.Transition transition9(condition = SOC >= 0.3)
   annotation(
      Placement(visible = true, transformation(origin = {-34, 12}, extent =
   {{10, -10}, {-10, 10}}, rotation = -90)));
    Modelica.StateGraph.Transition transition10(condition = SOC < 0.1)
   annotation(
      Placement(visible = true, transformation(origin = {-66, 12}, extent =
   {{-10, -10}, {10, 10}}, rotation = -90)));
    Modelica.StateGraph.Step MidMin(nIn = 3, nOut = 3) annotation(
      Placement(visible = true, transformation(origin = {-50, 64}, extent =
   {{-10, -10}, {10, 10}}, rotation = 0)));
    Modelica.StateGraph.Transition transition11(condition = SOH >= 0.3)
   annotation(
      Placement(visible = true, transformation(origin = {-14, 50}, extent =
   {{-10, -10}, {10, 10}}, rotation = 0)));
    Modelica.StateGraph.Transition transition12(condition = SOH < 0.1)
   annotation(
      Placement(visible = true, transformation(origin = {-14, 86}, extent =
   {{10, -10}, {-10, 10}}, rotation = 0)));
    Modelica.StateGraph.Transition transition13(condition = SOC < 0.7)
   annotation(
      Placement(visible = true, transformation(origin = {-68, 108}, extent =
   {{-10, -10}, {10, 10}}, rotation = -90)));
    Modelica.StateGraph.Transition transition14(condition = SOC >= 0.9)
   annotation(
      Placement(visible = true, transformation(origin = {-32, 106}, extent =
   {{10, -10}, {-10, 10}}, rotation = -90)));
    Modelica.StateGraph.Step MaxMin(nIn = 2, nOut = 2) annotation(
      Placement(visible = true, transformation(origin = {-56, 162}, extent =
   {{-10, -10}, {10, 10}}, rotation = 0)));
    Modelica.StateGraph.Transition transition15(condition = SOH < 0.1)
   annotation(
      Placement(visible = true, transformation(origin = {-14, 178}, extent =
   {{10, -10}, {-10, 10}}, rotation = 0)));
    Modelica.StateGraph.Transition transition16(condition = SOH >= 0.3)
   annotation(
```

**Figure A.3:** OpenModelica code for Controller (2/13).

```
      Placement(visible = true, transformation(origin = {-14, 144}, extent =
{{-10, -10}, {10, 10}}, rotation = 0)));
 Modelica.StateGraph.Step MaxMid(nIn = 3, nOut = 3) annotation(
    Placement(visible = true, transformation(origin = {30, 158}, extent =
{{-10, -10}, {10, 10}}, rotation = 0)));
 Modelica.StateGraph.Transition transition17(condition = SOC < 0.7)
annotation(
    Placement(visible = true, transformation(origin = {14, 110}, extent =
{{-10, -10}, {10, 10}}, rotation = -90)));
 Modelica.StateGraph.Transition transition18(condition = SOC >= 0.9)
annotation(
    Placement(visible = true, transformation(origin = {48, 110}, extent =
{{10, -10}, {-10, 10}}, rotation = -90)));
 Modelica.StateGraph.Transition transition19(condition = SOH >= 0.9)
annotation(
    Placement(visible = true, transformation(origin = {82, 50}, extent =
{{-10, -10}, {10, 10}}, rotation = 0)));
 Modelica.StateGraph.Transition transition20(condition = SOH < 0.7)
annotation(
    Placement(visible = true, transformation(origin = {82, 86}, extent = {{10,
-10}, {-10, 10}}, rotation = 0)));
 Modelica.StateGraph.Step MaxMax(nIn = 2, nOut = 2) annotation(
    Placement(visible = true, transformation(origin = {130, 160}, extent =
{{-10, -10}, {10, 10}}, rotation = 0)));
 Modelica.StateGraph.Transition transition21(condition = SOC >= 0.9)
annotation(
    Placement(visible = true, transformation(origin = {144, 112}, extent =
{{10, -10}, {-10, 10}}, rotation = -90)));
 Modelica.StateGraph.Transition transition22(condition = SOC < 0.7)
annotation(
    Placement(visible = true, transformation(origin = {114, 112}, extent =
{{-10, -10}, {10, 10}}, rotation = -90)));
 Modelica.StateGraph.Transition transition23(condition = SOH < 0.7)
annotation(
    Placement(visible = true, transformation(origin = {82, 178}, extent =
{{10, -10}, {-10, 10}}, rotation = 0)));
 Modelica.StateGraph.Transition transition24(condition = SOH >= 0.9)
annotation(
    Placement(visible = true, transformation(origin = {82, 144}, extent =
{{-10, -10}, {10, 10}}, rotation = 0)));
 Modelica.Blocks.Interfaces.RealOutput P_curt annotation(
    Placement(visible = true, transformation(origin = {210, 0}, extent =
{{-10, -10}, {10, 10}}, rotation = 0), iconTransformation(origin = {110,
-60}, extent = {{-10, -10}, {10, 10}}, rotation = 0)));
 Modelica.Blocks.Interfaces.RealInput SOC annotation(
    Placement(visible = true, transformation(origin = {-158, 140}, extent =
{{-10, -10}, {10, 10}}, rotation = 0), iconTransformation(origin = {-110,
100}, extent = {{-10, -10}, {10, 10}}, rotation = 0)));
 Modelica.Blocks.Interfaces.RealInput SOH annotation(
    Placement(visible = true, transformation(origin = {-158, 120}, extent =
{{-10, -10}, {10, 10}}, rotation = 0), iconTransformation(origin = {-110,
60}, extent = {{-10, -10}, {10, 10}}, rotation = 0)));
 Modelica.Blocks.Interfaces.RealOutput P_fc annotation(
```

**Figure A.4:** OpenModelica code for Controller (3/13).

```
        Placement(visible = true, transformation(origin = {210, 40}, extent =
{{-10, -10}, {10, 10}}, rotation = 0), iconTransformation(origin = {110,
-20}, extent = {{-10, -10}, {10, 10}}, rotation = 0)));
Modelica.Blocks.Interfaces.RealOutput P_b annotation(
        Placement(visible = true, transformation(origin = {210, 80}, extent =
{{-10, -10}, {10, 10}}, rotation = 0), iconTransformation(origin = {110, 20},
extent = {{-10, -10}, {10, 10}}, rotation = 0)));
Modelica.Blocks.Interfaces.RealOutput P_e annotation(
        Placement(visible = true, transformation(origin = {210, 120}, extent =
{{-10, -10}, {10, 10}}, rotation = 0), iconTransformation(origin = {110, 60},
extent = {{-10, -10}, {10, 10}}, rotation = 0)));
 Modelica.Blocks.Interfaces.RealInput P_diff annotation(
        Placement(visible = true, transformation(origin = {-158, 92}, extent =
{{-10, -10}, {10, 10}}, rotation = 0), iconTransformation(origin = {-110,
20}, extent = {{-10, -10}, {10, 10}}, rotation = 0)));
 Modelica.Blocks.Interfaces.RealInput P_prod annotation(
        Placement(visible = true, transformation(origin = {-158, 70}, extent =
{{-10, -10}, {10, 10}}, rotation = 0), iconTransformation(origin = {-110,
-20}, extent = {{-10, -10}, {10, 10}}, rotation = 0)));
 Modelica.Blocks.Interfaces.RealInput P_fc_set annotation(
        Placement(visible = true, transformation(origin = {-158, 44}, extent =
{{-10, -10}, {10, 10}}, rotation = 0), iconTransformation(origin = {-110,
-60}, extent = {{-10, -10}, {10, 10}}, rotation = 0)));
Modelica.Blocks.Interfaces.RealInput P_e_set annotation(
        Placement(visible = true, transformation(origin = {-158, 18}, extent =
{{-10, -10}, {10, 10}}, rotation = 0), iconTransformation(origin = {-110,
-98}, extent = {{-10, -10}, {10, 10}}, rotation = 0)));
Modelica.Blocks.Interfaces.RealInput P_e_m annotation(
        Placement(visible = true, transformation(origin = {-158, -32}, extent =
{{-10, -10}, {10, 10}}, rotation = 0), iconTransformation(origin = {40, 110},
extent = {{-10, -10}, {10, 10}}, rotation = -90)));
Modelica.Blocks.Interfaces.RealInput P_b_m annotation(
        Placement(visible = true, transformation(origin = {-158, -6}, extent =
{{-10, -10}, {10, 10}}, rotation = 0), iconTransformation(origin = {0, 110},
extent = {{-10, -10}, {10, 10}}, rotation = -90)));
Modelica.Blocks.Interfaces.RealInput P_fc_m annotation(
        Placement(visible = true, transformation(origin = {-158, -54}, extent =
{{-10, -10}, {10, 10}}, rotation = 0), iconTransformation(origin = {80, 110},
extent = {{-10, -10}, {10, 10}}, rotation = -90)));
equation
 if MinMin.active then
//state
    if P_diff < 0 then
// under
       P_b = 0;
       P_e = 0;
       P_fc = 0;
       P_curt = 0;
    else // over
      if P_diff <= P_b_max then
        P_b = -P_diff;
        P_e = 0;
        P_fc = 0;
```

**Figure A.5:** OpenModelica code for Controller (4/13).

```
            P_curt = 0;
          elseif P_diff <= (P_b_max + 0.5*P_e_max) then
            P_e = -0.5*P_e_max;
            P_b = -(P_diff + 0.5*P_e_m);
            P_fc = 0;
            P_curt = 0;
          else
            P_b = -P_b_max;
            P_e = -P_e_max;
            P_fc = 0;
            if P_prod > P_t_max + P_b_m + P_e_m   then
              P_curt = P_prod - P_t_max + P_b_m + P_e_m;
            else
              P_curt = 0;
            end if;
          end if;
        end if;
     elseif MinMid.active then
       if P_diff < 0 then
//Under
          if not P_fc_set == 0 and P_prod + P_fc_set < P_t_max then
            P_b = 0;
            P_e = 0;
            P_fc = P_fc_set;
            P_curt = 0;
          elseif not P_fc_set == 0 and P_prod + P_fc_set > P_t_max then
            P_b = P_prod + P_fc_m - P_t_max;
            P_e = 0;
            P_fc = P_fc_set;
            P_curt = 0;
          else
            P_b = -P_e_m;
            P_e = 0;
            P_fc = 0;
            P_curt = 0;
          end if;
       else
// Over production

          if P_diff <= P_b_max then
            P_b = -P_diff -P_e_m;
            P_e = 0;
            P_fc = 0;
            P_curt = 0;
          elseif P_diff <= P_b_max + 0.5*P_e_max then
            P_b = -(P_diff + P_e_m);
            P_e = -0.5*P_e_max;
            P_fc = 0;
            if P_prod > P_t_max - P_e_m - P_b_m then
              P_curt = P_prod - P_t_max + P_b_m + P_e_m;
            else
              P_curt = 0;
            end if;
```

**Figure A.6:** OpenModelica code for Controller (5/13).

```
        else
// P_diff > P_b_max + P_e_max
        P_b = -P_b_max;
        P_e = -P_e_max;
        P_fc = 0;
        if P_prod > P_t_max - P_e_m - P_b_m then
          P_curt = P_prod - P_t_max + P_b_m + P_e_m;
        else
          P_curt = 0;
        end if;
      end if;
    end if;
 elseif MinMax.active then
    if P_diff < 0 then
//Under
      if not P_fc_set == 0 and P_prod + P_fc_set < P_t_max then
        P_b = 0;
        P_e = 0;
        P_fc = P_fc_set;
        P_curt = 0;
      elseif not P_fc_set == 0 and P_prod + P_fc_set > P_t_max then
        P_b = P_prod + P_fc_m - P_t_max;
        P_e = 0;
        P_fc = P_fc_set;
        P_curt = 0;
      else
        P_b = -P_e_m;
        P_e = 0;
        P_fc = 0;
        P_curt = 0;
      end if;
    else
// Over
      if P_diff <= P_b_max then
        P_b = -P_diff;
        P_e = 0;
        P_fc = 0;
        P_curt = 0;
      else
//P_diff > P_b_max
        P_b = -P_b_max;
        P_e = 0;
        P_fc = 0;
        if P_prod > P_t_max - P_b_m - P_e_m then
          P_curt = P_prod - P_t_max + P_b_m + P_e_m;
        else
          P_curt = 0;
        end if;
      end if;
    end if;
 elseif MidMin.active then
    if P_diff < 0 then
//under
```

**Figure A.7:** OpenModelica code for Controller (6/13).

```
    P_e = -P_e_set;
    P_fc = 0;
    P_curt = 0;
    P_b = if -P_diff - P_e_m > P_b_max then P_b_max else -P_diff - P_e_m;
  else
// Over production
    P_fc = 0;
    if P_diff <= P_b_max + P_e_set then
      P_b = -(P_diff + P_e_m);
      P_e = -P_e_set;
      P_curt = 0;
    elseif P_diff <= P_b_max + P_e_max then
      P_b = -(P_diff + P_e_m);
      P_e = -P_e_max;
      P_curt = 0;
    else  //P_diff > P_b_max + P_e_max
      P_b = -P_b_max;
      P_e = -P_e_max;
      if P_prod >= P_t_max - P_b_m - P_e_m then
        P_curt = P_prod - P_t_max + P_b_m + P_e_m;
      else
        P_curt = 0;
      end if;
    end if;
  end if;
 elseif MidMax.active then
   if P_diff < 0 then
//under
     if -P_diff <= P_b_max and P_fc_set == 0 then
       P_b = -P_diff - P_e_m;
//P_b = -P_diff;
       P_e = 0;
       P_fc = 0;
       P_curt = 0;
     elseif -P_diff > P_b_max and P_fc_set == 0 then
       P_b = P_b_max - P_e_m;
       P_e = 0;
       P_fc = 0;
       P_curt = 0;
     else
// not P_fc_set == 0
       P_e = 0;
       P_curt = 0;
       if -P_diff <= P_b_max + P_fc_max then
         P_fc = P_fc_max;
         P_b = -P_diff - P_fc_m;
       else
//-P_diff > P_b_max + P_fc_max
         P_b = P_b_max;
         P_fc = P_fc_max;
       end if;
     end if;
   else
```

**Figure A.8:** OpenModelica code for Controller (7/13).

```
// over
    if P_diff <= P_b_max then
        P_b = -P_diff - P_e_m;
        P_e = 0;
        P_fc = 0;
        P_curt = 0;
    else
//P_diff > P_b_max
        P_b = -P_b_max - P_e_m;
        P_e = 0;
        P_fc = 0;
        if P_prod > P_t_max - P_b_m - P_e_m then
            P_curt = P_prod - P_t_max + P_b_m + P_e_m;
        else
            P_curt = 0;
        end if;
    end if;
  end if;
 elseif MaxMin.active then
   if P_diff < 0 then
//under
    if -P_diff <= P_b_max then
        if -P_diff + P_e_m < 0 then
            P_b = -(-P_diff + P_e_m);
        else
            P_b = 0;
        end if;
        P_e = 0;
        P_fc = 0;
        P_curt = 0;
    else
// -P_diff > P_b_max
        P_b = P_b_max;
        P_e = 0;
        P_fc = 0;
        P_curt = 0;
    end if;
    else
// Over production
    if P_diff <= 0.5*P_e_max and P_diff < P_e_m then
        P_b = -(P_diff + P_e_m);
        P_e = -0.5*P_e_max;
        P_fc = 0;
        P_curt = 0;
    elseif P_diff <= P_e_max and P_diff < P_e_m then
        P_b = -(P_diff + P_e_m);
        P_e = -P_e_max;
        P_fc = 0;
        P_curt = 0;
    else
// P_diff > P_e_max
        if P_diff + P_e_m < 0 then
            P_b = -(P_diff + P_e_m);
```

**Figure A.9:** OpenModelica code for Controller (8/13).

```
            else
              P_b = 0;
            end if;
            P_e = -P_e_max;
            P_fc = 0;
            if P_prod > P_t_max - P_e_m - P_b_m then
              P_curt = P_prod - P_t_max + P_e_m + P_b_m;
            else
              P_curt = 0;
            end if;
          end if;
        end if;
 elseif MaxMid.active then
    if P_diff < 0 then
//under
      if -P_diff <= P_b_max and P_fc_set == 0 then
        P_b = -P_diff - P_e_m;
        P_e = 0;
        P_fc = 0;
        P_curt = 0;
      elseif -P_diff > P_b_max and P_fc_set == 0 then
        P_b = P_b_max;
        P_e = 0;
        P_fc = 0;
        P_curt = 0;
      else
// P_fc_set != 0
        P_e = 0;
        P_curt = 0;
        if -P_diff <= P_b_max + 0.5*P_fc_max then
          P_fc = 0.5*P_fc_max;
          P_b = -P_diff - P_fc_m;
        else
//-P_diff <= P_b_max + P_fc_max
          P_fc = P_fc_max;
          P_b = -P_diff - P_fc_m;
        end if;
      end if;
    else
// over
      if P_diff <= 0.5*P_e_max and P_diff < P_e_m then
        P_b = -(P_diff + P_e_m);
        P_e = -0.5*P_e_max;
        P_fc = 0;
        P_curt = 0;
      elseif P_diff <= P_e_max and P_diff < P_e_m then
        P_b = -(P_diff + P_e_m);
        P_e = -P_e_max;
        P_fc = 0;
        P_curt = 0;
      else
// P_diff > P_e_max
        if P_diff + P_e_m < 0 then
```

**Figure A.10:** OpenModelica code for Controller (9/13).

```
        P_b = -(P_diff + P_e_m);
      else
        P_b = 0;
      end if;
      P_e = -P_e_max;
      P_fc = 0;
      if P_prod > P_t_max -P_b_m - P_e_m then
        P_curt = P_prod - P_t_max +P_b_m + P_e_m;
      else
        P_curt = 0;
      end if;
    end if;
  end if;
elseif MaxMax.active then
  if P_diff < 0 then
//under
    if -P_diff <= P_b_max and P_fc_set == 0 then
      if P_diff + P_e_m < 0 then
        P_b = -(P_diff + P_e_m);
      else
        P_b = 0;
      end if;
      P_e = 0;
      P_fc = 0;
      P_curt = 0;
    elseif -P_diff > P_b_max and P_fc_set == 0 then
      P_b = P_b_max;
      P_e = 0;
      P_fc = 0;
      P_curt = 0;
    else
// P_fc_set != 0
      P_e = 0;
      P_curt = 0;
      if -P_diff <= P_b_max + 0.5*P_fc_max then
        P_fc = 0.5*P_fc_max;
        P_b = -P_diff - P_fc_m;
      else
//-P_diff <= P_b_max + P_fc_max
        P_fc = P_fc_max;
        P_b = -P_diff - P_fc_m;
      end if;
    end if;
  else
// over
    if P_diff + P_e_m < 0 then
      P_b = -(P_diff + P_e_m);
    else
      P_b = 0;
    end if;
    P_e = 0;
    P_fc = 0;
    if P_prod >= P_t_max - P_e_m - P_b_m then
```

**Figure A.11:** OpenModelica code for Controller (10/13).

```
          P_curt = P_prod - P_t_max + P_e_m + P_b_m;
      else
        P_curt = 0;
      end if;
    end if;
  else
// MidMid
    if P_diff < 0 then
//under
      P_e = -P_e_set;
      P_fc = P_fc_set;
      P_curt = 0;
      P_b = if -P_diff - P_e_m > P_b_max then P_b_max else -P_diff - P_e_m;
    else
// Over
      P_fc = 0;
      if P_diff <= P_b_max + P_e_set then
        P_b = -(P_diff + P_e_m);
        P_e = -P_e_set;
        if P_prod >= P_t_max - P_b_m - P_e_m then
         P_curt = P_prod - P_t_max + P_b_m + P_e_m;
        else
         P_curt = 0;
        end if;
      elseif P_diff <= P_b_max + P_e_max then
        P_b = -(P_diff + P_e_m);
        P_e = -P_e_max;
        if P_prod >= P_t_max - P_b_m - P_e_m then
         P_curt = P_prod - P_t_max + P_b_m + P_e_m;
        else
         P_curt = 0;
        end if;
      else  //P_diff > P_b_max + P_e_max
        P_b = -P_b_max;
        P_e = -P_e_max;
        if P_prod >= P_t_max - P_b_m - P_e_m then
         P_curt = P_prod - P_t_max + P_b_m + P_e_m;
        else
         P_curt = 0;
      end if;
      end if;
    end if;
  end if;
  connect(transition.outPort, MinMid.inPort[1]) annotation(
    Line(points = {{-8.5, -66}, {2.25, -66}, {2.25, -46}, {25, -46}}));
  connect(transition3.outPort, MinMax.inPort[1]) annotation(
    Line(points = {{83.5, -62}, {98.25, -62}, {98.25, -46}, {119, -46}}));
  connect(initialStep.outPort[1], T1.inPort) annotation(
    Line(points = {{-98, 83.5}, {-98, -14}}));
  connect(transition4.outPort, initialStep.inPort[1]) annotation(
    Line(points = {{188, 167.5}, {188, 194}, {-98, 194}, {-98, 105}}));
  connect(transition6.outPort, MidMax.inPort[3]) annotation(
    Line(points = {{146, 11.5}, {146, 41.5}, {115, 41.5}, {115, 66}}));
```

**Figure A.12:** OpenModelica code for Controller (11/13).

```
connect(MidMax.outPort[3], transition5.inPort) annotation(
  Line(points = {{136.5, 66}, {136.5, 46}, {106, 46}, {106, 8}}));
connect(transition5.outPort, MinMax.inPort[2]) annotation(
  Line(points = {{106, 2.5}, {106, -9.75}, {119, -9.75}, {119, -46}}));
connect(MinMin.outPort[1], transition9.inPort) annotation(
  Line(points = {{-37.5, -52}, {-26, -52}, {-26, 2}, {-34, 2}, {-34, 8}}));
connect(MinMin.outPort[2], transition.inPort) annotation(
  Line(points = {{-37.5, -52}, {-37.5, -66}, {-13.5, -66}}));
connect(T1.outPort, MinMin.inPort[1]) annotation(
  Line(points = {{-98, -19.5}, {-98, -52}, {-59, -52}}));
connect(transition10.outPort, MinMin.inPort[2]) annotation(
  Line(points = {{-66, 10}, {-64, 10}, {-64, -52}, {-59, -52}}));
connect(transition1.outPort, MinMin.inPort[3]) annotation(
  Line(points = {{-11.5, -32}, {-33.25, -32}, {-33.25, -52}, {-59, -52}}));
connect(MidMin.outPort[1], transition14.inPort) annotation(
  Line(points = {{-39.5, 64}, {-32, 64}, {-32, 102}}));
connect(MidMin.outPort[2], transition11.inPort) annotation(
  Line(points = {{-39.5, 64}, {-28.75, 64}, {-28.75, 50}, {-18, 50}}));
connect(MidMin.outPort[3], transition10.inPort) annotation(
  Line(points = {{-39.5, 64}, {-66, 64}, {-66, 16}}));
connect(transition13.outPort, MidMin.inPort[1]) annotation(
  Line(points = {{-68, 106.5}, {-68, 64}, {-61, 64}}));
connect(transition12.outPort, MidMin.inPort[2]) annotation(
  Line(points = {{-15.5, 86}, {-20, 86}, {-20, 64}, {-61, 64}}));
connect(transition9.outPort, MidMin.inPort[3]) annotation(
  Line(points = {{-34, 13.5}, {-34, 64}, {-61, 64}}));
connect(transition14.outPort, MaxMin.inPort[2]) annotation(
  Line(points = {{-32, 107.5}, {-32, 162}, {-67, 162}}));
connect(MaxMin.outPort[2], transition13.inPort) annotation(
  Line(points = {{-45.5, 162}, {-72.75, 162}, {-72.75, 112}, {-68, 112}}));
connect(transition15.outPort, MaxMin.inPort[1]) annotation(
  Line(points = {{-15.5, 178}, {-71.25, 178}, {-71.25, 162}, {-67, 162}}));
connect(MaxMin.outPort[1], transition16.inPort) annotation(
  Line(points = {{-45.5, 162}, {-43.75, 162}, {-43.75, 144}, {-18, 144}}));
connect(transition16.outPort, MaxMid.inPort[1]) annotation(
  Line(points = {{-12.5, 144}, {16.25, 144}, {16.25, 158}, {19, 158}}));
connect(MaxMid.outPort[1], transition15.inPort) annotation(
  Line(points = {{40.5, 158}, {8.25, 158}, {8.25, 178}, {-10, 178}}));
connect(transition17.outPort, MidMid.inPort[2]) annotation(
  Line(points = {{14, 108.5}, {14, 63.25}, {23, 63.25}, {23, 62}}));
connect(MidMid.outPort[2], transition18.inPort) annotation(
  Line(points = {{44.5, 62}, {48, 62}, {48, 106}}));
connect(transition18.outPort, MaxMid.inPort[3]) annotation(
  Line(points = {{48, 111.5}, {48, 158}, {19, 158}}));
connect(MaxMid.outPort[3], transition17.inPort) annotation(
  Line(points = {{40.5, 158}, {44.25, 158}, {44.25, 114}, {14, 114}}));
connect(MidMid.outPort[1], transition12.inPort) annotation(
  Line(points = {{44.5, 62}, {21.25, 62}, {21.25, 86}, {-10, 86}}));
connect(transition11.outPort, MidMid.inPort[1]) annotation(
  Line(points = {{-12.5, 50}, {4.25, 50}, {4.25, 62}, {23, 62}}));
connect(MidMid.outPort[3], transition19.inPort) annotation(
  Line(points = {{44.5, 62}, {60.25, 62}, {60.25, 50}, {78, 50}}));
connect(MidMid.outPort[4], transition8.inPort) annotation(
```

**Figure A.13:** OpenModelica code for Controller (12/13).

```
    Line(points = {{44.5, 62}, {20, 62}, {20, 10}}));
  connect(transition7.outPort, MidMid.inPort[4]) annotation(
    Line(points = {{52, 9.5}, {52, 62}, {23, 62}}));
  connect(transition19.outPort, MidMax.inPort[1]) annotation(
    Line(points = {{83.5, 50}, {83.5, 66}, {115, 66}}));
  connect(MidMax.outPort[1], transition20.inPort) annotation(
    Line(points = {{136.5, 66}, {99.25, 66}, {99.25, 86}, {86, 86}}));
  connect(MidMax.outPort[2], transition21.inPort) annotation(
    Line(points = {{136.5, 66}, {144, 66}, {144, 108}}));
  connect(transition22.outPort, MidMax.inPort[2]) annotation(
    Line(points = {{114, 110.5}, {115, 110.5}, {115, 66}}));
  connect(transition21.outPort, MaxMax.inPort[2]) annotation(
    Line(points = {{144, 113.5}, {144, 140}, {119, 140}, {119, 160}}));
  connect(MaxMax.outPort[2], transition22.inPort) annotation(
    Line(points = {{140.5, 160}, {160, 160}, {160, 134}, {114, 134}, {114,
116}}));
  connect(MaxMid.outPort[2], transition24.inPort) annotation(
    Line(points = {{40.5, 158}, {72.25, 158}, {72.25, 144}, {78, 144}}));
  connect(transition23.outPort, MaxMid.inPort[2]) annotation(
    Line(points = {{80.5, 178}, {42.75, 178}, {42.75, 158}, {19, 158}}));
  connect(MaxMax.outPort[1], transition23.inPort) annotation(
    Line(points = {{140.5, 160}, {142.25, 160}, {142.25, 178}, {86, 178}}));
  connect(transition24.outPort, MaxMax.inPort[1]) annotation(
    Line(points = {{83.5, 144}, {105.25, 144}, {105.25, 160}, {119, 160}}));
  connect(MinMid.outPort[2], transition7.inPort) annotation(
    Line(points = {{46.5, -46}, {52, -46}, {52, 4}}));
  connect(transition8.outPort, MinMid.inPort[2]) annotation(
    Line(points = {{20, 4.5}, {20, -23.75}, {25, -23.75}, {25, -46}}));
  connect(MinMax.outPort[1], transition2.inPort) annotation(
    Line(points = {{140.5, -46}, {108.25, -46}, {108.25, -34}, {86, -34}}));
  connect(MinMax.outPort[3], transition4.inPort) annotation(
    Line(points = {{140.5, -46}, {188, -46}, {188, 162}}));
  connect(MinMax.outPort[2], transition6.inPort) annotation(
    Line(points = {{140.5, -46}, {146, -46}, {146, 6}}));
  connect(transition20.outPort, MidMid.inPort[3]) annotation(
    Line(points = {{80.5, 86}, {55.75, 86}, {55.75, 62}, {23, 62}}));
  connect(MinMid.outPort[1], transition1.inPort) annotation(
    Line(points = {{46.5, -46}, {20.25, -46}, {20.25, -32}, {-6, -32}}));
  connect(transition2.outPort, MinMid.inPort[3]) annotation(
    Line(points = {{80.5, -34}, {52.75, -34}, {52.75, -46}, {25, -46}}));
  connect(MinMid.outPort[3], transition3.inPort) annotation(
    Line(points = {{46.5, -46}, {56.25, -46}, {56.25, -62}, {78, -62}}));
  annotation(
    preserveAspectRatio=true,
    Diagram(coordinateSystem(extent = {{-100, -100}, {200, 200}})),
    Icon(coordinateSystem(extent = {{-100, -100}, {100, 100}})));
end Controller;
```

**Figure A.14:** OpenModelica code for Controller (13/13).

# Appendix B

# Scheduler

```
model Scheduler

 parameter Real P_t_max = 130e+06 "in watts";
 parameter Real P_e_max = 70e+06 "maximum electrolyser power in watts";
 parameter Real P_fc_max = 30e+06 "maximum electrolyser power in watts";
 parameter Real P_fc_min = 2e+06 "maximum electrolyser power in watts";
 parameter Real P_e_min = 1e+06 "minimum electrolyser power in watts";
 parameter Real P_b_max = 80e+06 "maximum battery power in watts";
 parameter Real e_eff  = 0.6 "electrolyser efficiency";
 parameter Real fc_eff  = 0.6 "Fuel cell efficiency";
 parameter Real profitmargin = 0.2 "profit";
 parameter Real h2_Price = 1000 "price for hydrogen in kr/MWh";
 parameter Real batteryStorageCap = 100e+6 "Maximum capacity in battery in
Wh";
 parameter Real hydrogenStorageCap= 1000e+6 "Maximum capacity in hydrogen
storage in Wh";
 parameter Real SOC_high = 0.75 "SOC scheduler wants to plan to stay below";
 parameter Real SOC_low = 0.3 "SOC scheduler wants to plan to stay above";
 parameter Real SOC_nom = 0.5 "SOC scheduler wants to plan to stay at";
 parameter Real SOH_high = 0.75 "SOH scheduler wants to plan to stay below";
 parameter Real SOH_low = 0.3 "SOH scheduler wants to plan to stay above";
 Boolean very_high;
 Boolean high;
 Boolean low;
 Boolean very_low;
 Boolean hydrogen_best;
 Boolean fuel_cell_on;
 Real SOCT0 "State of charge at t0";
 Real SOCT1 "State of charge at t1";
 Real SOCT2 "State of charge at t2";
 Real SOHT0 "State of hydrogen at t0";
 Real correctionPower;
 Real correctionPower_0to1;
  Modelica.Blocks.Interfaces.RealInput P_progT0 annotation(
    Placement(visible = true, transformation(origin = {-180, 0}, extent =
{{-140, 60}, {-100, 100}}, rotation = -90), iconTransformation(origin =
{-100, 110}, extent = {{-10, -10}, {10, 10}}, rotation = -90)));
 Modelica.Blocks.Interfaces.RealInput P_progT1 annotation(
    Placement(visible = true, transformation(origin = {-160, 0}, extent =
{{-140, 60}, {-100, 100}}, rotation = -90), iconTransformation(origin = {-80,
110}, extent = {{-10, -10}, {10, 10}}, rotation = -90)));
 Modelica.Blocks.Interfaces.RealInput dayaheadT0 annotation(
    Placement(visible = true, transformation(origin = {-110, 60}, extent =
{{-10, -10}, {10, 10}}, rotation = 0), iconTransformation(origin = {-110,
60}, extent = {{-10, -10}, {10, 10}}, rotation = 0)));
 Modelica.Blocks.Interfaces.RealInput dayaheadT1 annotation(
    Placement(visible = true, transformation(origin = {-110, 40}, extent =
{{-10, -10}, {10, 10}}, rotation = 0), iconTransformation(origin = {-110,
40}, extent = {{-10, -10}, {10, 10}}, rotation = 0)));
 Modelica.Blocks.Interfaces.RealInput SOC annotation(
    Placement(visible = true, transformation(origin = {120, -2}, extent =
{{-140, 60}, {-100, 100}}, rotation = 90), iconTransformation(origin = {140,
0}, extent = {{-140, 60}, {-100, 100}}, rotation = 90)));
```

```
Modelica.Blocks.Interfaces.RealInput SOH annotation(
  Placement(visible = true, transformation(origin = {160, 0}, extent =
{{-140, 60}, {-100, 100}}, rotation = 90), iconTransformation(origin = {180,
0}, extent = {{-140, 60}, {-100, 100}}, rotation = 90)));
 Modelica.Blocks.Interfaces.RealOutput P annotation(
  Placement(visible = true, transformation(origin = {0, 0}, extent = {{100,
-10}, {120, 10}}, rotation = 0), iconTransformation(origin = {0, 0}, extent =
{{100, -10}, {120, 10}}, rotation = 0)));
 Modelica.Blocks.Interfaces.RealOutput P_e_set annotation(
  Placement(visible = true, transformation(origin = {0, 40}, extent = {{100,
-10}, {120, 10}}, rotation = 0), iconTransformation(origin = {0, -40}, extent
= {{100, -10}, {120, 10}}, rotation = 0)));
 Modelica.Blocks.Interfaces.RealOutput P_fc_set annotation(
 Placement(visible = true, transformation(origin = {0, -40}, extent = {{100,
-10}, {120, 10}}, rotation = 0), iconTransformation(origin = {0, 42}, extent
= {{100, -10}, {120, 10}}, rotation = 0)));
 parameter Modelica.SIunits.Time period(final min=Modelica.Constants.small,
     start=3600) "Sample period";
 parameter Modelica.SIunits.Time startTime=-3599.99;
 Modelica.Blocks.Interfaces.RealInput upper_band annotation(
  Placement(visible = true, transformation(origin = {-40, 0}, extent =
{{-140, 60}, {-100, 100}}, rotation = -90), iconTransformation(origin = {-30,
0}, extent = {{-140, 60}, {-100, 100}}, rotation = -90)));
 Modelica.Blocks.Interfaces.RealInput average annotation(
  Placement(visible = true, transformation(origin = {0, 0}, extent = {{-140,
60}, {-100, 100}}, rotation = -90), iconTransformation(origin = {20, 0},
extent = {{-140, 60}, {-100, 100}}, rotation = -90)));
 Modelica.Blocks.Interfaces.RealInput lower_band annotation(
  Placement(visible = true, transformation(origin = {-80, 0}, extent =
{{-140, 60}, {-100, 100}}, rotation = -90), iconTransformation(origin = {-80,
0}, extent = {{-140, 60}, {-100, 100}}, rotation = -90)));
 Modelica.Blocks.Interfaces.RealInput dayaheadT2 annotation(
  Placement(visible = true, transformation(origin = {-110, 20}, extent =
{{-10, -10}, {10, 10}}, rotation = 0), iconTransformation(origin = {-110,
20}, extent = {{-10, -10}, {10, 10}}, rotation = 0)));
 Modelica.Blocks.Interfaces.RealInput dayaheadT3 annotation(
  Placement(visible = true, transformation(origin = {-110, 0}, extent =
{{-10, -10}, {10, 10}}, rotation = 0), iconTransformation(origin = {-110, 0},
extent = {{-10, -10}, {10, 10}}, rotation = 0)));
 Modelica.Blocks.Interfaces.RealInput dayaheadT5 annotation(
  Placement(visible = true, transformation(origin = {-110, -40}, extent =
{{-10, -10}, {10, 10}}, rotation = 0), iconTransformation(origin = {-110,
-40}, extent = {{-10, -10}, {10, 10}}, rotation = 0)));
 Modelica.Blocks.Interfaces.RealInput dayaheadT4 annotation(
  Placement(visible = true, transformation(origin = {-110, -20}, extent =
{{-10, -10}, {10, 10}}, rotation = 0), iconTransformation(origin = {-110,
-20}, extent = {{-10, -10}, {10, 10}}, rotation = 0)));
 Modelica.Blocks.Interfaces.RealInput dayaheadT7 annotation(
  Placement(visible = true, transformation(origin = {-110, -80}, extent =
{{-10, -10}, {10, 10}}, rotation = 0), iconTransformation(origin = {-110,
-80}, extent = {{-10, -10}, {10, 10}}, rotation = 0)));
 Modelica.Blocks.Interfaces.RealInput dayaheadT6 annotation(
```

**Figure B.2:** OpenModelica code for Scheduler (2/7).

```
      Placement(visible = true, transformation(origin = {-110, -60}, extent =
   {{-10, -10}, {10, 10}}, rotation = 0), iconTransformation(origin = {-110,
   -60}, extent = {{-10, -10}, {10, 10}}, rotation = 0)));
   /*Modelica.Blocks.Interfaces.RealInput dayaheadT8 annotation(
      Placement(visible = true, transformation(origin = {-110, -100}, extent =
   {{-10, -10}, {10, 10}}, rotation = 0), iconTransformation(origin = {-110,
   -100}, extent = {{-10, -10}, {10, 10}}, rotation = 0)));
   */equation
   when sample(startTime,period) then
      correctionPower_0to1 = correctionPower/130e+6;
      if dayaheadT0 >= upper_band and dayaheadT0 > h2_Price *
   (e_eff-profitmargin) and dayaheadT0 < h2_Price / (fc_eff-profitmargin) then
         very_high = true;
         high = false;
         low = false;
         very_low = false;
         hydrogen_best = false;
         fuel_cell_on = false;
      elseif dayaheadT0 >= average and dayaheadT0 > h2_Price *
   (e_eff-profitmargin) and dayaheadT0 < h2_Price / (fc_eff-profitmargin) then
         very_high = false;
         high = true;
         low = false;
         very_low = false;
         hydrogen_best = false;
         fuel_cell_on = false;
      elseif dayaheadT0 >= lower_band and dayaheadT0 > h2_Price *
   (e_eff-profitmargin) and dayaheadT0 < h2_Price / (fc_eff-profitmargin) then
         very_high = false;
         high = false;
         low = true;
         very_low = false;
         hydrogen_best = false;
         fuel_cell_on = false;
      elseif dayaheadT0 < lower_band and dayaheadT0 > h2_Price *
   (e_eff-profitmargin) and dayaheadT0 < h2_Price / (fc_eff-profitmargin) then
         very_high = false;
         high = false;
         low = false;
         very_low = true;
         hydrogen_best = false;
         fuel_cell_on = false;
         elseif dayaheadT0 >= h2_Price / (fc_eff-profitmargin) then
         very_high = false;
         high = false;
         low = false;
         very_low = false;
         hydrogen_best = false;
         fuel_cell_on = true;
      else
         very_high = false;
         high = false;
         low = false;
```

**Figure B.3:** OpenModelica code for Scheduler (3/7).

```
      very_low = false;
      hydrogen_best = true;
      fuel_cell_on = false;
    end if;

    SOCT0 = SOC;
    SOHT0 = SOH;
    if P_progT0 > P_t_max then //over production at t0?
      P_fc_set = 0;
      P = P_t_max;
      SOCT1 = SOCT0 + (P_progT0 - P_t_max)/batteryStorageCap "Calculate SOC
after one hour of over production";
        if P_progT1 > P_t_max then // over production at t1?
          SOCT2 = SOCT1 + (P_progT1 - P_t_max)/batteryStorageCap;
          if SOCT2 >= SOC_high then
            correctionPower = (SOCT2 - SOC_high)*batteryStorageCap;
            if correctionPower > (SOCT1-SOC_low)*batteryStorageCap and
(SOCT1-SOC_low) > 0 then
              P_e_set = (SOCT1-SOC_low)*batteryStorageCap;
            elseif (SOCT1-SOC_nom) <= 0 then
              P_e_set = if (P_progT1 - P_t_max)> P_e_max then P_e_max else
P_progT1 - P_t_max;
            elseif correctionPower >= P_e_max then
              P_e_set = P_e_max;
            else
              P_e_set = correctionPower;
            end if;
          else
            correctionPower = 0;
            P_e_set = 0;
          end if;
        else //under production t1
          SOCT2 = 0;
          if SOCT1 >= SOC_nom then
            correctionPower = (SOCT1 - SOC_nom)*batteryStorageCap;
            if correctionPower >= P_e_max then
              P_e_set = P_e_max;
            else
              P_e_set = correctionPower;
            end if;
          else
              correctionPower = 0;
              P_e_set = 0;
          end if;
        end if;
      else // under production at t0
        if P_progT1 > P_t_max then // over production at t1?
          P_fc_set = 0;
          SOCT1 = SOCT0;
          SOCT2 = SOCT1 + (P_progT1 - P_t_max)/batteryStorageCap;
          if SOCT2 >= SOC_high then
            correctionPower = (SOCT2 - SOC_high)*batteryStorageCap;
            if dayaheadT0 < h2_Price*0.6 then // better to produce hydrogen?
```

**Figure B.4:** OpenModelica code for Scheduler (4/7).

```
          P_e_set = if correctionPower >= P_e_max then P_e_max elseif
correctionPower < P_e_min then 0 else correctionPower;
          P = if correctionPower > P_e_max and P_progT0 + (correctionPower -
P_e_set) < P_t_max then P_progT0 + (correctionPower - P_e_set) elseif
correctionPower > P_e_max and P_progT0 + (correctionPower - P_e_set) >=
P_t_max then P_t_max else P_progT0;
        else // better to sell to grid
          P = if correctionPower < P_b_max and P_progT0 + correctionPower <
P_t_max then P_progT0 + correctionPower elseif correctionPower < P_b_max and
P_progT0 + correctionPower >= P_t_max then P_t_max elseif correctionPower >
P_b_max and P_progT0 + correctionPower >= P_t_max then P_t_max else  P_progT0
+ P_b_max;
          P_e_set = 0; // could also activate P_e here if battery can't
reach the right SOC on its own. Problem with logical statments
        end if;
      else // SOCT2 < SOC_nom Om fuel cell är rimligt, kör den
        correctionPower = 0;
        P = P_progT0;
        P_e_set = 0 ;
      end if;
    else // under production at t1
      SOCT1 = 0;
      SOCT2 = 0;
        if very_high then
        correctionPower = if abs((SOCT0 - SOC_low)*batteryStorageCap) >=
P_b_max then P_b_max else (SOCT0 - SOC_low)*batteryStorageCap;
        if dayaheadT0 >= dayaheadT1 and dayaheadT0 >= dayaheadT2 and
dayaheadT0 >= dayaheadT3 and dayaheadT0 >= dayaheadT4 and dayaheadT0 >=
dayaheadT5 and dayaheadT0 >= dayaheadT6 and dayaheadT0 >= dayaheadT7 and
correctionPower > 0 then
            P = if correctionPower + P_progT0 >= P_t_max then P_t_max elseif
correctionPower + P_progT0 <= 0 then 0 else P_progT0 + correctionPower;
            P_e_set = 0;
            P_fc_set = 0;
          else
            P = P_progT0;
            P_e_set = 0;
            P_fc_set = 0;
          end if;
        elseif high then
        correctionPower = if abs((SOCT0 - SOC_nom)*batteryStorageCap) >=
P_b_max then P_b_max else (SOCT0 - SOC_nom)*batteryStorageCap;
        if dayaheadT0 >= dayaheadT1 and dayaheadT0 >= dayaheadT2 and
dayaheadT0 >= dayaheadT3 and dayaheadT0 >= dayaheadT4 and dayaheadT0 >=
dayaheadT5 and dayaheadT0 >= dayaheadT6 and dayaheadT0 >= dayaheadT7 and
correctionPower > 0 then
            P = if correctionPower + P_progT0 >= P_t_max then P_t_max elseif
correctionPower + P_progT0 <= 0 then 0 else P_progT0 + correctionPower;
            P_e_set = 0;
            P_fc_set = 0;
          else
            P = P_progT0;
            P_e_set = 0;
```

**Figure B.5:** OpenModelica code for Scheduler (5/7).

```
                        P_fc_set = 0;
                    end if;
              elseif low then
                    correctionPower = if abs((SOCT0 - SOC_high*7/8)*batteryStorageCap)
>= P_b_max then P_b_max else (SOCT0 - SOC_high*7/8)*batteryStorageCap;
                    if dayaheadT0 <= dayaheadT1 and dayaheadT0 <= dayaheadT2 and
dayaheadT0 <= dayaheadT3 and dayaheadT0 <= dayaheadT4 and dayaheadT0 <=
dayaheadT5 and dayaheadT0 <= dayaheadT6 and dayaheadT0 <= dayaheadT7 and
correctionPower < 0 then
                        P = if correctionPower + P_progT0 >= P_t_max then P_t_max elseif
correctionPower + P_progT0 <= 0 then 0 else P_progT0 + correctionPower;
                        P_e_set = 0;
                        P_fc_set = 0;
                    else
                        P = P_progT0;
                        P_e_set = 0;
                        P_fc_set = 0;
                    end if;
              elseif very_low then
                    correctionPower = if abs((SOCT0 - SOC_high)*batteryStorageCap) >=
P_b_max then P_b_max else (SOCT0 - SOC_high)*batteryStorageCap;
                    if dayaheadT0 <= dayaheadT1 and dayaheadT0 <= dayaheadT2 and
dayaheadT0 <= dayaheadT3 and dayaheadT0 <= dayaheadT4 and dayaheadT0 <=
dayaheadT5 and dayaheadT0 <= dayaheadT6 and dayaheadT0 <= dayaheadT7 and
correctionPower < 0 then
                        P = if correctionPower + P_progT0 >= P_t_max then P_t_max elseif
correctionPower + P_progT0 <= 0 then 0 else P_progT0 + correctionPower;
                        P_e_set = 0;
                        P_fc_set = 0;
                    else
                        P = P_progT0;
                        P_e_set = 0;
                        P_fc_set = 0;
                    end if;
              elseif fuel_cell_on then
                    correctionPower = if abs((SOCT0 - SOC_low)*batteryStorageCap) >=
P_b_max then P_b_max else (SOCT0 - SOC_low)*batteryStorageCap;
                    if dayaheadT0 >= dayaheadT1 and dayaheadT0 >= dayaheadT2 and
dayaheadT0 >= dayaheadT3 and dayaheadT0 >= dayaheadT4 and dayaheadT0 >=
dayaheadT5 and dayaheadT0 >= dayaheadT6 and dayaheadT0 >= dayaheadT7 and
correctionPower > 0 then
                        P_fc_set = if correctionPower + P_progT0 >= P_fc_min and
correctionPower + P_progT0 <= P_fc_max and -(correctionPower +
P_progT0)/hydrogenStorageCap+SOHT0 >= SOH_low then correctionPower + P_progT0
elseif (correctionPower + P_progT0) > P_fc_max and
(-P_fc_max)/hydrogenStorageCap+SOHT0 >= SOH_low then P_fc_max else 0;
                        P = if correctionPower + P_progT0 + P_fc_set >= P_t_max then
P_t_max elseif correctionPower + P_progT0 + P_fc_set <= 0 then 0 else
P_progT0 + correctionPower + P_fc_set;
                        P_e_set = 0;
                    else
                        P_fc_set = if P_t_max - P_progT0 < P_fc_max and -(P_t_max -
P_progT0)/hydrogenStorageCap+SOHT0 >= SOH_low then P_t_max - P_progT0 elseif
```

**Figure B.6:** OpenModelica code for Scheduler (6/7).

```
P_t_max - P_progT0 >= P_fc_max and (-P_fc_max)/hydrogenStorageCap+SOHT0 >=
SOH_low then P_fc_max else 0;
            P = if P_progT0 + P_fc_set>=P_t_max then P_t_max else P_progT0 +
P_fc_set;
            P_e_set = 0;
          end if;
        else // hydrogen_best
          correctionPower = if ((SOCT0 - SOC_high)*batteryStorageCap) >=
P_b_max then P_b_max else ((SOCT0 - SOC_high)*batteryStorageCap);
          if dayaheadT0 <= dayaheadT1 and dayaheadT0 <= dayaheadT2 and
dayaheadT0 <= dayaheadT3 and dayaheadT0 <= dayaheadT4 and dayaheadT0 <=
dayaheadT5 and dayaheadT0 <= dayaheadT6 and dayaheadT0 <= dayaheadT7 and
correctionPower < 0 then
            P_e_set = if correctionPower + P_progT0 >= P_e_min and
correctionPower + P_progT0 <= P_e_max and (correctionPower +
P_progT0)/hydrogenStorageCap+SOHT0 <= SOH_high then correctionPower +
P_progT0 elseif (correctionPower + P_progT0) > P_e_max and
(P_e_max)/hydrogenStorageCap+SOHT0 <= SOH_high then P_e_max else 0;
            P = if correctionPower + P_progT0 - P_e_set >= P_t_max then
P_t_max elseif correctionPower + P_progT0 - P_e_set <= 0 then 0 else P_progT0
+ correctionPower - P_e_set;
            P_fc_set = 0;
          else
            P_e_set = if P_progT0 < P_e_max and
(P_progT0)/hydrogenStorageCap+SOHT0 <= SOH_high then P_progT0 elseif P_progT0
>= P_e_max and (P_e_max)/hydrogenStorageCap+SOHT0 <= SOH_high then P_e_max
else 0;
            P = if P_progT0 - P_e_set>=P_t_max then P_t_max else P_progT0 -
P_e_set;
            P_fc_set = 0;
          end if;
        end if;
    end if;
  end if;
 end when;
 annotation(
   Diagram,
   Icon);
end Scheduler;
```

**Figure B.7:** OpenModelica code for Scheduler (7/7).

# Appendix C

# Operational strategy performance overview
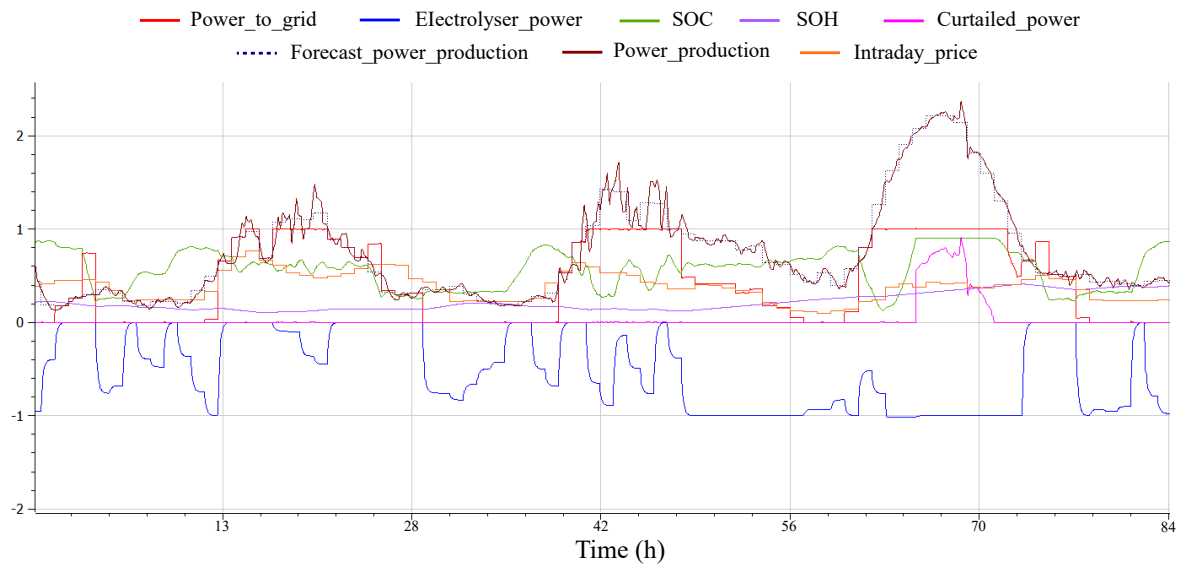


**Figure C.1:** Simulation plot of power to grid, forecast production, real production, curtailed solar power, state of charge in battery, state of hydrogen storage, intraday price, and power flow through electrolyser.

# Appendix D

# Investment appraisal of optimised model
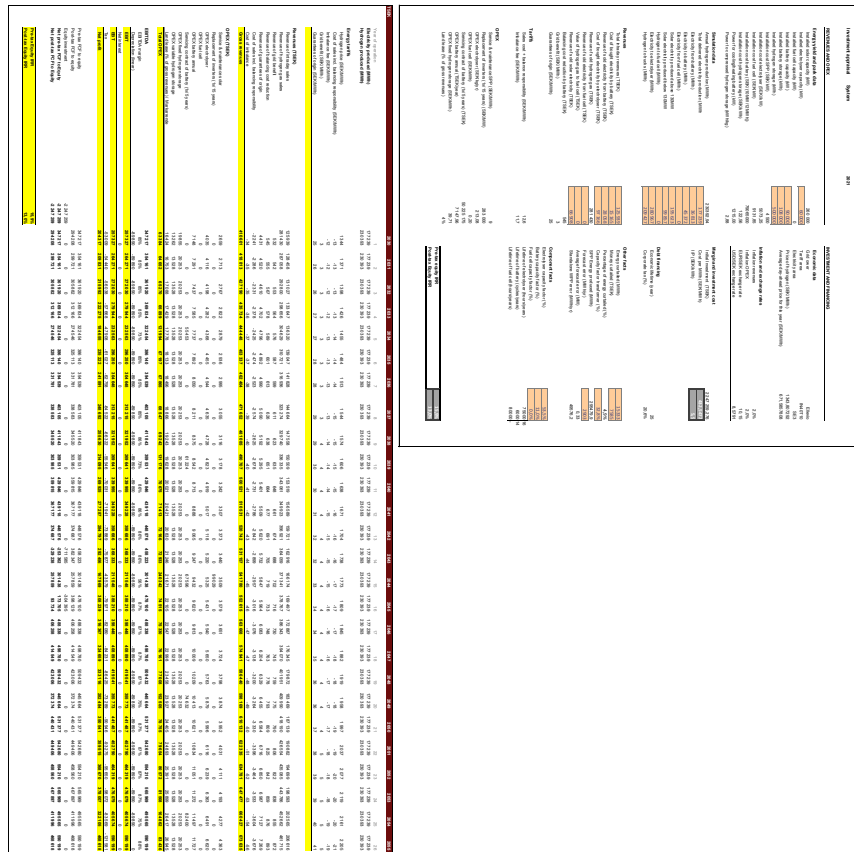


**Figure D.1:** Investment appraisal of entire system.

**Figure D.2:** Investment appraisal of electrolyser and hydrogen storage.

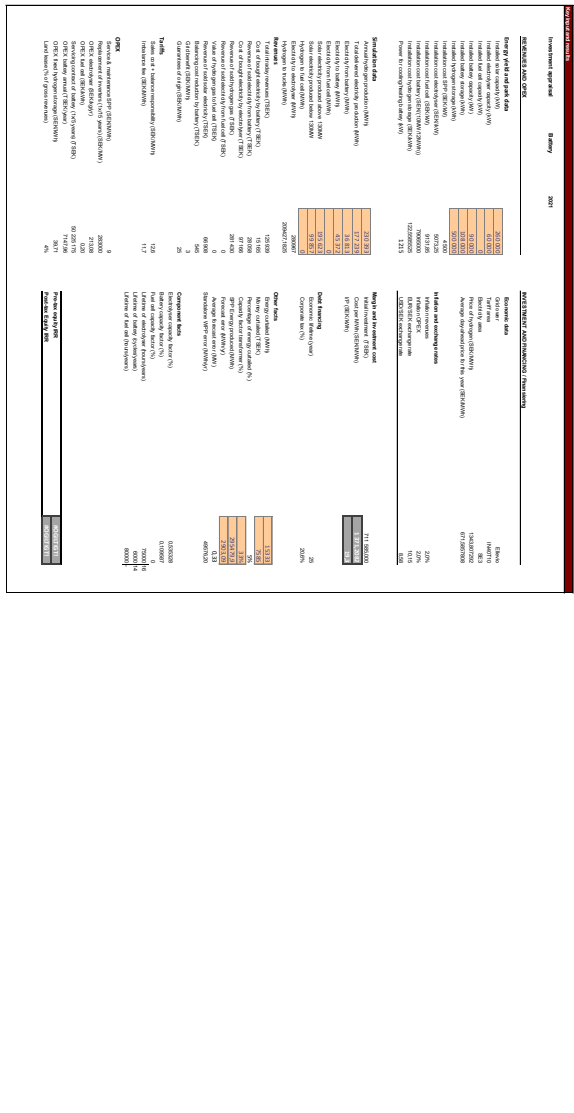**Figure D.3:** Investment appraisal of battery storage.

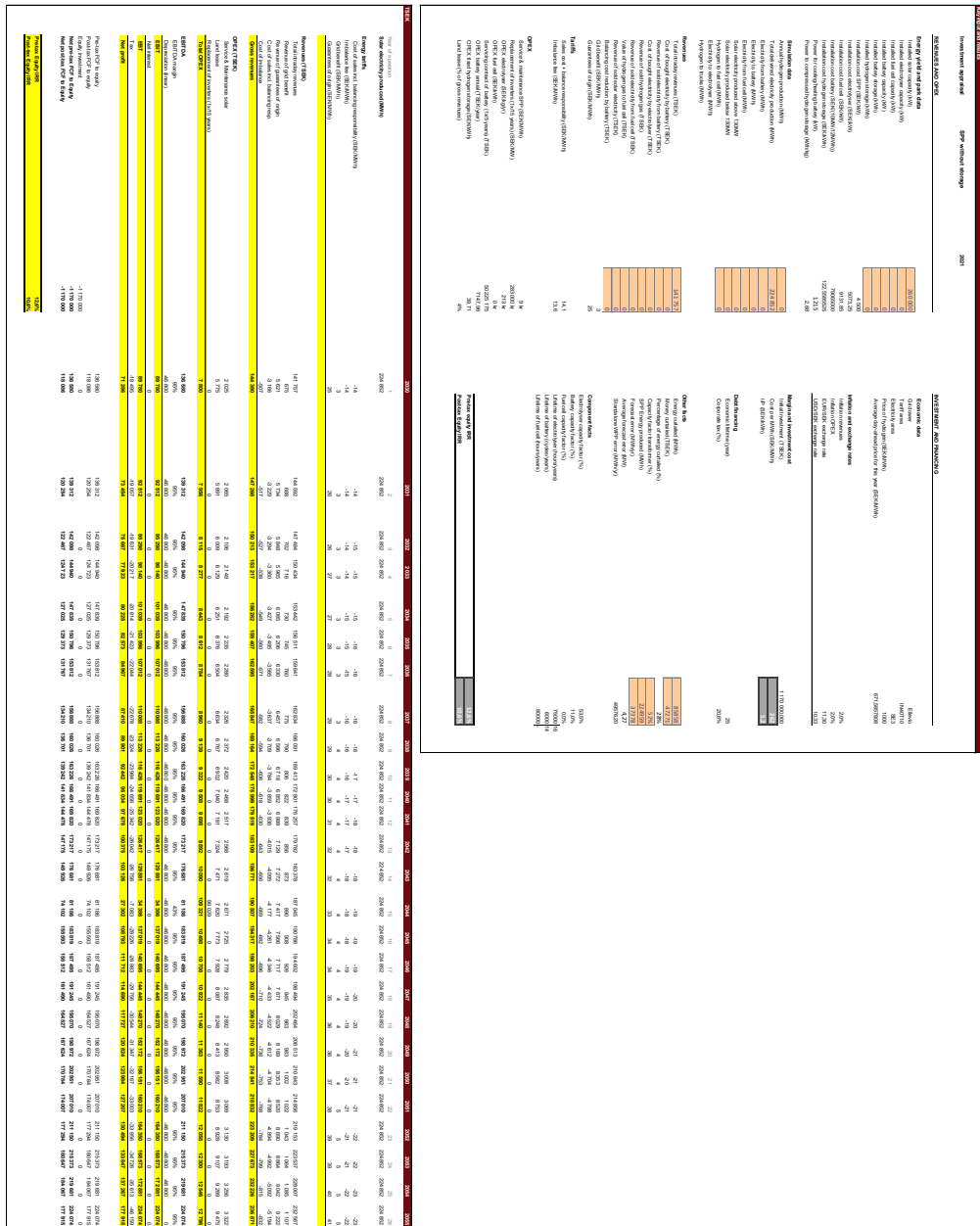**Figure D.4:** Investment appraisal of solar power plant.

**Figure D.5:** Investment appraisal of solar power plant with no storage.